공학석사 학위논문

유공케이슨 방파제의 활동에 대한 설계법 비교 연구

Comparative study of design methods for sliding of perforated wall caisson breakwater

2014년 02월

서울대학교 대학원

건설환경공학부

김 남 훈

ABSTRACT

Comparative Study of Design Methods for Sliding of Perforated Wall Caisson Breakwater

Nam-Hoon, Kim

Department of Civil and Environmental Engineering

The Graduate School

Seoul National University

In the design of a caisson breakwater against sliding, the deterministic design method has been used with consideration of certain margin of safety factor. However, it is difficult to quantitatively and comparatively evaluate the sliding distance using the safety factor because of the uncertainty of the design variables. It may cause the over- or under-design of the structure. Therefore, it is required to develop probabilistic design methods (e.g., performance-based design method) to consider the uncertainties of the design variables by computing the sliding distance of the caisson. The performance-based design method of a solid-wall caisson breakwater has been investigated by many researchers and its framework is almost completed. On the other hand, researches on a perforated-wall caisson breakwater have been scarcely made despite the fact that it has greater structural safety due to decreased impulsive wave force at the perforated-wall.

In this study, the conventional performance-based design method of the solid-wall caisson breakwater has been expanded and applied to the perforated-wall caisson breakwater in order to examine the feasibility of its application. In addition, a comparative analysis is made between the deterministic design method and performance-based design method. It will serve as a basic research to standardize the criteria of the performance-based design method of a perforated-wall caisson breakwater. Moreover, it is expected to be an important and useful tool in designing a stable perforated-wall caisson breakwater in the future.

Keywords: Perforated-wall caisson breakwater, reliability design method, performance-based design method, expected sliding distance, exceedance rate

Student number: 2012-20892

CONTENTS

LIST OF TABLES

LIST OF FIGURES

LIST OF SYMBOLS

Latin upper case

B	Caisson width
B_c	Chamber width
B_M	Berm width
F_D	Force related sliding velocity including the wave-making resistance force
F_R	Resistance force
$G(\theta \mid f)$	Directional spreading function
H	Individual wave height
H_b	Breading wave height
$H_{\max}$	Maximum wave height at breakwater site
H_0	Offshore wave height
H_0'	Equivalent deepwater wave height
$H_{1/3}$	Significant wave height
$H_{1/3e}$	Significant wave height through wave transformation
H_{0e}	Sample of extreme distribution of deepwater wave height
$(K_r)_{eff}$	Effective refraction coefficient
K_s	Nonlinear shoaling coefficient
K_{si}	Linear shoaling coefficient

L	Probabilistic variable of load component or Wave length
L'	Wave length at d'
L_0	Deep water wave length
M_a	Added mass
N	Total number of simulation
P_e	Exceedance rate
P_f	Probability of failure
P_H	Horizontal wave force
P_I	Horizontal wave force at Crest I
P_{IIa}	Horizontal wave force at Crest IIa
P_{IIaM}	Wave force acting on the chamber at Crest IIa
P_{IIb}	Horizontal wave force at Crest IIb
P_{IIbM}	Wave force acting on the chamber at Crest IIb
P_U	Uplift force
P_V	Chamber force
R	Probabilistic variable of resistance component
$S_0(f)$	Frequency spectrum
$S_0(f,\theta)$	Offshore directional wave spectrum
$T_{1/3}$	Significant wave period
U	Uplift force
U_I	Uplift force at Crest I
U_{IIa}	Uplift force at Crest IIa

U_{IIb}	Uplift force at Crest IIb
W	Caisson weight in the air
W'	Caisson weight in water
Z	Design criterion that can judge the success and failure of structure

Latin lower case

d	Water depth at the top of foot protection
d'	Water depth of the wave chamber
f	Wave frequency
f_{DTN}	Probability density function of doubly truncated normal distribution
f_p	Peak wave frequency
h	Water depth
h'	Water depth at the top of rubble mound foundation
h_c	Crest elevation
h_{c1}	Crest elevation of perforated wall
h_{c2}	Crest elevation of solid wall
m_0	Zeroth moments of the frequency spectrum
n	Number of failure state in the simulation
n_e	Number of limit state in the simulation
r	Random variables
r'	Random variables using doubly-truncated normal distribution

s	Directional spreading parameter
s_a	Allowable sliding distance
$s_{\max}$	Peak value of directional spreading parameter
t_d	Time difference of wave force between Crest I and Crest IIa
t_m	Start time of wave force acting on the wave chamber
x_G	Horizontal displacement of caisson

Greek upper case

$\Gamma(\cdot)$	Gamma function

Greek lower case

α	Scale parameter of Weibull distribution
α_1	Parameter for a standing wave force
α_2	Parameter for an impulsive wave force
α_I	Parameter for an impulsive wave force proposed by Takahashi et al. (1994)
α_{X_i}	Bias coefficient of design variables
α^*	Maximum value between α_2 and α_I
β	Wave direction
η^*	Run-up height

ε	Opening ratio of the perforated wall
ε'	Reduction rate of wave force
γ_{X_i}	Variation coefficient of design variables
ξ	Location parameter of Weibull distribution
κ	Shape parameter of Weibull distribution
$\lambda_1, \lambda_2, \lambda_3$	Correction coefficient for vertical caisson breakwater
λ_S	Correction coefficient for perforated front wall
λ_L	Correction coefficient for solid front wall
λ_R	Correction coefficient for solid rear wall
λ_M	Correction coefficient for wave chamber
λ_U	Correction coefficient for uplift
μ	Friction coefficient
μ_{X_i}	Mean of design variables
σ_{X_i}	Standard deviation of design variables
θ	Angle of the bottom slope
τ_0	Duration of impulsive wave
τ_0'	Duration of wave force at Crest IIa

CHAPTER 1 INTRODUCTION

1.1 Necessity and background of research

Existing harbor structures have been generally designed by the deterministic design method. The safety factor is calculated with the force acting on the structure during the lifetime. The safety factor is then compared against the requirement of safety factor to judge the safety of the structure. It is assumed that the uncertainty of the load on and resistance of the structure can be determined by using the safety factor as an evaluation index. However, it poses a possibility of over- or under-estimation of structure dimension since the quantitative and comparative evaluations of a structure displacement are not easy.

In order to overcome the shortcomings of the deterministic design method, a probabilistic design method has been used since 1970's, which now is known as a reliability design method. The reliability design methods for coastal structures have been studied since the mid 1980's. In place of the safety factor of the deterministic design method, reliability design method considers the probabilistic uncertainty of the design variables affecting the failure of the structure. This method is such that probability of failure is within an allowable limit to satisfy stability, functionality, and economic feasibility of the structure.

Failure modes of caisson breakwaters are sliding, overturning, and geotechnical failure of rubble mound foundation. Failure of caisson breakwaters is dominated by sliding among these modes. A concept of

expected sliding distance of caisson breakwaters has been adapted first in Japan. It uses a probability distribution of wave height and time series of wave force and makes repeated computations of cumulative sliding distances that may occur during the lifetime. The sliding distances are then averaged to determine the expected sliding distance. This has been recognized as a significant measure to evaluate performance of breakwaters. There are two typical types of caisson breakwaters: a solid-wall caisson breakwater and a perforated-wall caisson breakwater; the former consists a solid frontal wall and the latter a perforated frontal wall.

Computation models for the expected sliding distance of a solid-wall caisson breakwater have been researched in large volume and its framework is almost fully established. On the other hand, researches on the perforated-wall caisson breakwaters are scarce either at home or abroad despite the fact that it poses great structural stability due to decreased impulsive wave force with good wave dissipation at the perforated wall.

This research is done as a fundamental study to develop a performance-based design method of the perforated-wall caisson breakwater. Its main purpose is to compare and analyze the pros and cons of the perforated-wall caisson breakwater, while the performance-based design method mostly applied to the solid-wall caisson breakwater is expanded to be applied to the design of the perforated-wall caisson breakwater.

1.2 Research trends

The reliability design method which reflects uncertainties of the design variables into the structure design has become to be recognized as a major technology to proactively manage the structural risks throughout the world. A design criteria ISO 2394 of International Organization for Standardization (ISO) requires a probabilistic design of a structure. The reliability theory has already been introduced all over the world in harbor structure designs for this reason and the establishments of international standards have been centered around Japan (JPHA, 2007; OCDI, 2009) and Europe (ECS, 1991, 1992). Thus, the trend of civil engineering structure design is moving away from the deterministic design method toward the probabilistic design method. In order to come up with performance-based reliability design criteria against natural disaster in Korea to be in line with global trends, the Ministry of Land, Transport and Maritime Affairs had initiated the reliability design method studies to be applied to harbor structure designs with Korea Institute of Ocean Science and Technology (formerly the Korea Ocean Research and Development Institute) since 2006. In 2011, it published the standards for the breakwater reliability design (2011).

A performance-based design method which determines the reliability of the caisson structure with the expected sliding distance has been suggested by Shimosako and Takahashi (1999) and Goda and Takagi (2000), and has been used by numerous researchers at home and abroad. In Korea, Hong et al. (2003) expanded Shimosako and Takahashi (1999) model and computed the expected sliding distance of the solid-wall caisson breakwater considering the

variability of wave directions. While Shimosako and Takahashi (1999) had only considered the unidirectional irregular wave entering a harbor with normal incidence to an area with shore-parallel contours, Hong et al. (2003) had considered effects of shoaling, refraction and breaking of multi-directional irregular wave that are closer to actual situations. The reliability analysis shows that the variability of wave direction significantly affects the expected sliding distance of caissons and gives possibility of a cost-effective design. Kim et al. (2003) computed the expected sliding distance of the solid-wall caisson breakwater using the doubly-truncated normal distribution for the friction coefficient and wave force in order to overcome limitations of the normal distribution. Since the normal distribution of the horizontal wave force and friction coefficient may be distributed from negative infinity to positive infinity, there is a possibility to extract a design value that may not occur. To correct this, a doubly-truncated normal distribution using the upper and lower limits based on research results of Takayama and Ikeda (1992) that were closer to actual situations are used. Kim (2005) proposed to use time series of wave force based on Shimosako and Takahashi (1999) model and made computations of the expected sliding distance for the perforated-wall caisson breakwater. Kim et al. (2009) identified the limitations while evaluating the reliability with the expected sliding distance and came up with solutions to structural reliability evaluation by computing the exceedance rate of an allowable sliding distance. Suh et al. (2012) made a computation of expected sliding distance of the solid-wall caisson breakwater considering the climate change effect. They predicted increases in expected sliding distance of the

solid-wall caisson breakwater in the future due to sea level rise caused by climate change effect.

Computation of expected sliding distance has been studied by numerous researchers and Table 1. 1 demonstrates the summary. However, majority of researches were on the expected sliding distance of the solid-wall caisson breakwaters except Kim (2005). There is not much study available on the expected sliding distance of the perforated-wall caisson breakwaters until recently.

The reliability design method is being actively researched worldwide and Japan and other countries are already using the new design method. The clarified standards for domestic introduction are believed to be very important at this point. Thus, it is very critical to study the less researched perforated-wall caisson breakwaters and appropriate standards should be established.

Table 1. 1 Research trend of performance-based design of caisson breakwater

Year	Author	Contribution	Caisson type
1999	Shimosako and Takahashi	First proposal of performance-based design method	Solid wall
2000	Goda and Takagi	Improvement of the method proposed by Shimosako and Takahashi (1999)	Solid wall
2003	Hong et al.	Variability in wave direction	Solid wall
2003	Kim et al.	Doubly-truncated normal distribution	Solid wall
2005	Kim	Time series of perforated-wall caisson breakwater	Perforated wall
2009	Kim et al.	Exceedance rate of allowable sliding distance	Solid wall
2012	Suh et al.	Effect of climate change	Solid wall

1.3 Research details and methodology

This study mainly uses the performance-based design method among the probability design methods that is used in Japan. The performance-based design method uses a pre-determined acceptable expected damage to design a structure within that expected damage (Standards for the breakwater reliability design, 2011). Basic concept of the performance-based design method assumes that every load and resistance factors have different probability density functions, makes enough number of simulations in order to simulate the uncertainty of randomly fluctuating load and resistance factors and computes approximated probability of failure. It basically is the same concept as the Level III reliability design method with only difference in evaluation criteria of structural reliability which could be either a probability of failure or expected damage.

The performance-based design method of caisson breakwaters uses the expected sliding distance as the expected damage which requires wave data at the location of the breakwaters. The wave height may be the most important factor in computing the wave force of the structure in designing the caisson breakwaters and it plays a major role in determining the cross-section of the structure. To predict the structural reliability against the uncertainty of wave height in the performance-based design method, deepwater wave heights defined by the probability distribution function are used. Deepwater waves will be transformed into the waves at breakwater site by water depth, tidal level, wave direction and boundary conditions. The wave force acting on the caisson breakwater is computed using the transformed shallow water waves.

Total sliding distance during lifetime can be computed based on this and the expected sliding distance is computed with an average of the repeated simulations. But one limitation of this method is that an actual sliding distance may exceed the expected sliding distance since it is an average of simulated sliding distance within lifetime. In order to overcome this limitation, Kim et al. (2009) evaluated the stability by computing the exceedance rate for an allowable sliding distance.

The most dominant factor that affects the sliding of the caisson breakwaters is the wave force acting on the caisson. Caissons are typically either a solid-wall or perforated-wall shapes; former having solid frontal walls, latter perforated frontal walls. Sliding distance of the solid-wall caisson breakwater can be computed using the maximum wave force proposed by Goda (1974) with application of the wave force and time series model developed by Shimosako and Takahashi (1998 and 1999). However, it cannot be applied to the perforated-wall caisson breakwaters which have different maximum wave force and time series due to the wave dissipation at the perforated frontal wall. In general, the wave force acting on the perforated-wall caisson breakwaters is less than that of the solid-wall caisson breakwaters because of wave force reduction due to the wave dissipation at the perforated frontal wall. Takahashi et al. (1991) computed the wave force acting on the perforated-wall caisson breakwaters by expanding the Goda (1974) model and Kim (2005) computed the expected sliding distance by developing and applying the wave force and time series model of the perforated-wall caisson breakwaters using previous research results. In this

study, the expected sliding distance and exceedance rate is computed by applying the wave force time series model of the perforated-wall caisson breakwaters developed by Kim (2005) to the performance-based design method. This study is very important in providing information to the performance-based design of the perforated-wall caisson breakwaters in the future with its comparison analysis of the pros and cons of the existing deterministic design method and performance-based design method of the solid-wall caisson breakwaters.

CHAPTER 2 THEORITICAL BACKGROUND

2.1 Deterministic design method

In the deterministic design method, the caisson is considered to be safe against sliding if the safety factor does not exceed 1.2 (Goda, 2010).

$$S.F = \frac{\mu\left[\left(W' + P_V\right) - P_U\right]}{P_H} \tag{2.1}$$

The Eq. (2.1) represents a safety factor of a caisson sliding used in the deterministic design method, where μ is a friction coefficient between the caisson and rubble mound foundation, W' the caisson weight in water, P_U the uplift force, P_H the horizontal wave force acting on the caisson, and P_V is the wave force acting on the lower part of the wave chamber. In the deterministic design method, sliding of caisson will occur if the S.F. exceeds 1.2 and the caisson will be unstable.

S.F. of the caisson breakwater can be computed according to Fig 2. 1, and the stability can be determined by changing the structure dimension in comparison with allowed safety factor of 1.2.

In the perforated-wall caisson breakwaters, there is a phase difference between the forces acting on the perforated frontal wall and solid rear wall. To cope with this situation, Takahashi et al. (1991) had distinguished the phase by Crest I, Crest IIa and Crest IIb in terms of the acting states of wave force. In addition, there are wave chambers in the perforated-wall caisson breakwaters to dissipate the wave energy. Thus, the horizontal wave force,

wave force acting on the lower part of the wave chamber and the uplift force can be computed for different phases to determine different S.F's. The minimum S.F. will be used in the design. In the solid-wall caisson breakwater, S.F. is computed with the horizontal wave force and uplift force from the wave force formula of Goda (1975). Since there is no wave chamber in the solid-wall caisson breakwaters, the wave force acting on the lower part of the wave chamber should be 0 in Eq. (2.1).

2.2 Reliability design method

2.2.1 Overview of reliability design method

The reliability design method uses a pre-determined design standard Z and analyzes the relationship between structural load L and resistance R to validate the structural safety.

$$Z = R - L \tag{2.2}$$

where the structure is safe if $Z > 0$, there is sliding if $Z < 0$, and it is on safety boundary if $Z = 0$. Eq. (2.2) is an equation derived depending on the form of failure of the target structure and defined as a failure function, limit state function or safety margin.

In the existing deterministic design method, the structural safety was determined by the safety factor in consideration of representative $\overline{R}$ and $\overline{L}$ without considering the statistical characteristics of R and L: where there is a safety margin if $\overline{R} > \overline{L}$ to maintain a proper safety factor. However, the concept of the reliability design method takes into consideration the statistical properties of the design variables with changing characteristics of R and L, even if the same safety factor is maintained with consistent representative values.

Therefore, considering the probability of failure depending on the statistical characteristics of the design variables is a much better alternative than the safety factor method considering only the representative values of the design variables in evaluating the structural stability.

2.2.2 Level III reliability design method

The reliability design method is classified as Level I, II and III depending on the degree of probabilistic concepts. Level III reliability design method directly assigns the randomly generated probabilistic variables that follow certain distribution functions into the limit state function by considering every design variables as probabilistic variables. Level III reliability design method mostly used the Monte-Carlo Simulation (MCS) which is one of the most common ways to estimate the probability of failure. In the MCS, uniformly distributed random number between 0 and 1 is extracted and changed to a random number that best reflects the distribution characteristic of the probability variables, to generate samples of sufficient size. Generated probabilistic variables will be assigned into the limit state function to determine the structural safety. The probability of failure for $Z \le 0$ in the limit state function of Eq. (2.2) is expressed as the following.

$$P_f = P\left(Z \le 0\right) = \lim_{x \to \infty} \frac{n}{N} \tag{2.3}$$

where, N is the number of total simulations, and n is the number of simulations for $Z \le 0$ in the limit state function. The accuracy of the probability of failure estimated by Eq. (2.3) depends on the number of simulations. n / N is a statistical variable of the extracted distribution and is dependent on the number of simulations N, especially for a variance. In case of small N or a low probability of failure, the probability of failure given by n / N has considerable uncertainty. Thus, the number of total simulations N

has to be determined depending on the probability of failure.

2.2.3 Performance-based design method

The performance-based design method designs a structure such that the expected failure is within a pre-determined allowable expected failure by assuming that a structure will maintain its function within the pre-determined allowable expected failure. The performance-based design method has basically the same concept as the Level III reliability design method. In other words, the breakwater is designed to maintain its function during its lifetime without any problems. But the two methods have a slightly different interpretation. Level III reliability design method computes the probability of failure of the load that might exceed the resistance considering the uncertainty of randomly changing load and resistance factors with an assumption that all load and resistance factors have different probability density functions. On the other hand, the performance-based design method predicts the sliding distance kinetically per each wave conditions to keep the expected values of the sliding distance below the allowable value (Standards for the breakwater reliability design, 2011).

In the performance-based design method, the sliding distance of the caisson is considered as the criterion of the structural functionality so that the expected sliding distance during the lifetime of the structure is calculated to determine the stability of the caisson breakwater. However, the expected sliding distance of the caisson breakwater possesses a limitation to be an

evaluation standard of the stability of the caisson. Since the expected sliding distance is an average of a number of simulations, sometimes the actual sliding distance can exceed the average. In order to overcome such shortcoming, Kim et al. (2009) identified the limitations that might occur in evaluating the stability with the expected sliding distance and computed the exceedance rate for an allowable sliding distance and evaluated the structural stability.

The expected sliding distance and the exceedance rate of the caisson breakwaters can be computed following the procedure in Fig 2. 2 and the structural reliability can be determined by comparing with the allowable values.

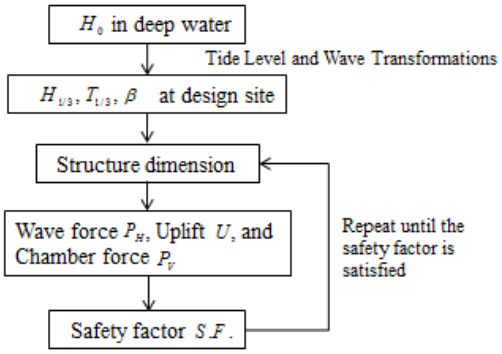

Fig 2. 1 Schematic flow chart for computation of safety factor

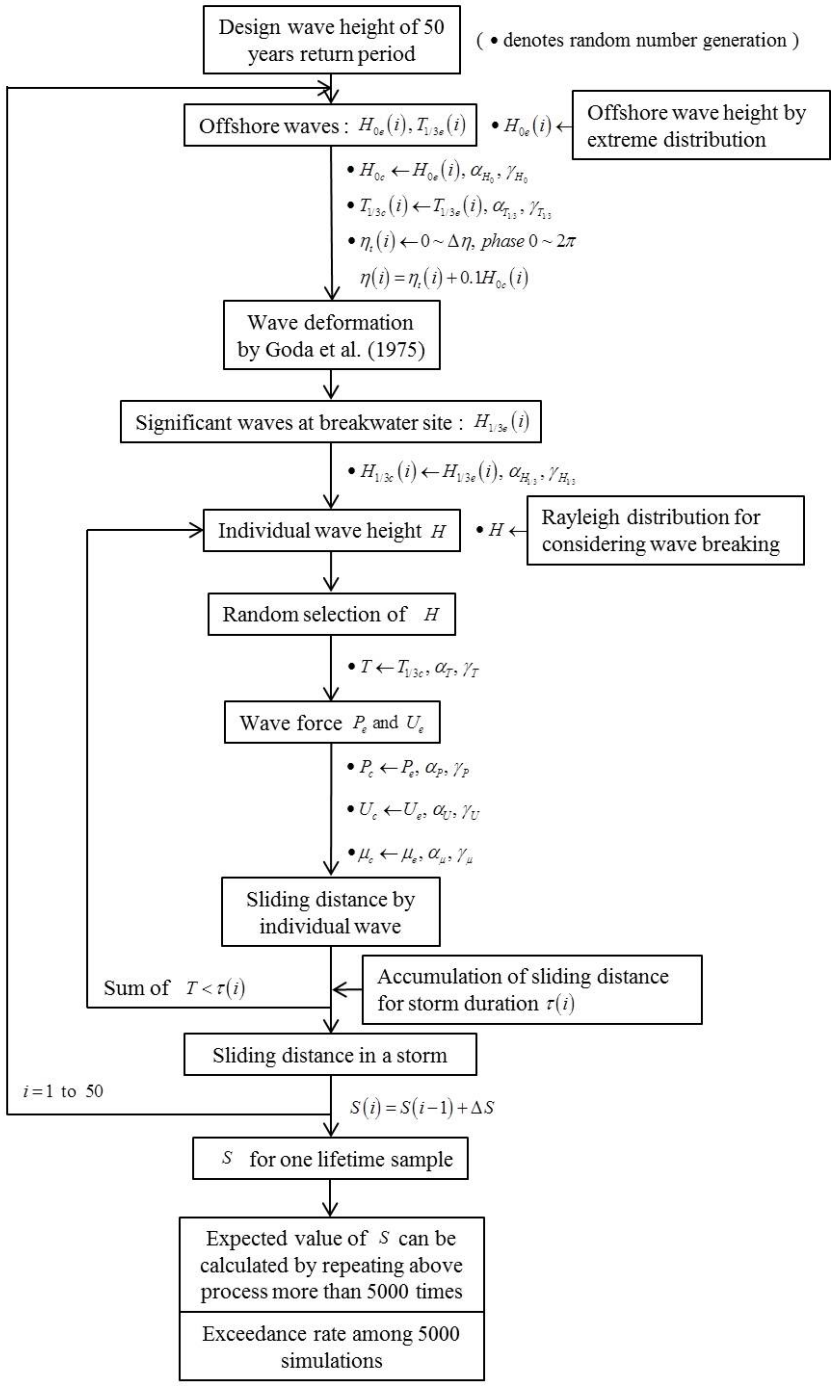

Fig 2. 2 Schematic flow chart for computation of expected sliding distance and exceedance rate given by Hong et al. (2004)

CHAPTER 3 DESIGN VARIABLES

3.1 Deepwater wave

In general, failures of the caisson breakwaters are caused by high waves corresponding to the design waves. Thus, it should be allowed to use the annual maximum deepwater wave in the computation. Deepwater wave height used in the performance-based design method is generally determined by the extreme wave height distribution from the wave data of a long-term observation or hindcasts.

$$F_{Weibull}(X) = 1 - \left[\exp\left(-\left(\frac{X - \xi}{\alpha} \right) \right)^{\kappa} \right] \tag{3.1}$$

The weibull distribution for deepwater wave height given by Eq. (3.1) is used in this study, where X is an annual maximum deepwater wave height and, α, ξ and κ are scale, location and shape parameter, respectively. The probabilistic wave is the 50-year lifetime used by Kim (2005) of 6.5m significant wave height whose scale, location and shape parameters are 2.005, 1.595 and 1.525, respectively. H_{0e} is a randomly extracted annual maximum significant wave height from extreme distribution of given deepwater wave height. Since these wave heights have uncertainty due to finite characteristic of parameter of extreme wave data or inaccuracy of the hindcasts data, probabilistic changes of the normal distribution which has an average μ_{H_0} and a standard deviation σ_{H_0} proposed by Takayama and Ikeda (1992) have

to be considered.

$$\mu_{H_0} = \left(1+\alpha_{H_0}\right) H_{0e}, \quad \sigma_{H_0} = \gamma_{H_0} H_{0e} \tag{3.2}$$

where α_{H_0} and γ_{H_0} are bias coefficient and coefficient of variation, respectively. Shimosako and Takahashi (1999) have suggested 0.0 and 0.1 for the bias coefficient and coefficient of variation of the deepwater wave height. As a result, the normal distribution of Eq. (3.2) determines the deepwater wave height H_{0c} to be used in the computation of wave force. Fig 3. 1 demonstrates an example of 50-year deepwater wave height generated using the parameters of the distribution function.

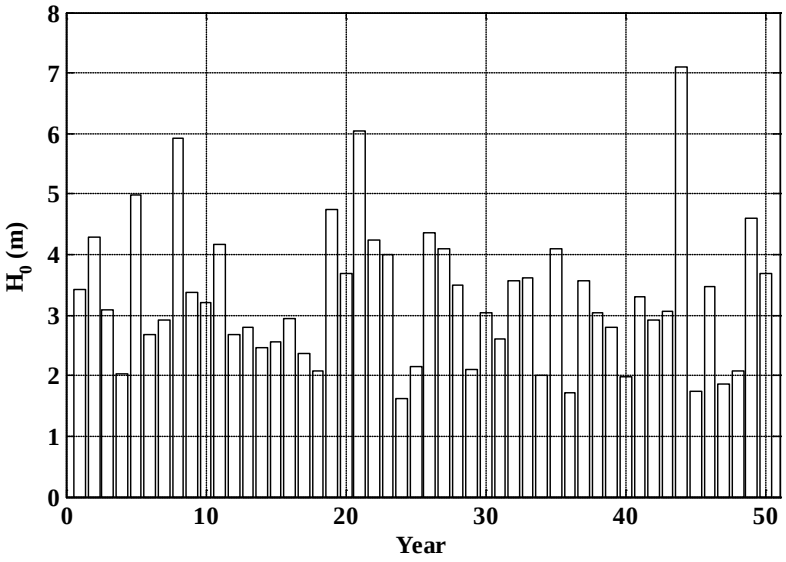

Fig 3. 1 Sample of offshore wave height for one lifetime of structure

3.2 Significant wave period

Goda (2003) and Wilson (1965) analyzed the significant wave height and significant wave period of fully developed wind wave with varied wind speed under an assumption that their equation used long enough fetch length, to come up with the following equation to express the relation between significant wave height and significant wave period.

$$T_{1/3} \cong 3.3 H_{1/3}{}^{0.63} \tag{3.3}$$

Shore Protection Manual (1977) published by Coastal Engineering Research Center of U.S. proposed the following equation to express the relation between significant wave height and significant wave period.

$$T_{1/3} \cong 3.85 H_{1/3}{}^{0.5} \tag{3.4}$$

On the other hand, Suh at al. (2010) used data and hindcasts observed in Korean coast and an actual long-term observation data of Japan to analyze; Eq. (3.3) of Goda (2003) and Eq. (3.4) of U.S. Army (Shore Protection Manual, 1977) were averaged into Eq. (3.5); both are used to express the relationship between the significant wave height and significant wave period for a high wave that close to the designed wave.

$$T_{1/3e} = \frac{1}{2}\left(3.3 H_{1/3}{}^{0.63} + 3.85 H_{1/3}{}^{0.5}\right) \tag{3.5}$$

The sample significant wave period $T_{1/3c}$ is determined by assigning the

probabilistic change of normal distribution with the average $\mu_{T_{1/3}}$ and standard deviation $\sigma_{T_{1/3}}$, i.e.

$$\mu_{T_{1/3}} = (1+\alpha_T)T_{1/3e}, \quad \sigma_{T_{1/3}} = \gamma_T T_{1/3e} \tag{3.6}$$

where α_T and γ_T are bias coefficient and coefficient of variation of the wave period, respectively. Fig 3. 2 demonstrates a sample significant wave period generated with a probabilistic change of the normal distribution showing relationship between the significant wave height and significant wave period in Eq. (3.5) whose bias coefficient and coefficient of variation are 0.0 and 0.1, respectively.

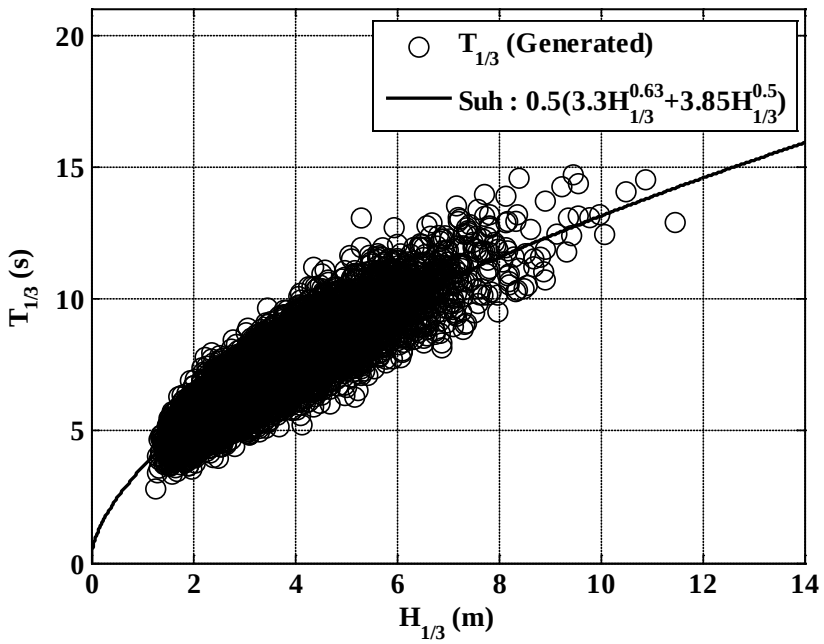

Fig 3. 2 Relation between significant wave height and significant wave period

3.3 Significant wave height at breakwater site

The wave height at the location of the breakwater is computed using a wave transformation model which considered wave breaking effect. To overcome the long computation time in the performance-based design method due to large number of simulations, a simplified equation proposed by Goda (1975) is used. As in Shimosako and Takahashi (1999), irregular waves propagating to the coast with parallel contours are used. Tidal levels were assumed to possess a sinusoidal wave type change between low water level (LWL) and high water level (HWL). Thus, a random number uniformly distributed between 0 and 2π is extracted as the phase of the sinusoidal curve and a sample tidal level with respect to the mean sea level η is determined.

3.3.1 Directional spreading function

The directional spreading function indicates how the wave energy is distributed around the principal wave direction when the wave propagates to the coast. Mitsuyasu et al. (1977) suggested the directional spreading function as shown in Eq. (3.7) based on the observation data of the clover-leaf buoy. It is called the Mitsuyasu-type directional spreading function.

$$G(\theta \mid f) = G_0 \cos^{2s}\left(\frac{\theta - \theta_0}{2}\right) \tag{3.7}$$

where f is frequency of the wave, θ the direction of the wave, θ_0 the

principal wave direction, and s the parameter indicating the directional spreading of the energy which is also called a directional spreading parameter. The larger the directional spreading parameter, more wave energy concentrated near the principal wave direction. If wave direction is spread from $-\pi$ to π in reference to the principal wave $(\theta = 0°)$, G_0 is defined as follows:

$$G_0 = \frac{1}{\pi} 2^{2s-1} \frac{\Gamma^2(s+1)}{\Gamma(2s+1)} \tag{3.8}$$

where Γ is a Gamma function. Goda and Suzuki (1975) proposed the following directional spreading parameter.

$$s = \begin{cases} (f / f_p)^5 s_{\max} & : f \le f_p \\ (f / f_p)^{-2.5} s_{\max} & : f > f_p \end{cases} \tag{3.9}$$

where f_p is a peak frequency which has a relationship of $f_p = 1/(1.05T_{1/3})$ with the significant wave period for the Bretschneider-Mitsuyasu spectrum. $s_{\max}$ is a peak value at $f = f_p$. $s_{\max}$ uses the following values in engineering terms.

$$s_{\max} = \begin{cases} 10 & \text{for wind waves} \\ 25 & \text{for swell with short decay distance} \\ 75 & \text{for swell with long decay distance} \end{cases} \tag{3.10}$$

3.3.2 Frequency spectrum

The frequency spectrum of wave indicates how the wave energy is distributed for each frequency. Directional spectrum considering the directional spreading function is as follows:

$$S(f,\theta) = S(f)G(\theta \mid f) \tag{3.11}$$

where $S(f)$ is the frequency spectrum. Various frequency spectra have been proposed. Eqs. (3.12), (3.13), (3.14) and (3.15) are Bretschneider-Mitsuyasu spectrum, Modified Bretschneider-Mitsuyasu spectrum modified by Goda, JONSWAP (Joint North Sea Wave Project) spectrum, and TMA spectrum, respectively.

$$S_{BM}(f) = 0.257 H_{1/3}{}^2 T_{1/3}{}^{-4} f^{-5} \exp\left[-1.03\left(T_{1/3} f\right)^{-4}\right] \tag{3.12}$$

$$S_{MBM}(f) = 0.205 H_{1/3}{}^2 T_{1/3}{}^{-4} f^{-5} \exp\left[-0.75\left(T_{1/3} f\right)^{-4}\right] \tag{3.13}$$

$$S_J(f) = \beta_J H_{1/3}{}^2 T_p{}^{-4} f^{-5} \exp\left[-1.25\left(T_p f\right)^{-4}\right] \gamma^{\exp\left[-\left(T_p f - 1\right)^2 / 2\sigma^2\right]} \tag{3.14}$$

$$S_{TMA}(f) = S_J(f) \cdot \phi(kh) \;:\; \phi(kh) = \frac{\tanh^2 kh}{1 + 2kh / \sinh 2kh} \tag{3.15}$$

The Bretschneider-Mitsuyasu spectrum is a spectrum for fully developed wind waves, which was modified by Goda to come up with the Modified Bretschneider-Mitsuyasu spectrum. The JONSWAP spectrum is a spectrum for developing wind waves in a fetch-limited state. The TMA spectrum is an

expanded version of the JONSWAP spectrum which expressed wave height changes by the depth-limited breaking in $\phi(kh)$ format in terms of the relative depth (kh). Variables in Eq. (3.14) are as follows:

$$\beta_J = \frac{0.0624}{0.230 + 0.0336\gamma - 0.185(1.9+\gamma)^{-1}}\left[1.094 - 0.01915\ln\gamma\right] \tag{3.16}$$

$$T_p \cong T_{1/3} / \left[1 - 0.132(\gamma + 0.2)^{-0.559}\right] \tag{3.17}$$

$$\sigma = \begin{cases} \sigma_a \ : \ f \le f_p \\ \sigma_b \ : \ f \ge f_p \end{cases} \tag{3.18}$$

$$\gamma = 1 \sim 7(\text{mean of } 3.3), \ \sigma_a \cong 0.07, \ \sigma_b \cong 0.09 \tag{3.19}$$

3.3.3 Wave transformation

Goda (1975) proposed the following equations to compute the wave transformation on the coast including the surf zone.

$$H_s = \begin{cases} K_s H_0' & : h / L_0 \ge 0.2 \\ \min\left\{(\beta_0 H_0' + \beta_1 h),\ \beta_{\max} H_0',\ K_s H_0'\right\} & : h / L_0 < 0.2 \end{cases} \tag{3.20}$$

$$H_{\max} = \begin{cases} 1.8 K_s H_0' & : h / L_0 \ge 0.2 \\ \min\left\{(\beta_0^* H_0' + \beta_1^* h),\ \beta_{\max}^* H_0',\ 1.8 K_s H_0'\right\} & : h / L_0 < 0.2 \end{cases} \tag{3.21}$$

where H_s is a significant wave height at the location of the breakwater, $H_{\max}$ the maximum wave height, H_0' an equivalent deepwater wave height

corresponding to the significant wave height, K_s the shoaling coefficient, h water depth and L_0 is the deepwater wave length. β_0, β_1, $\beta_{\max}$, β_0^*, β_1^*, and $\beta_{\max}^*$ are the coefficients depending on deepwater wave steepness and bottom slope, which are expressed as follows:

$$\beta_0 = 0.028\left(H_0'/L_0\right)^{-0.38}\exp\left[20\tan^{1.5}\theta\right] \tag{3.22}$$

$$\beta_1 = 0.52\exp\left[4.2\tan\theta\right] \tag{3.23}$$

$$\beta_{\max} = \max\left\{0.92, 0.32\left(H_0'/L_0\right)^{-0.29}\times\exp\left[2.4\tan\theta\right]\right\} \tag{3.24}$$

$$\beta_0^* = 0.052\left(H_0'/L_0\right)^{-0.38}\exp\left[20\tan^{1.5}\theta\right] \tag{3.25}$$

$$\beta_1^* = 0.63\exp\left[3.8\tan\theta\right] \tag{3.26}$$

$$\beta_{\max} = \max\left\{1.65, 0.53\left(H_0'/L_0\right)^{-0.29}\times\exp\left[2.4\tan\theta\right]\right\} \tag{3.27}$$

where $\tan\theta$ is the bottom slope. To compute the equivalent deepwater wave height H_0', a computation of the refraction coefficient has to be preceded. Refraction coefficient computations of irregular wave are as follows:

$$\left(K_r\right)_{eff} = \left(\frac{m_0}{m_{s0}}\right)^{1/2} \tag{3.28}$$

$$m_0 = \int_0^\infty S(f)\,df = \int_0^\infty\int_{\theta_{\min}}^{\theta_{\max}} S_0(f,\theta_0)K_s^{\,2}(f,h)K_r^{\,2}(f,h,\theta_0)\,d\theta_0\,df \tag{3.29}$$

$$m_{s0} = \int_0^{\infty} \int_{\theta_{\min}}^{\theta_{\max}} S_0(f,\theta_0) K_s^{\,2}(f,h)\, d\theta_0 df \tag{3.30}$$

where m_0 is the zeroth moment considering both shoaling coefficient and refraction coefficient, and m_{s0} is the zeroth moment considering only the shoaling coefficient. From the ratio of the two zeroth moments, the effective refraction coefficient $(K_r)_{eff}$ is determined. $K_s(f,h)$ is a linear shoaling coefficient for the regular wave, f is a frequency, θ_0 is a wave direction of the deepwater wave, and h is water depth.

Goda (1975) used a non-linear shoaling coefficient in his equation which was proposed by Iwagaki et al. (1981).

$$K_s = K_{si} + 0.0015\left(\frac{h}{L_0}\right)^{-2.87}\left(\frac{H_0'}{L_0}\right)^{1.27} \tag{3.31}$$

where K_s, K_{si} are non-linear and linear shoaling coefficients, respectively. Fig 3. 3 shows the refraction coefficient derived by the Modified BM spectrum and directional spreading function. As the principal direction increases, the refraction coefficient tends to decrease. The refraction coefficient is the greatest when the wave normally propagates to the coast. The breaking wave height can be computed using the equation for breaking wave height in shallow water region proposed by Goda (1974).

$$\frac{H_b}{L_0} = A\left\{1 - \exp\left[-1.5\frac{\pi h}{L_0}\left(1 + 15\tan^{4/3}\theta\right)\right]\right\} \tag{3.32}$$

A is 0.18 and 0.12, respectively, for the upper and lower limits of the breaking wave height. This study used 0.18 to satisfy the condition that the individual wave height cannot be greater than the upper limit of the breaking wave height. Fig 3. 4 and Fig 3. 5 represent the wave height with respect to water depth using Eqs. (3.20), (3.21) and (3.32) with bottom slope of 1/50 and 1/20. It is found that a surf zone forms at 14m when the bottom slope is 1/50, and at 12m when the bottom slope is 1/20.

The wave height $H_{1/3e}$ at the location of the breakwater is assumed to have a computational uncertainty, and the probabilistic change is given according to the normal distribution with an average μ_{H_s} and a standard deviation σ_{H_s}.

$$\mu_{H_{1/3}} = \left(1+\alpha_{H_{1/3}}\right) H_{1/3e}, \quad \sigma_{H_{1/3}} = \gamma_{H_{1/3}} H_{1/3e} \tag{3.33}$$

where $\alpha_{H_{1/3}}$ and $\gamma_{H_{1/3}}$ are the bias coefficient and coefficient of variation, respectively. Shimosako and Takahashi (1999) proposed 0.0 and 0.1 for the bias coefficient and coefficient of variation of the significant wave height, respectively. A normal distribution of Eq. (3.33) determines the sample significant wave height $H_{1/3c}$ to be used in the computation. Fig 3. 6 demonstrates an example of the significant wave height at the location of the breakwater generated in 50-year lifetime.

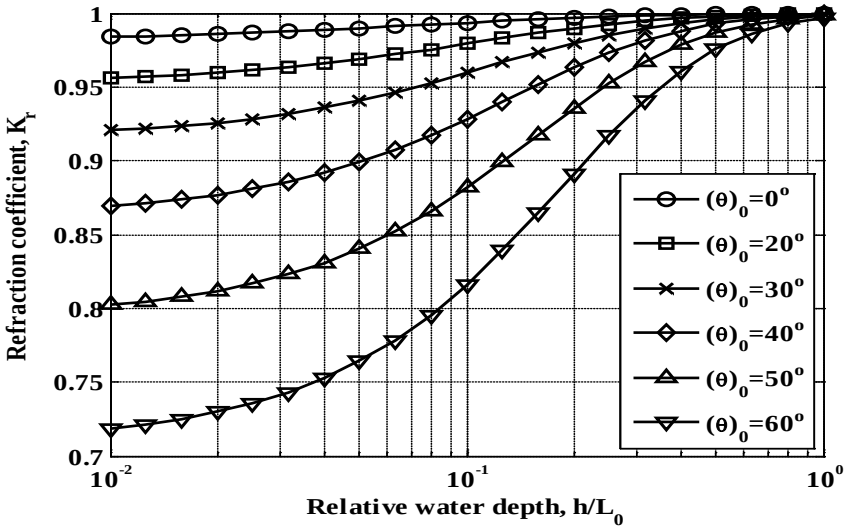

Fig 3. 3 Refraction coefficient of random sea waves with $s_{max} = 25$ on a coast with straight and parallel depth-contours

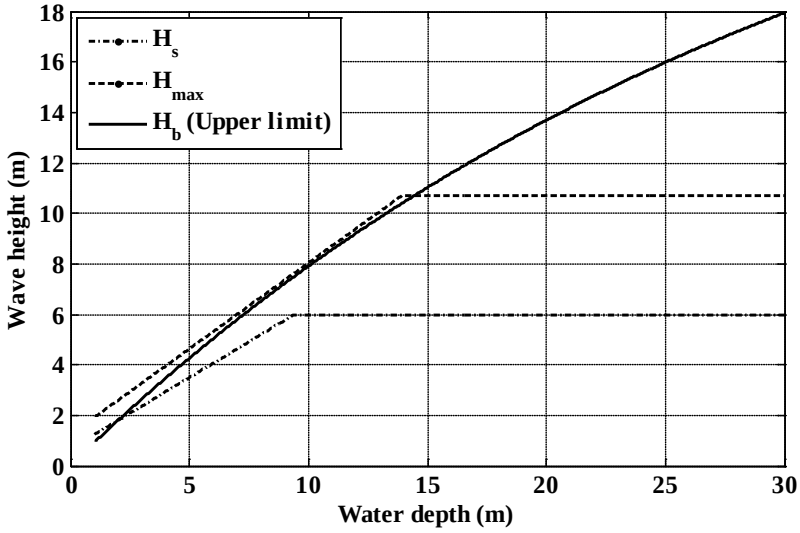

Fig 3. 4 Wave heights in different water depths on a coast with bottom slope of 1/50

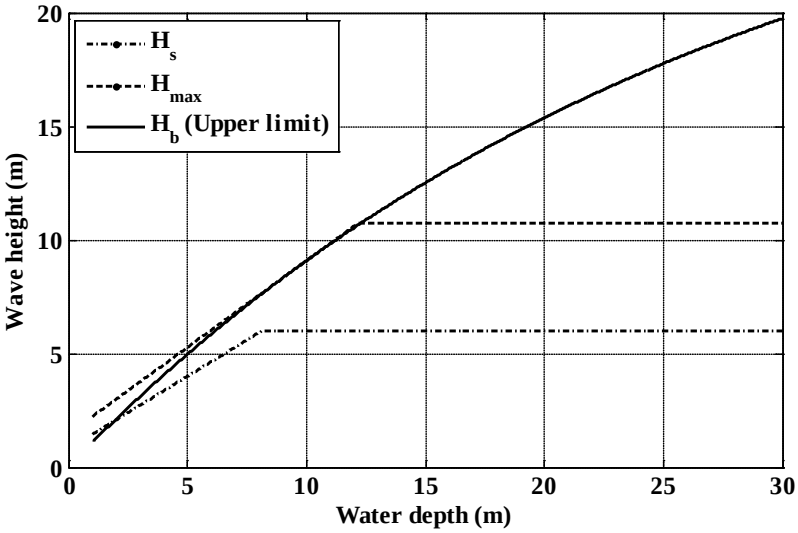

Fig 3. 5 Wave heights in different water depths on a coast with bottom slope of 1/20

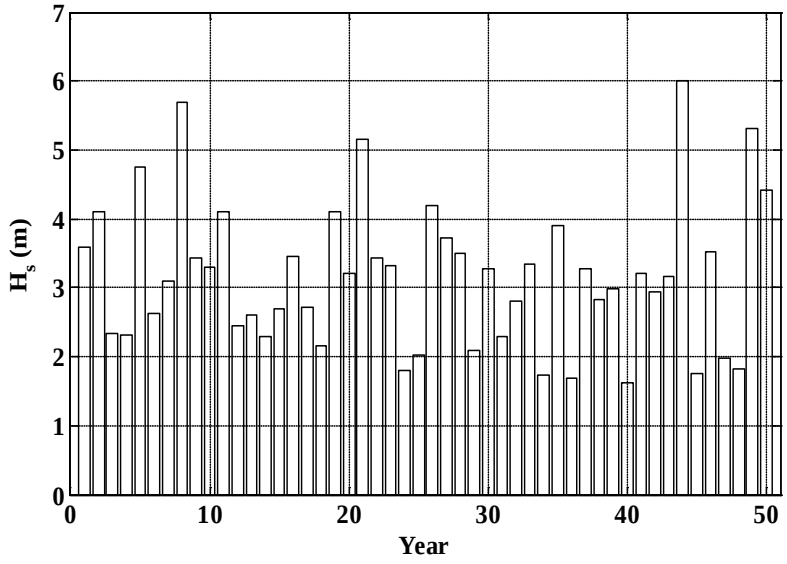

Fig 3. 6 Sample of design wave height at the breakwater for one lifetime of structure

3.4 Individual wave

After the significant wave height at the location of the breakwater is computed, the individual wave during a storm can be extracted by the Rayleigh distribution.

$$P_{Rayleigh}\left(H\right)=e^{-\left(H/H_{rms}\right)^2} \tag{3.34}$$

$$H_{rms}=\frac{H_s}{1.416} \tag{3.35}$$

If the extracted individual wave height is greater than the breaking wave height computed by Eq. (3.32), then the breaking wave height should be used instead of the extracted individual wave height.

In the case of the individual wave period, the wave period T to be used in the computation is determined by giving the probabilistic change of the normal distribution in a same manner as in the significant wave period.

$$\mu_T=\left(1+\alpha_{T_{1/3}}\right)T_{1/3c},\quad \sigma_T=\gamma_{T_{1/3}}T_{1/3c} \tag{3.36}$$

where $\alpha_{T_{1/3}}$ and $\gamma_{T_{1/3}}$ are bias coefficient and coefficient of variation, respectively. Their values use the same values for the significant wave period. Fig 3. 7 shows the occurrence frequency of the individual wave height when the significant wave height is 6.28m. The Rayleigh distribution is also presented in the same figure.

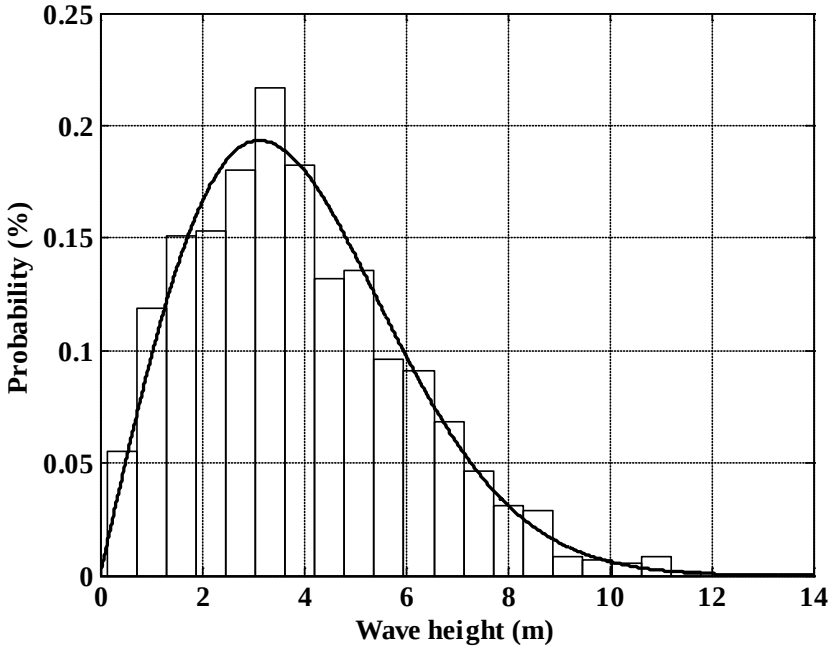

Fig 3. 7 Frequency of individual wave heights in a storm event of significant wave height of 6.28 m

3.5 Calculation of wave force acting on solid-wall caisson breakwater

For the computation of the wave force acting on the solid-wall caisson breakwater, the Goda (1974) formula expanded by Takahashi et al. (1991) and Takahashi and Tanimoto (1994) is used. This equation assumes that the wave pressure is distributed in a trapezoidal shape on the front of the caisson wall as illustrated in Fig 3. 8.

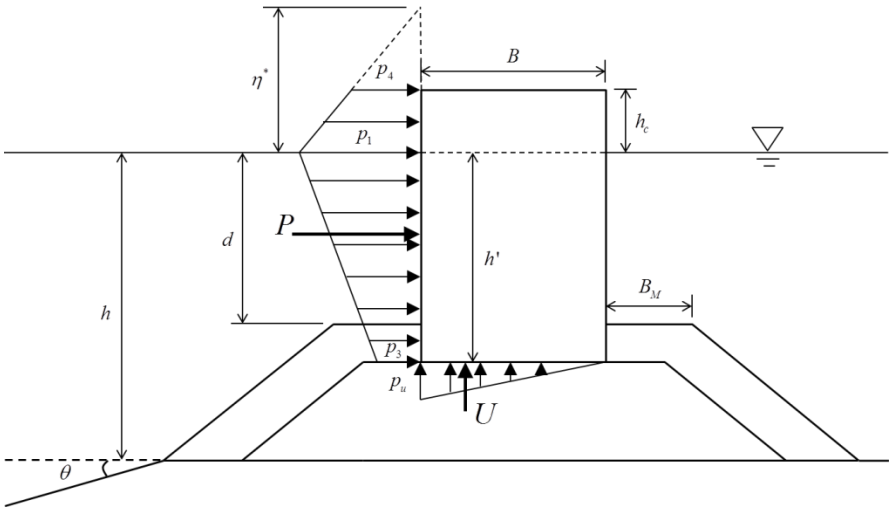

Fig 3. 8 Pressure distribution for solid-wall caisson breakwater

However, it is not much different from the Goda (1974) formula since the correction coefficients λ_1, λ_2, and λ_3 for a typical solid-wall caisson breakwater are 1. The wave force computation by Goda (1974) is as follows:

$$P = \frac{1}{2}\left(p_1 + p_3\right)h' + \frac{1}{2}\left(p_1 + p_4\right)h_c^* \tag{3.37}$$

$$U = \frac{1}{2}p_u B \tag{3.38}$$

where P is a horizontal wave force and U is an uplift force, with each terms in Eqs. (3.37) and (3.38) are computed as follows:

$$p_1 = \frac{1}{2}\left(1+\cos\beta\right)\left(\alpha_1\lambda_1 + \alpha_2\lambda_2\cos^2\beta\right)w_0 H_{\max} \tag{3.39}$$

$$p_2 = \frac{p_1}{\cosh\left(2\pi h / L\right)} \tag{3.40}$$

$$p_3 = \alpha_3 p_1 \tag{3.41}$$

$$p_4 = \alpha_4 p_1 \tag{3.42}$$

$$p_u = \frac{1}{2}\left(1+\cos\beta\right)\alpha_1\alpha_3\lambda_3 w_0 H_{\max} \tag{3.43}$$

$$h_c^* = \min\left\{\eta^*, h_c\right\} \tag{3.44}$$

$$\eta^* = 0.75\left(1+\lambda_1\cos\beta\right)H_{\max} \tag{3.45}$$

where β is an angle between the direction of wave approach and a line normal to the breakwater. w_0 is the unit weight of sea water, $H_{\max}$ is the maximum wave height at the location of the breakwater, h is a depth in front of the breakwater, h_c is the crest elevation of upright section, and η^* is a run-up parameter. Coefficients of Eqs. (3.39) to (3.45) are computed as follows:

$$\alpha_1 = 0.6 + \frac{1}{2}\left[\frac{4\pi h / L}{\sinh\left(4\pi h / L\right)}\right]^2 \tag{3.46}$$

$$\alpha_2 = \min\left\{\frac{h_b - d}{3h_b}\left(\frac{H_{\max}}{d}\right)^2, \frac{2d}{H_{\max}}\right\} \tag{3.47}$$

$$\alpha_3 = 1 - \frac{h'}{h}\left[1 - \frac{1}{\cosh(2\pi h / L)}\right] \tag{3.48}$$

$$\alpha_4 = 1 - \frac{h_c^*}{\eta^*} \tag{3.49}$$

where α_1, α_2, α_3, and α_4 are the correction factors of wave pressure, and h_b is the water depth at $5H_{1/3}$ away from the breakwater. α_2 is a coefficient to consider the effect of the rubble mound. Since this coefficient is not sufficient to express the impulsive wave pressure, Takahashi and Shimosako (1994) had introduced a correction coefficient of impulsive wave α_I for the cases that impulsive wave breaking occurs easily such as relatively high and wide mound or very steep bottom slope. A relation between α_2 and α_I are as follows:

$$\delta_{11} = 0.93\left(\frac{B_M}{L} - 0.12\right) + 0.36\left(0.4 - \frac{d}{h}\right) \tag{3.50}$$

$$\delta_{22} = -0.36\left(\frac{B_M}{L} - 0.12\right) + 0.93\left(0.4 - \frac{d}{h}\right) \tag{3.51}$$

$$\delta_1 = \begin{cases} 20\delta_{11} & \text{when } \delta_{11} \le 0 \\ 15\delta_{11} & \text{when } \delta_{11} > 0 \end{cases} \tag{3.52}$$

$$\delta_2 = \begin{cases} 4.9\delta_{22} & \text{when } \delta_{22} \le 0 \\ 3.0\delta_{22} & \text{when } \delta_{22} > 0 \end{cases} \tag{3.53}$$

$$\alpha_{IH} = \min\left\{H_{\max} / d,\ 2.0\right\} \tag{3.54}$$

$$\alpha_{IB} = \begin{cases} \cos\delta_2 / \cosh\delta_1 & \text{when } \delta_2 \le 0 \\ 1/\left(\cosh\delta_1 \cosh^{1/2}\delta_2\right) & \text{when } \delta_2 > 0 \end{cases} \tag{3.55}$$

$$\alpha_I = \alpha_{IH}\alpha_{IB} \tag{3.56}$$

$$\alpha^* = \max\left\{\alpha_2,\ \alpha_I\right\} \tag{3.57}$$

To consider the effect of the impulsive wave pressure in the existing wave force equation, α^* is used in place of α_2 through the above computation processes.

3.6 Calculation of wave force acting on perforated-wall caisson breakwater

Takahashi et al. (1991) had performed hydraulic experiments under various conditions to come up with a computation of wave force acting on the perforated-wall caisson breakwaters. He had classified waves into Crest I, Crest IIa, and Crest IIb as shown in Fig 3. 9. Crest I occurs at the moment when the wave makes a first contact with the front of the perforated wall; horizontal wave pressure acts on both perforated wall and solid-wall on the front face of the caisson and the uplift force acts on the bottom of the caisson. Crest IIa occurs at the moment when the wave passes through the perforated front wall and makes a contact with the solid-wall at the rear; horizontal wave pressure acts not only on the front wall but also on the rear wall and wave pressure increases at the bottom of the wave chamber due to raised water level. Crest IIb occurs at the moment when the previous Crest IIa becomes the standing waves. The computation of the wave force is the same as that for the solid-wall caisson breakwater by Takahashi et al. (1991) and Takahashi and Tanimoto (1994). Correction coefficients $\lambda_1, \lambda_2,$ and λ_3, however, should be applied according to the phase of wave pressure as shown in Table 3.1 by Takahashi et al. (1991); where B' is the width of the wave chamber plus a thickness of the front wall, and L' is the wave length at a depth d' within the wave chamber. When calculating the correction coefficient of the impulsive wave α^* for the rear wall which is required in computing the correction coefficient of λ_{R2} for Crest IIa, the water depth within the wave

chamber d', wave length within the wave chamber L', and $B'-(d-d')$ should be used in place of the water depth d, wave length L, and B_M. Fig 3. 10, Fig 3. 11, and Fig 3. 12 demonstrate the wave pressure distribution and example of applied correction coefficients of Crest I, Crest IIa and Crest IIb, respectively. It is assumed that the wave pressure is distributed in a trapezoidal shape along the front and rear wall of the wave chamber and the pressure at the bottom of the wave chamber is assumed to be hydrostatic. Computations of the front-wall wave pressure for the perforated and solid parts are done separately using an interpolation, and the same for the computation for the wave pressure at the rear wall. The pressure acting on the bottom of the wave chamber is computed with the correction coefficient λ_M, the same as the computation for the pressure acting on the rear wall. Since the perforated-wall caisson breakwater has a wave absorbing structure, unlike the solid-wall caisson breakwater, it effectively decreases the maximum wave force. Thus the wave force decrease according to the porosity of the front wall is as follows, when the wave force is computed.

$$\varepsilon = \frac{\ell \times h \times N}{L \times H} \tag{3.58}$$

$$\varepsilon' = 1 - \varepsilon \tag{3.59}$$

where ε and ε' are the porosity and dissipation rate of the wave force, respectively, and ℓ, h, N, L and H are the width, height and the number of the slit, the length of a caisson (in a parallel direction with the

breakwater) and the height from crest to bottom of the slit, respectively. The correction coefficient of the wave force computed above is only applied to the perforated part of the front wall.

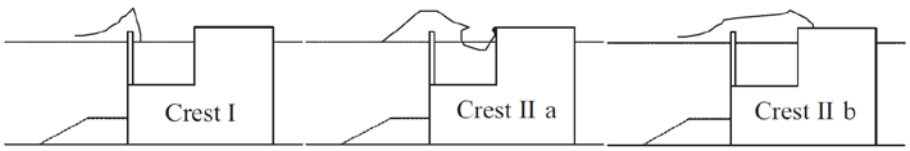

Fig 3. 9 Phase difference for wave action on a perforated caisson defined by Takahashi et al. (1991)

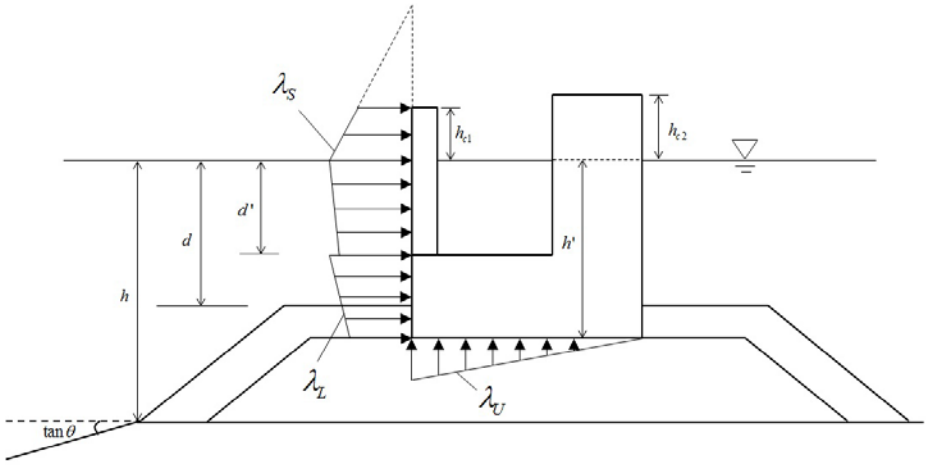

Fig 3. 10 Pressure distributions on a perforated caisson at Crest I given by Takahashi et al. (1991)

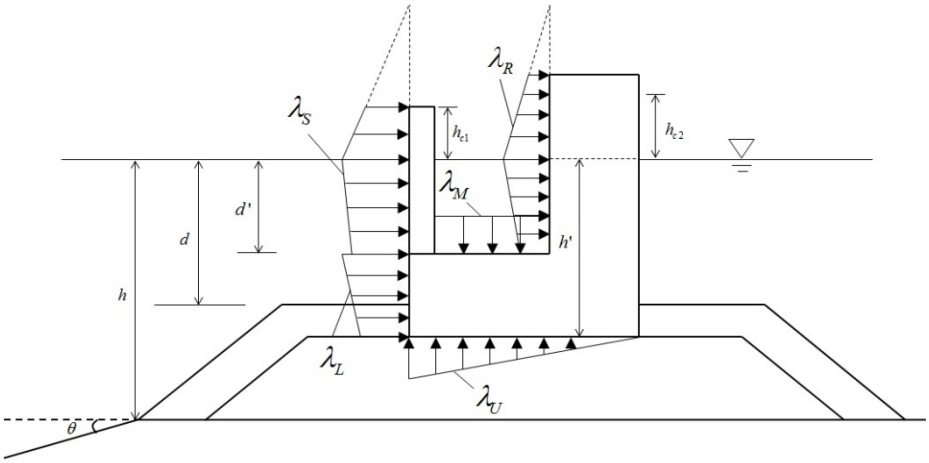

Fig 3. 11 Pressure distributions on a perforated caisson at Crest IIa given by Takahashi et al. (1991)

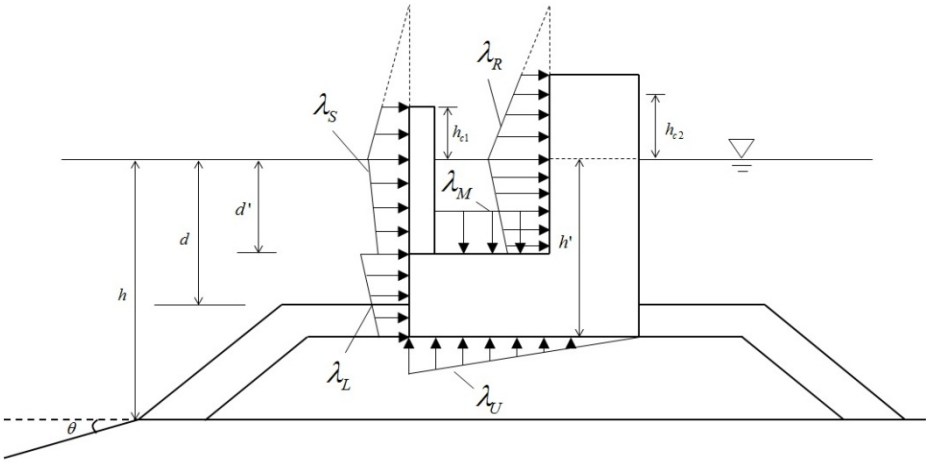

Fig 3. 12 Pressure distributions on a perforated caisson at Crest IIb given by Takahashi et al. (1991)

Table 3.1 Correction coefficients for perforated caissons given by Takahashi et al. (1991)

		Crest I	Crest IIa	Crest IIb
Perforated part of the front wall	λ_{S1}	0.85	0.7	0.3
	λ_{S2}	$0.4 \quad (\alpha^* \le 0.75)$ $0.3/\alpha^* \quad (\alpha^* > 0.75)$	0.0	0.0
Solid part of the front wall	λ_{L1}	1.0	0.75	0.65
	λ_{L2}	$0.4 \quad (\alpha^* \le 0.75)$ $0.2/\alpha^* \quad (\alpha^* > 0.75)$	0.0	0.0
Wave chamber rear wall	λ_{R1}	0.0	$20B'/3L' \quad (B'/L' \le 0.15)$ $1.0 \quad (B'/L' > 0.15)$	$1.4 \quad (H_d/d \le 0.1)$ $1.6-2H_d/d \quad (0.1 < H_d/d < 0.3)$ $1.0 \quad (H_d/d \ge 0.3)$
	λ_{R2}	0.0	$0.56 \quad (\alpha^* \le 25/28)$ $0.5/\alpha^* \quad (\alpha^* > 25/28)$	0.0
Wave chamber bottom slab	λ_{M1}	0.0	$20B'/3L' \quad (B'/L' \le 0.15)$ $1.0 \quad (B'/L' > 0.15)$	$1.4 \quad (H_d/d \le 0.1)$ $1.6-2H_d/d \quad (0.1 < H_d/d < 0.3)$ $1.0 \quad (H_d/d \ge 0.3)$
	λ_{M2}	0.0	0.0	0.0
Uplift	λ_{U3}	1.0	0.75	0.65

3.7 Doubly-truncated normal distribution

The stochastic variability of most design variables can be expressed in a normal distribution. Since the design variables are randomly extracted from negative infinity to positive infinity, some extracted variable may not be realistic. In order to overcome such shortcoming, Kim et al. (2003) used a doubly-truncated normal distribution, using the upper limit x_1 and lower limit x_2 for the wave force and friction coefficient based on the experiment data of Takayama and Ikeda (1992). This study also used his method. Other design variables use the assumption of the normal distribution due to lack of available data.

$$\int_{x_1}^{x_2} f_{DTN}(x)\,dx = 1 \tag{3.60}$$

$$f_{DTN}(x) = \frac{1}{p_{12}} f(x) \tag{3.61}$$

$$p_{12} = \int_{x_1}^{x_2} f(x)\,dx \tag{3.62}$$

The doubly-truncated normal distribution $f_{DTN}(x)$ in Eq. (3.60) is related to the normal distribution $f(x)$ as in Eq. (3.61). The cumulative distribution function $F_{DTN}(x)$ of the doubly-truncated normal distribution is the same as the cumulative distribution function $F(x)$ of the normal distribution and expressed as follows:

$$F_{DTN}(x)=\frac{1}{p_{12}}\left[\int_{-\infty}^{x} f(x)dx-\int_{-\infty}^{x_1} f(x)dx\right]=\frac{F(x)-F(x_1)}{p_{12}} \tag{3.63}$$

$F(x_1)$ and p_{12} can be computed once the upper and lower limits are determined. The random number $r(0\le r\le 1)$ of the doubly-truncated normal distribution has the following relation with the random number r' of the normal distribution.

$$r=F_{DTN}(x)=\frac{r'-F(x_1)}{p_{12}} \tag{3.64}$$

Thus, the random variable X of the doubly-truncated normal distribution can be computed as follows:

$$X=\begin{cases}\mu_X+\sqrt{2}\sigma_X\sqrt{-\dfrac{\pi}{4}\ln\left(4r'-4r'^2\right)} & r'\ge 0.5\\ \mu_X-\sqrt{2}\sigma_X\sqrt{-\dfrac{\pi}{4}\ln\left(4r'-4r'^2\right)} & r'<0.5\end{cases} \tag{3.65}$$

Fig 3. 13, Fig 3. 14, and Fig 3. 15 represent randomly extracted wave force acting on the perforated-wall caisson breakwater, wave force acting on the solid-wall caisson breakwater, and friction coefficients, respectively. Takayama and Ikeda (1992) had suggested the following upper and lower limits of the wave force; 1.28 and 0.57 for the perforated-wall caisson breakwater, 1.42 and 0.48 for the solid-wall caisson breakwater; and 1.43 and 0.71 for the friction coefficients. This indicates that the values outside the upper and lower limits that are not likely in the normal distribution are

eliminated so that reasonable wave forces and friction coefficients will be generated.

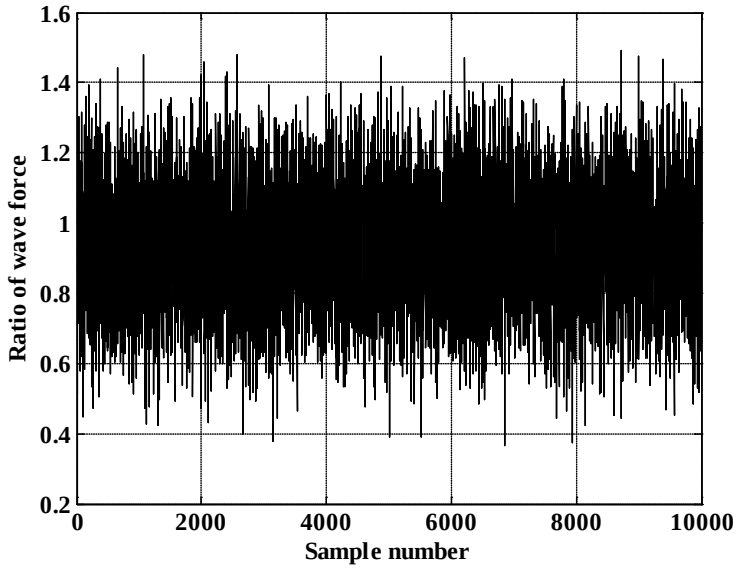

(a)

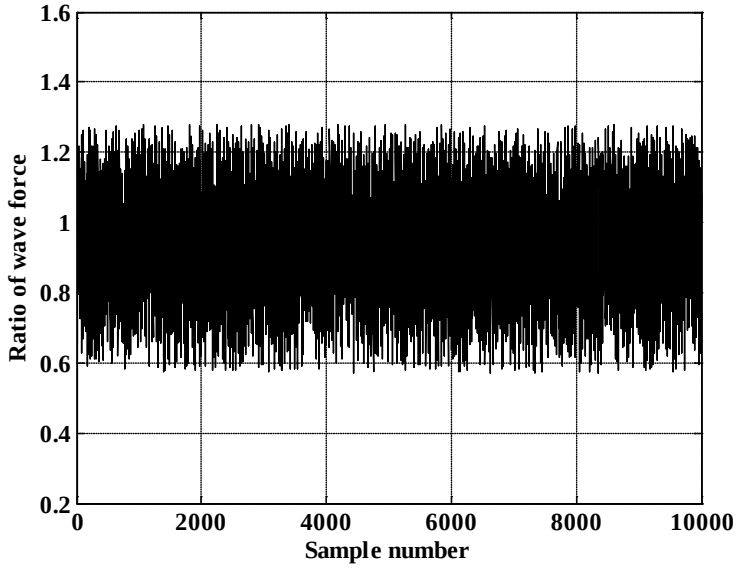

(b)

Fig 3. 13 Random sample of wave force from (a) normal distribution and (b) doubly-truncated normal distribution (Perforated-wall caisson)

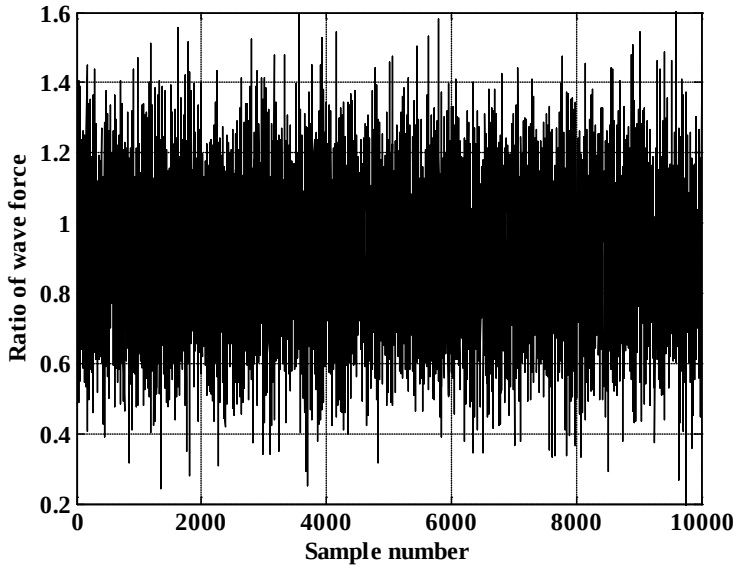

(a)

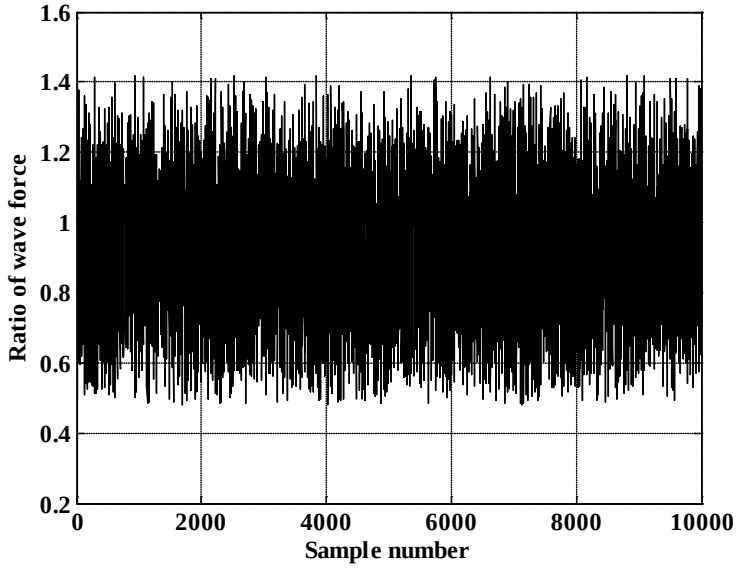

(b)

Fig 3. 14 Random sample of wave force from (a) normal distribution and (b) doubly-truncated normal distribution (Solid-wall caisson)

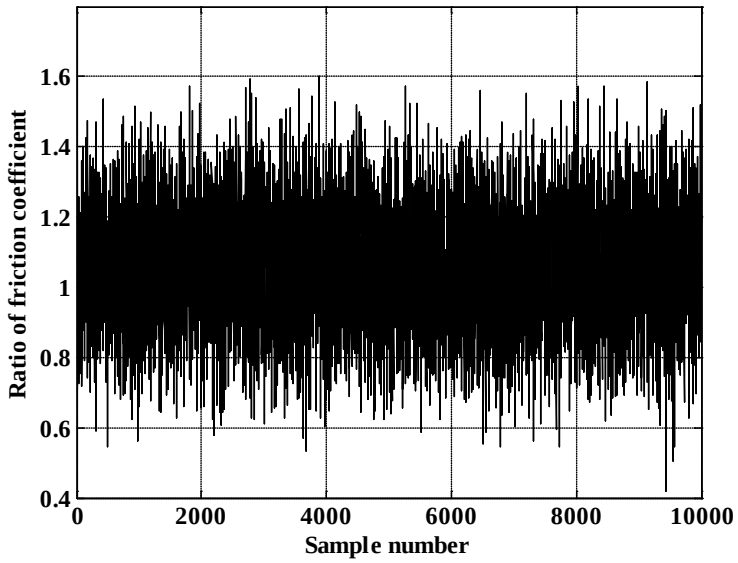

(a)

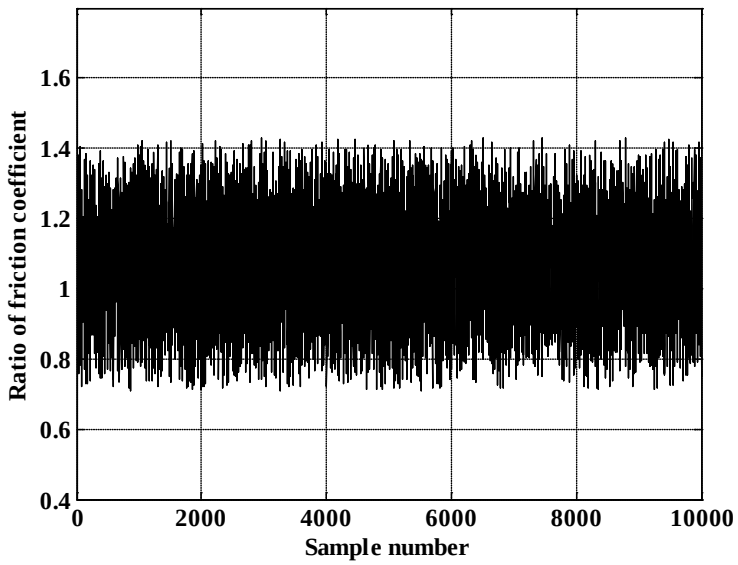

(b)

Fig 3. 15 Random sample of friction coefficient from (a) normal distribution and (b) doubly-truncated normal distribution

3.8 Uncertainty of design variables

The uncertainty of the design variables can be expressed as Eq. (3.66), and statistical characteristics of each variable are presented in Table 3.2.

$$\mu_{X_i} = \left(1+\alpha_{X_i}\right) X_i, \quad \sigma_{X_i} = \gamma_{X_i} X_i \tag{3.66}$$

where X_i, α_{X_i}, and γ_{X_i} are design variables, bias coefficient, and coefficient of variation, respectively.

Table 3.2 Statistical characteristics of design variables

Description	X_i	α_{X_i}	γ_{X_i}	References
Offshore wave height	Various	0.0	0.1	Shimosako and Takahashi (1999)
Significant wave period	Various	0.0	0.1	Suh et al. (2010)
Wave transformation	Various	0.0	0.1	Shimosako and Takahashi (1999)
Horizontal wave force (Solid)	Various	-0.09	0.19	Takayama and Ikeda (1992) Kim and Takayama (2003)
Horizontal wave force (Perforated)	Various	-0.10	0.17	Takayama and Ikeda (1992)
Vertical wave force	Various	-0.23	0.20	Oumeraci et al. (2001)
Friction coefficient	0.6	0.06	0.16	Takayama and Ikeda (1992) Kim and Takayama (2003)

3.9 Time series of wave force

3.9.1 Time series of wave force acting on solid-wall caisson

Shimosako and Takahashi (1998) proposed that the time series of the wave force used in the computation of the expected sliding distance of the solid-wall caisson breakwater is a combined form of the impulsive wave force and standing wave force; and thus expressed as follow:

$$P(t) = \max\left\{P_1(t), P_2(t)\right\} \tag{3.67}$$

$$P_1(t) = \gamma_P P_{1\max} \sin\frac{2\pi t}{T} \tag{3.68}$$

$$P_2(t) = \begin{cases} \left(\dfrac{2t}{\tau_0}\right) P_{2\max} & 0 \le t \le \tau_0 / 2 \\ 2\left(\dfrac{1-t}{\tau_0}\right) P_{2\max} & \tau_0 / 2 \le t \le \tau_0 \\ 0 & t \ge \tau_0 \end{cases} \tag{3.69}$$

$$\gamma_P = 1 - \frac{\pi}{P_{1\max}} \int_{t_1}^{t_2} \left[P_2(t) - P_{1\max} \sin\frac{2\pi t}{T} \right] dt \tag{3.70}$$

$$P_2(t) - P_{1\max} \sin\frac{2\pi t}{T} \ge 0 \tag{3.71}$$

where $P_{1\max}$ is the horizontal wave force of Goda (1974) considering only α_1, $P_{2\max}$ the wave force considering α^*, and $P_1(t)$ and $P_2(t)$ are the standing wave component and impulsive wave component, respectively. τ_0

is the duration of $P_2(t)$, T is the wave period, γ_P is the modification factor which indicates the reduction of standing wave force due to the occurrence of the impulsive wave force. The range of integration of Eq. (3.70) is the range of $P_2(t)-P_1(t)\geq 0$. The uplift force $U(t)$ may also be computed by using the following time series.

$$U(t)=\max\left\{U_1(t),U_2(t)\right\} \tag{3.72}$$

$$U_1(t)=\gamma_U U_{\max}\sin\frac{2\pi t}{T} \tag{3.73}$$

$$U_2(t)=\begin{cases}\left(\dfrac{2t}{\tau_0}\right)U_{\max} & 0\leq t\leq \tau_0/2\\ 2\left(\dfrac{1-t}{\tau_0}\right)U_{\max} & \tau_0/2\leq t\leq \tau_0\\ 0 & t\geq \tau_0\end{cases} \tag{3.74}$$

$$\gamma_U=1-\frac{\pi}{U_{\max}}\int_{t_1}^{t_2}\left[U_2(t)-U_{\max}\sin\frac{2\pi t}{T}\right]dt \tag{3.75}$$

$$U_2(t)-U_{\max}\sin\frac{2\pi t}{T}\geq 0 \tag{3.76}$$

τ_0 is the duration of the impulsive wave force and is defined as follows:

$$\tau_0=k\tau_{0F} \tag{3.77}$$

$$\tau_{0F}=\begin{cases}\left(0.5-\dfrac{H}{8h}\right) & 0\leq\dfrac{H}{h}\leq 0.8\\ 0.4T & \dfrac{H}{h}>0.8\end{cases} \tag{3.78}$$

$$k = \left(\frac{1}{\left(\alpha^*\right)^{0.3} + 1} \right)^2 \tag{3.79}$$

where τ_{0F} is the time when the water level is positive in the finite-amplitude standing wave theory, H wave height, h water depth, and α^* is an impulsive wave pressure coefficient.

Fig 3. 16 shows the time series of the wave force of combined impulsive wave and standing wave components acting on the solid-wall caisson breakwater.

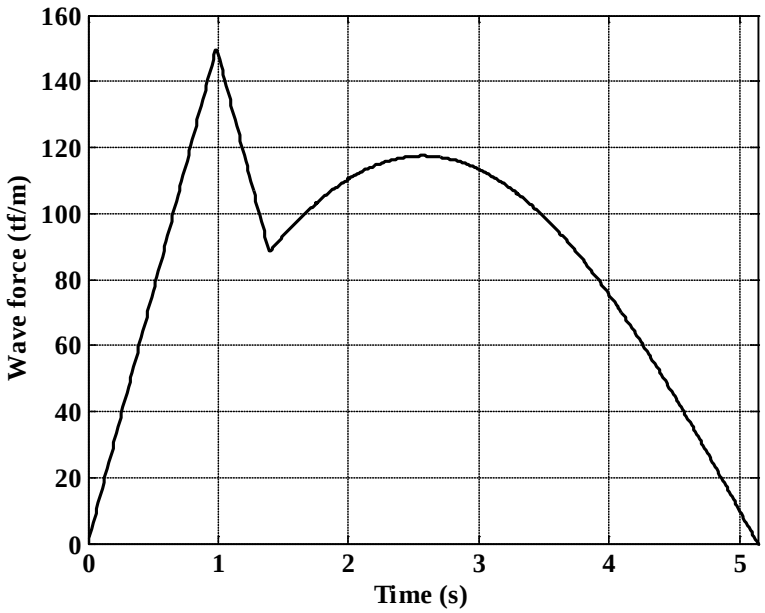

Fig 3. 16 Time series for horizontal wave force acting on solid-wall caisson breakwater

3.9.2 Time series of wave force acting on perforated-wall caisson

Kim (2005) proposed the method to compute the time series of the wave force acting on the perforated-wall caisson breakwater by combining the time series of solid-wall caisson breakwater described in the previous section with the formula proposed by Takahashi et al. (1991) to compute the wave pressure computation acting on the perforated-wall caisson breakwater. In other words, the wave forces of Crest I, Crest IIa and Crest IIb that act on the perforated-wall caisson breakwater with phase difference are expressed by two impulsive waves and one standing wave as follow:

$$P(t) = \max\left\{P_1(t), P_2(t), P_3(t)\right\} \tag{3.80}$$

$$P_1(t) = \begin{cases} \left(\dfrac{2t}{\tau_0}\right)P_I & 0 \le t < \dfrac{\tau_0}{2} \\ 2\left(\dfrac{1-t}{\tau_0}\right)P_I & \dfrac{\tau_0}{2} \le t < \tau_0 \\ 0 & t \ge \tau_0 \end{cases} \tag{3.81}$$

$$P_2(t) = \begin{cases} 0 & 0 \le t < t_d \\ \left(\dfrac{2(t-t_d)}{\tau_0'}\right)P_{IIa} & t_d \le t < \dfrac{\tau_0'}{2} + t_d \\ 2\left(\dfrac{1-(t-t_d)}{\tau_0'}\right)P_{IIa} & \dfrac{\tau_0'}{2} + t_d \le t < \tau_0' + t_d \\ 0 & t \ge \tau_0' + t_d \end{cases} \tag{3.82}$$

$$P_3(t) = \begin{cases} 0 & 0 \le t < t_d \\ P_{IIb}\sin\dfrac{2\pi(t-t_d)}{T} & t \ge t_d \end{cases} \tag{3.83}$$

where P_I, P_{IIa} and P_{IIb} are the maximum wave forces obtained using the correction coefficients in Table 3.1. The uplift force $U(t)$ for the perforated-wall caisson breakwater can be obtained by the same method of horizontal wave force.

$$U(t) = \max\left\{U_1(t), U_2(t), U_3(t)\right\} \tag{3.84}$$

$$U_1(t) = \begin{cases} \left(\dfrac{2t}{\tau_0}\right)U_I & 0 \le t < \dfrac{\tau_0}{2} \\ 2\left(\dfrac{1-t}{\tau_0}\right)U_I & \dfrac{\tau_0}{2} \le t < \tau_0 \\ 0 & t \ge \tau_0 \end{cases} \tag{3.85}$$

$$U_2(t) = \begin{cases} 0 & 0 \le t < t_d \\ \left(\dfrac{2(t-t_d)}{\tau_0'}\right)U_{IIa} & t_d \le t < \dfrac{\tau_0'}{2} + t_d \\ 2\left(\dfrac{1-(t-t_d)}{\tau_0'}\right)U_{IIa} & \dfrac{\tau_0'}{2} + t_d \le t < \tau_0' + t_d \\ 0 & t \ge \tau_0' + t_d \end{cases} \tag{3.86}$$

$$U_3(t) = \begin{cases} 0 & 0 \le t < t_d \\ U_{IIb} \sin\dfrac{2\pi(t-t_d)}{T} & t \ge t_d \end{cases} \tag{3.87}$$

where U_I, U_{IIa} and U_{IIb} are the uplift forces obtained using the correction coefficients in Table 3.1. t_d is the time difference between the wave forces $P_1(t)$ and $P_2(t)$, and τ_0' is the duration of Crest IIa, and these can be obtained as follows:

$$t_d = \frac{\tau_0}{2} + \frac{B'}{\sqrt{gd}} - \frac{\tau_0'}{2} \tag{3.88}$$

$$\tau_0' = k'\tau_{0F}' \tag{3.89}$$

$$k' = \left(\frac{1}{\left(\alpha^*\right)^{0.3} + 1} \right)^2 \tag{3.90}$$

$$\tau_{0F}' = \begin{cases} \left(0.5 - \frac{H_{\max}}{8d}\right)T & 0 < \frac{H_{\max}}{d} \le 0.8 \\ 0.4T & \frac{H_{\max}}{d} > 0.8 \end{cases} \tag{3.91}$$

Eqs. (3.89) to (3.91) use the water depth inside the wave chamber d' instead of h. In Eq. (3.91), the wave height must be the value on the rubble mound, but the wave height in front of the breakwater is used by assuming that the wave height change on the mound is small enough to be ignored (Kim, 2005).

Unlike the solid-wall caisson breakwater, the perforated-wall caisson breakwater has a wave chamber that can dissipate the wave force acting on the caisson. The force acting at the bottom of the wave chamber is caused by the increase of water level in the wave chamber and it will increase the caisson stability. The force of at the bottom of the wave chamber was calculated by assuming a triangular distribution; by using the maximum value $\left(P_{IIaM}\right)$ at the moment $\left(t_d + \tau_0'/2\right)$ when the impulsive wave impacts the rear wall and the maximum value $\left(P_{IIbM}\right)$ at the moment $\left(t_d + T/4\right)$ when the wave becomes a standing wave. (Kim, 2005).

$$P_V = \begin{cases} 0 & 0 \le t < t_m \\ \dfrac{4\left(P_{IIbM} - P_{IIaM}\right)}{T - 2\tau_0'}\left[t - \left(t_d + \dfrac{\tau_0'}{2}\right)\right] + P_{IIaM} & t_m \le t < t_d + \dfrac{T}{4} \\ -\dfrac{4\left(P_{IIbM} - P_{IIaM}\right)}{T - 2\tau_0'}\left[t - \left(t_d + \dfrac{\tau_0'}{2}\right)\right] + 2P_{IIbM} - P_{IIaM} & t_d + \dfrac{T}{4} \le t < t_d + \dfrac{T}{2} \\ 0 & t \ge t_d + \dfrac{T}{2} \end{cases}$$

(3.92)

$$t_m = \frac{-P_{IIa}\left(T - 2\tau_0'\right)}{4\left(P_{IIb} - P_{IIa}\right)} + t_d + \frac{\tau_0'}{2} \tag{3.93}$$

where t_m is the time then the vertical pressure starts occurring at the bottom of the wave chamber due to the increase of water level in the wave chamber.

Fig 3. 17 shows the time series of the perforated-wall caisson breakwater which is the combination of two impulsive wave components and one standing wave component. Fig 3. 18 shows a comparison of the time series between the perforated-wall caisson breakwater and the solid-wall caisson breakwater under the same wave condition. The perforated-wall caisson breakwater has the perforated structure that causes the reduction of wave force, and shows a smaller wave force than the solid-wall caisson breakwater, and it can be confirmed that the influence of the impulsive wave has reduced unlike the solid-wall caisson breakwater. From the shape of time series, depending on the configuration of structure, one can find out if the impulsive wave is dominant or the standing wave is dominant.

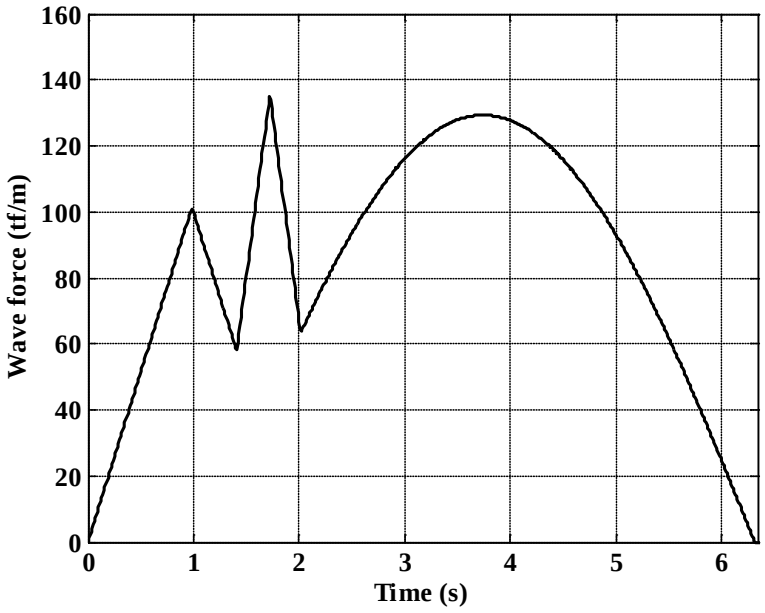

Fig 3. 17 Time series for horizontal wave force acting on perforated-wall caisson breakwater

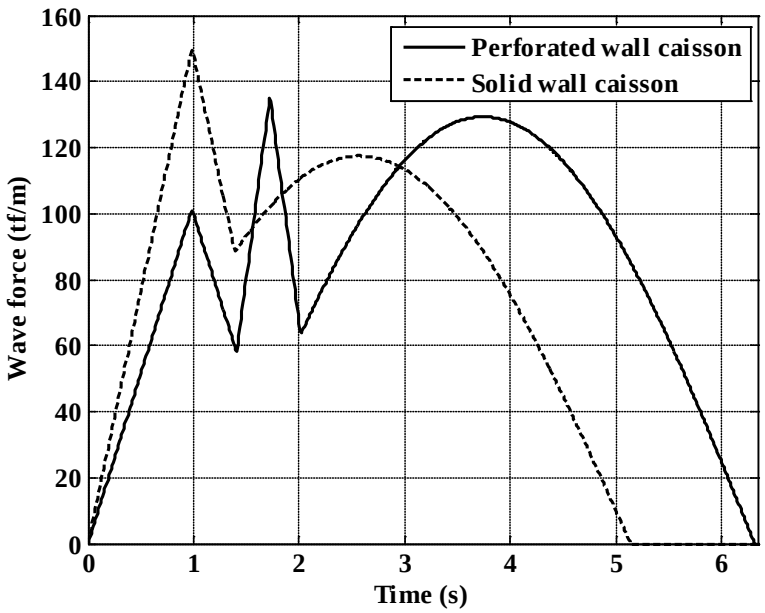

Fig 3. 18 Comparison of time series for horizontal wave force between perforated-wall caisson and solid-wall caisson

3.10 Expected sliding distance

The sliding distance of a caisson can be calculated by accumulating for the lifetime of the breakwater and by assuming the following: the storm that can cause high waves for caisson sliding landed once a year, and 1000 waves occur during the storm. For the calculation of the expected sliding distance, in order to consider the distribution of wave transformation or wave force, the accumulated sliding distance must be calculated repeatedly by changing the random numbers. These processes repeat a number of times and the average value of accumulated sliding distance calculated in each process is defined as the expected sliding distance. In other words, the expected sliding distance means the expected value of total sliding distance obtained by using the high wave that is possible to occur during the lifetime. Monte-carlo simulation was used to generate the random processes of caisson sliding. This is appropriate to the calculation of the process with complexity and many steps, and is sufficiently practical using a personal computer. In the performance-base design method, the caisson can maintain its function even if some sliding occurs. This has the possibility of producing different results than with the conventional deterministic design method. The caisson sliding can be calculated from the time series of wave force.

$$\left(\frac{W}{g}+M_a\right)\frac{d^2x_G}{dt^2}=P_H-F_R-F_D \tag{3.94}$$

$$F_R=\mu\left(W'-U\right) \tag{3.95}$$

Eq. (3.94) is the equation of motion of caisson for sliding. W is the caisson weight in the air, g is gravitational acceleration, M_a is added mass $\left(=1.0855\rho_0 h'^2\right)$, ρ_0 is density of sea water, h' is water depth in front of the caisson, x_G is the horizontal displacement of the caisson, P_H is horizontal wave force, F_R is the frictional resistance, W' is the caisson weight in water, U is the uplift force, and F_D is the wave resistance force.

In general, wave resistance force is not considered because the sliding speed is small enough to ignore. Based on the time series of wave force, if the wave force is smaller than the friction resistance, no sliding occurs, and if the wave force exceeds the friction resistance, sliding occurs and can be calculated by performing the numerical integration of Eq. (3.94) twice with respect to time. Total sliding distance can be calculated by accumulating the sliding distance during the lifetime of the breakwater. In order to estimate the expected sliding distance, the calculation of total sliding distance was repeated for 5000 times and the averaged value was obtained.

Shimosako and Takahashi (1999) proposed the allowable sliding distance of 0.3 m, but Goda and Takagi (2000) thought that 0.3 m was too large and proposed 0.1 m instead. Takahashi et al. (2001) proposed the stability criteria for the expected sliding distance as shown in Table 3.3. If only the expected sliding distance is chosen as the criteria for stability without considering the probability as shown in Table 3.3, the allowable expected sliding distance of the structure having a medium importance is less than 0.3 m.

3.11 Exceedance rate

Since the expected sliding distance is calculated as the average of the simulated sliding distances over the lifetime of the structure, the actual sliding distance can exceed the average. To overcome this, Kim et al. (2009) pointed out the limitation that can occur in evaluating the stability with the expected sliding distance, and evaluated the stability of structure by calculating the exeedance probability of an allowable sliding distance. Exceedance rate can be calculated as shown in Eq. (3.96), which can solve the problem of the structure stability evaluation.

$$P_e = \lim_{N\to\infty} \frac{n_e}{N} \tag{3.96}$$

where n_e is the number of simulations in which the total sliding distance has exceeded the allowable sliding distance, and N is the total number of simulation.

Shimosako and Tada (2004) proposed the exceedance rate criteria of an allowable sliding distance depending on the importance of structure and limit state as shown in Table 3.4 based on the observed damage of caisson breakwater for sliding. This is being used as the criteria for JPHA (2007) in Japan and standards for the breakwater reliability design (2011) in Korea. If the criteria of Table 3.4 are used, the same stability can be maintained even under any design conditions that the sliding distance changes by the environmental conditions such as the occurrence frequency of high waves. The probability exceeding an allowable sliding distance(0.1, 0.3, and 1.0 m)

during the lifetime of a medium-importance structure is proposed as 30%, 10%, and 5% for repairable limit state, extreme limit state, and collapse limit state, respectively, as shown in Table 3.4.

Table 3.3 Allowable expected sliding distance by Takahashi et al. (2001)

	Importance of structure		
	High	Medium	Low
Expected sliding distance (m)	0.03	0.3	1.0

Table 3.4 Acceptable exceedance rate of total sliding distance for breakwaters of different levels of importance, as proposed by Shimosako and Tada (2004)

Limit state (allowable sliding distance)	Importance of structure		
	High	Medium	Low
Repairable(0.1 m)	15%	30%	50%
Ultimate(0.3 m)	5%	10%	20%
Collapse(1.0 m)	2.5%	5%	10%

CHAPTER 4 RESULTS AND ANALYSIS

4.1 Validation of model

In order to validate the model which is used in this study, the experimental results of the hydraulic model tests conducted by the Korea Ocean Research and Development Institute (1992). Fig 4. 1 shows a standard cross-section which was used in the experiment, and is the perforated-wall caisson with vertical slits. Irregular waves were used in the experiment, with the significant wave height of 100-year return period is 9.5m, significant wave period 15 s, and the storm duration is 380 times the significant wave period. The conditions used in validating the model are identical to the conditions in hydraulic experiments. The wave periods of individual waves were calculated by using the coefficient of variation of 0.1 to the significant wave period, 15 s. The expected sliding distance was estimated by averaging the total sliding distances simulated 5000 times. The wave chamber in the hydraulic model test has two wave chambers, each having 4.6-m width as shown in Fig 4. 1. The calculation in this study was conducted for one narrow chamber with 4.6-m width and one wide chamber with 9.6-m width. Fig 4. 2 shows a comparison between the results of hydraulic model test and the calculation in this study.

The sliding distance calculated in this study is greater than the experimental results. The caisson used in the experiment has two wave chambers that dissipate the wave energy twice. However, the caisson used in the calculation has one wave chamber with different widths.

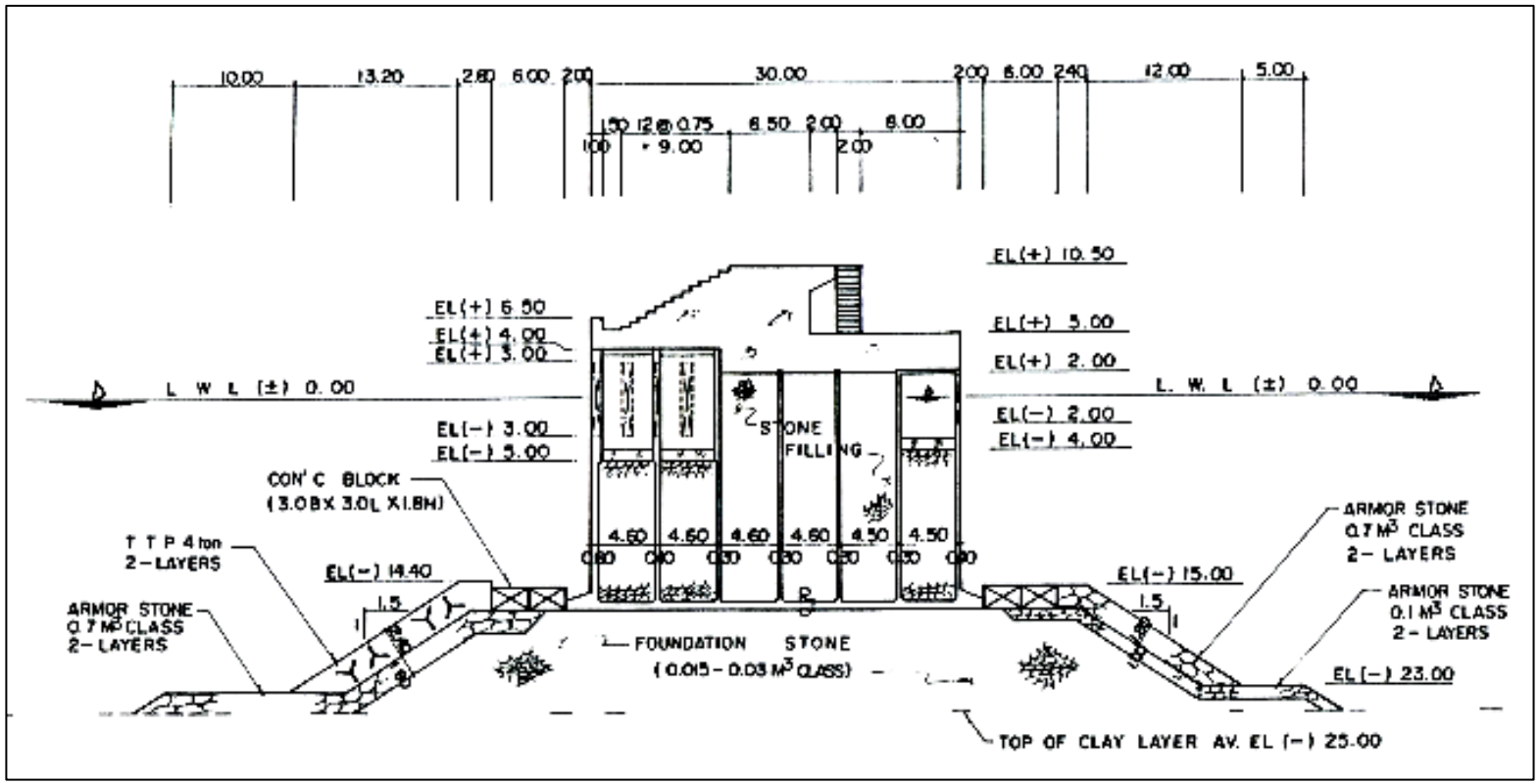

Fig 4. 1 Cross-section II of vertical slit caisson breakwater

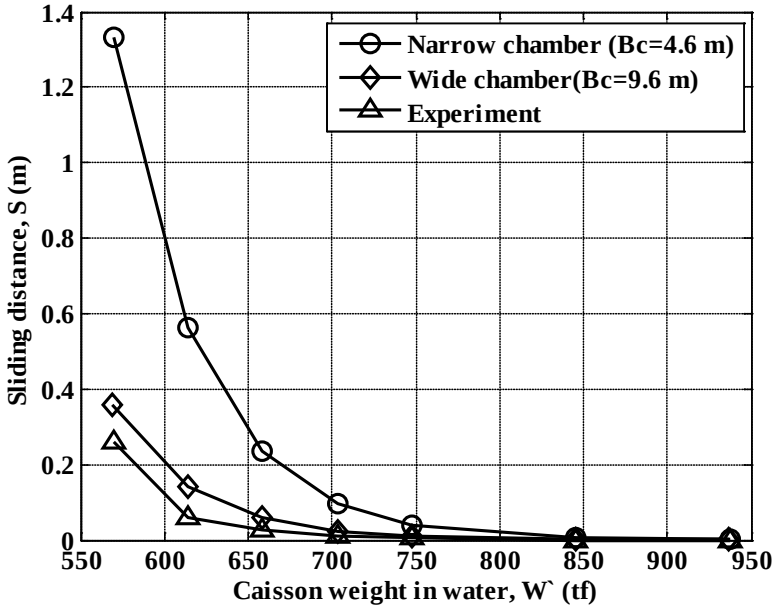

Fig 4. 2 Comparison of sliding distance versus caisson weight in water between experiment and calculation

The narrow-chamber caisson has a relatively large sliding distance since the phase difference of the wave forces acting on the front and rear wall is smaller than that of wider chamber. The caisson used in the experiment has two wave chambers, while the wide chamber in the calculation has one wave chamber. Since the wave dissipating effect by two wave chambers is greater than that in one wide chamber, the sliding distance in the calculation is estimated to be a little larger than the experimental value. The result of the calculation in this study shows the same tendency as the experimental result, although its value is slightly larger than the experimental results. Therefore, the performance-based design method used in this study seems to give a reasonable result.

4.2 Design conditions of caisson breakwater

The typical cross-section of a perforated-wall caisson breakwater is shown in Fig 4. 3, and the design conditions used in estimating the sliding distance of the perforated-wall caisson breakwater is shown in Table 4. 1.

In order to compare the deterministic design method and performance-based design method, the safety factor of sliding was changed at intervals of 0.1 from 1.0 to 1.3, and at intervals of 0.2 from 1.3 to 1.9 to determine the width of caisson that satisfies each safety factor, and the performance-based design was also performed. Water depths at the breakwater site were set at intervals of 4 m from DL(-)14 m to DL(-)30 m, and at intervals of 2 m from DL(-)10 m to DL(-)14 m. Two bottom slopes were used: 1/50 and 1/20. The ratio of the depth on top of mound to total water depth (h'/h) is set at 0.7, the ratio of the water depth inside wave chamber to the depth on top of mound (d'/h') is set at 0.5. The ratio of the wave chamber width to wave length (B_c/L) is set to be 0.12, which can significantly reduce wave reflection without significantly increasing the wave chamber width. The ratio of berm width on the mound to wave length (B_M/L) used the value of 0.05. The high water level is assume to be DL(+)0.66 m. The crest elevation of the front perforated wall is set at $0.5H_{1/3}$, and the crest elevation of the rear wall is set at $0.6H_{1/3}$. The porosity (ε) of the perforated wall is set to be 30%, which gives a minimum reflection.

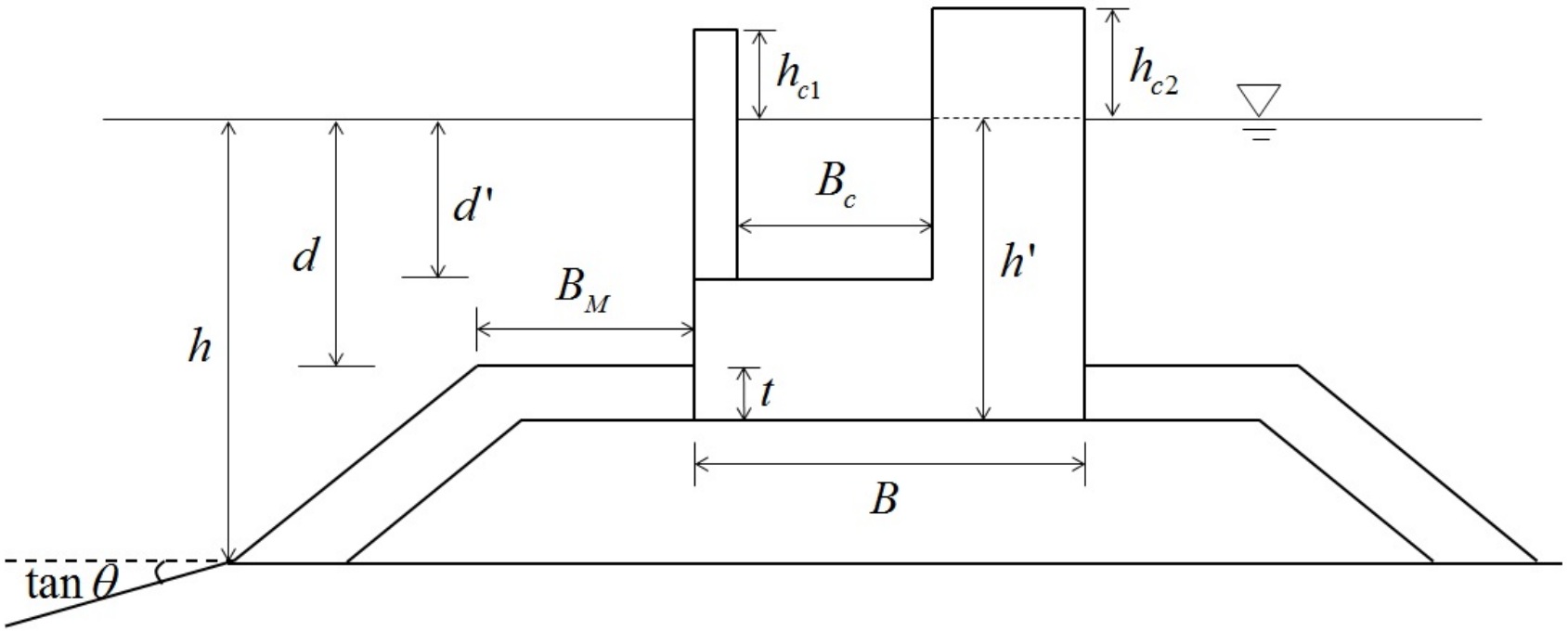

Fig 4. 3 Typical cross-section of perforated-wall caisson breakwater

Table 4. 1 Design condition

	Variable	Condition
Incident wave condition	$H_{1/3}(m)$	Weibull distribution
	$T_s(\mathrm{s})$	Suh et al. (2010b)
	$\beta(\mathrm{deg})$	0
Geometries of caisson breakwater	B	1.0, 1.1, 1.2, 1.3, 1.5, 1.7, 1.9
	h	10, 12, 14, 18, 22, 26, 30 m
	$\tan\theta$	1/50, 1/20
	h'/h	0.7
	Height of armor layer, t	$AH_{1/3}(h'/h)^{-0.787}$, $A=0.21$
	d	$h'-t$
	d'/h'	0.5
	B_c/L	0.12
	B_M/L	0.05
	HWL	0.66 m
	h_{c1}	$0.5H_{1/3}$
	h_{c2}	$0.6H_{1/3}$
	Porosity, ε	0.3

4.3 Computation results

This study was conducted by expanding the performance-based design method for a solid-wall caisson breakwater to the perforated-wall caisson breakwater.

Fig 4. 4~Fig 4. 9 show the computation results of the solid-wall caisson breakwater and perforated-wall caisson breakwater in different water depths designed by using different safety factors. Both expected sliding distance and exceedance rate decreases with decreasing water depth outside the surf zone, but they increase inside the surf zone, i.e. from 14 m for the case of bottom slope of 1/50, and from 12 m for the case of 1/20. The water depths of 14 m and 12 m are the points where wave breaking starts for the bottom slope of 1/50 and 1/20, respectively (see Fig 3. 4 and Fig 3. 5). Both expected sliding distance and exceedance rate reduce as the water depth decreases on the outside of surf zone. As shown in Fig 3. 4 and Fig 3. 5, it is because the limiting breaker height increases with the water depth so that the number of individual waves of larger wave height increases. This result has also been demonstrated for the solid-wall caisson breakwater in Suh et al. (2013). Both expected sliding distance and exceedance rate increase with decreasing water depth inside the surf zone. It is believed that inside the surf zone, as the water depth decreases, the range of wave heights that can cause caisson sliding becomes narrower so that the relative occurrence frequency of large waves close to the limiting breaker height becomes higher.

Fig 4. 10~Fig 4. 15 compare the result of computation between the deterministic design method and the performance-based design method. The

computation result shows the solid-wall caisson breakwater and the perforated-wall caisson breakwater separately.

Fig 4. 10 and Fig 4. 11 show the computation results of expected sliding distance of the solid-wall caisson breakwater and the perforated-wall caisson breakwater installed in various water depths. For both solid-wall and perforated-wall caissons, and in the case of bottom slope of 1/50, if the caisson is designed to satisfy the criterion for the expected sliding distance of the structure of medium importance (i.e. $s_E = 0.3$ m), the corresponding safety factor is smaller than 1.2 inside the surf zone $(h \le 14 \text{ m})$, while it is greater than 1.2 outside the surf zone. This implies that the caisson designed by the performance-based design method satisfies the design criterion of the deterministic design method (i.e. $S.F. = 1.2$) outside the surf zone, but it does not satisfy the criterion inside the surf zone. Also, the safety factor corresponding to $s_E = 0.3$ m increases with water depth outside the surf zone. The same is true for the case of bottom slope of 1/20, in which the boundary of the surf zone is $h = 12$ m .

This can be looked at the other way round. If the caisson is designed to satisfy the criterion of the deterministic design method (i.e. $S.F. = 1.2$), the expected sliding distance is smaller than 0.3 m inside the surf zone, while it is greater than 0.3 m outside the surf zone. Therefore, the caisson trends to be over-designed inside the surf zone and under-designed outside the surf zone from the point of view of the performance-based design method using $s_E = 0.3$ m .

Fig 4. 12 and Fig 4. 13 show the exeedance rate of solid-wall caisson breakwater and perforated-wall caisson breakwater for the ultimate limit state for the structure of medium importance. For both solid-wall and perforated-wall caissons, and for both bottom slopes of 1/20 and 1/20, if the caisson is designed to satisfy the criterion for the exceedance rate for the structure of medium importance in the ultimate limit state (i.e. $P_E\left(S > 0.3\,E\right) = 10\ \%$), the corresponding safety factor is smaller than 1.2 only at the incipient wave breaking point (i.e. $h = 14$ m for 1/50 slope and $h = 12$ m for 1/20 slope), while it is greater than 1.2 in other water depths. This implies that the caisson designed by the performance-based design method satisfies the design criterion of the deterministic design method (i.e. $S.F. = 1.2$) in all water depths except the incipient wave breaking point. On the other hand, if the caisson is designed to satisfy the criterion of the deterministic design method (i.e. $S.F. = 1.2$), the exceedance rate is smaller than 10 % only at the incipient wave breaking point, while it is greater than 10 % in other water depths. This implies that the caisson is under-designed except at the incipient wave breaking point from the view point of the performance-based design method using $P_E\left(S > 0.3\ \mathrm{m}\right) = 10\ \%$.

Fig 4. 14 and Fig 4. 15 show the exceedance rate of solid-wall caisson and perforated-wall caisson breakwater for the repairable limit state for the structure of medium importance. If the caisson is designed by the performance-based design method (i.e. $P_E\left(S > 0.1\ \mathrm{m}\right) = 30\ \%$), the safety factor is smaller than 1.2 in most cases except $h = 30$ m. This implies that

the caisson designed by the performance-based design method to satisfy the criterion of $P_E\left(S > 0.1\ \mathrm{m}\right) = 30\ \%$ does not satisfy the criterion of $S.F. = 1.2$ except at the large water depth of $h = 30\ \mathrm{m}$. On the other hand, if the caisson is designed by the deterministic design method to satisfy the criterion of $S.F. = 1.2$, the exceedance rate, $P_E\left(S > 0.1\ \mathrm{m}\right)$, is smaller than 30 % in most water depths except $h = 30\ \mathrm{m}$. This implies that the caisson in over-designed in most cases from the view point of the performance-based design method using $P_E\left(S > 0.1\ \mathrm{m}\right) = 30\ \%$.

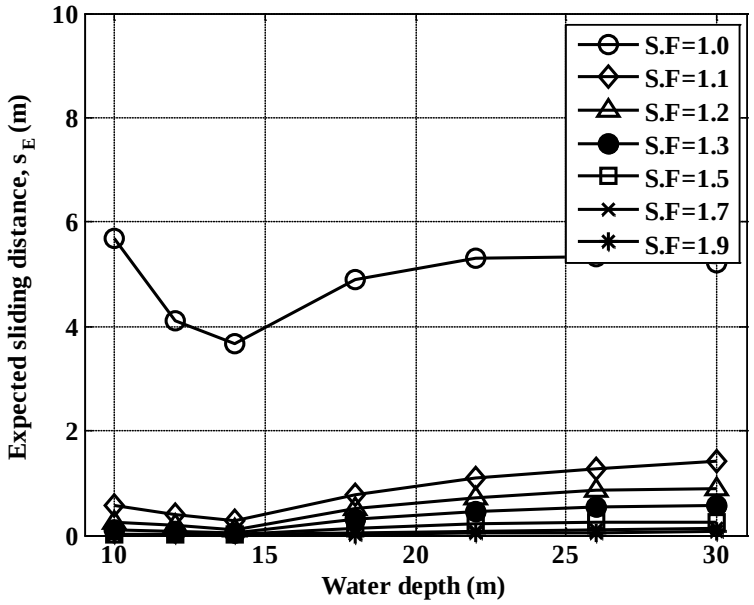

(a)

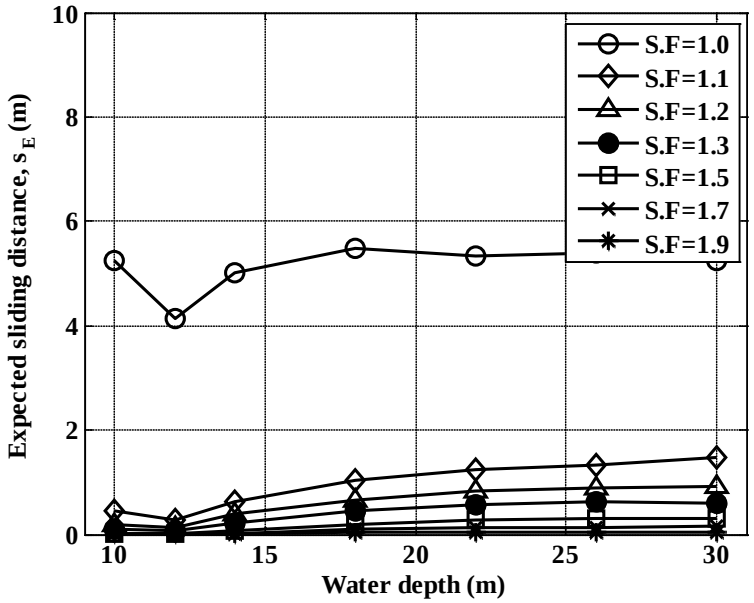

(b)

Fig 4. 4 Expected sliding distance of solid-wall caisson breakwater in different water depths of (a) bottom slope=1/50, (b) bottom slope=1/20

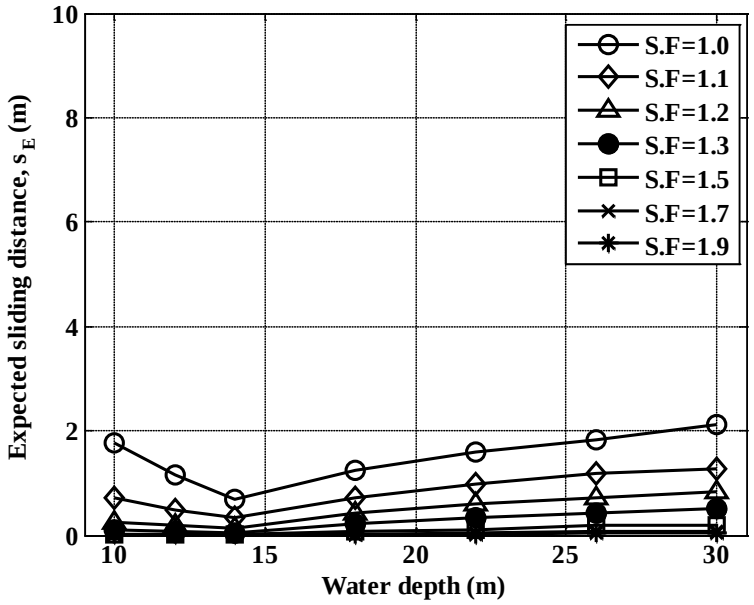

(a)

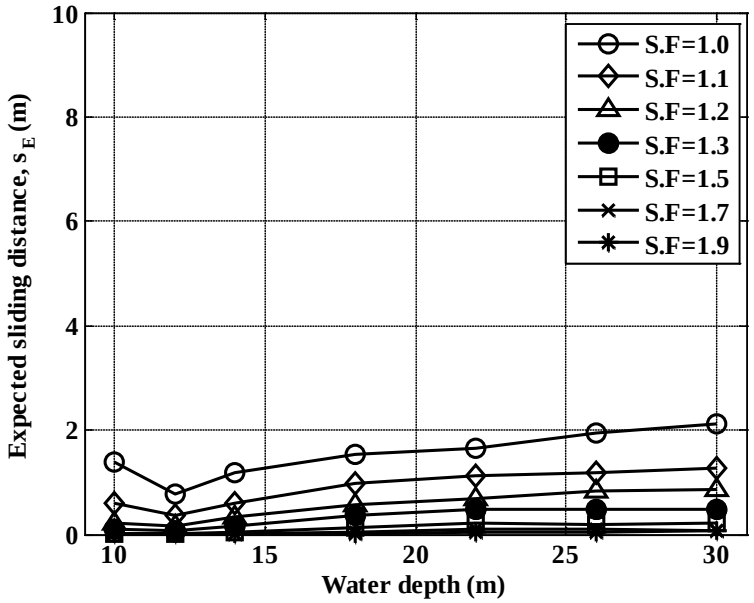

(b)

Fig 4. 5 Expected sliding distance of perforated-wall caisson breakwater in different water depths of (a) bottom slope=1/50, (b) bottom slope=1/20

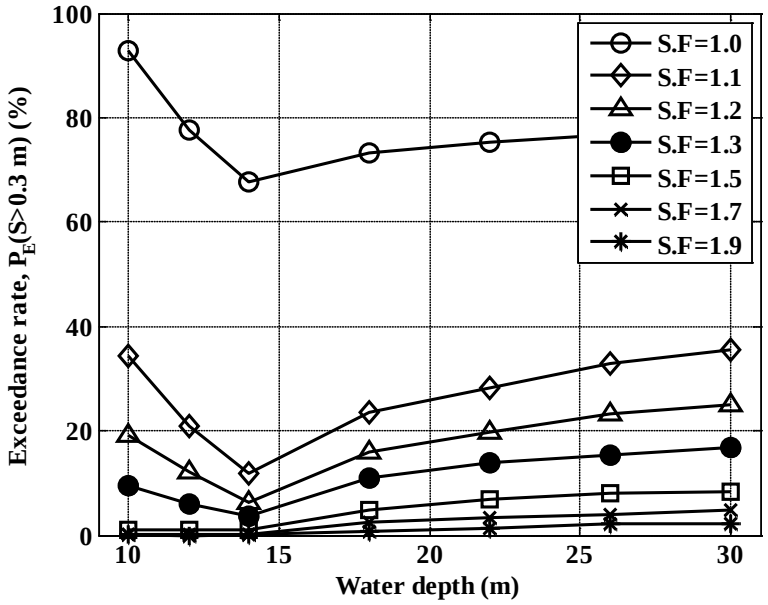

(a)

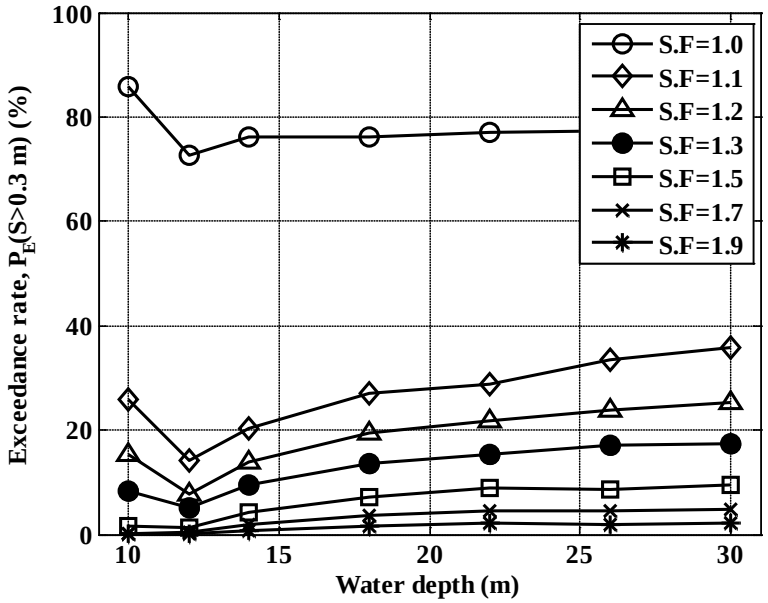

(b)

Fig 4. 6 Exceedance rate(S>0.3 m) of solid-wall caisson breakwater in different water depths of (a) bottom slope=1/50, (b) bottom slope=1/20

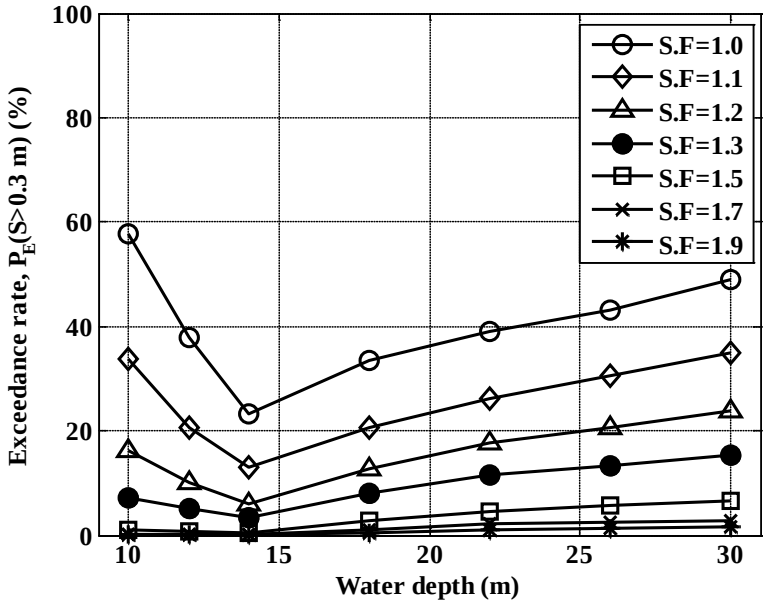

(a)

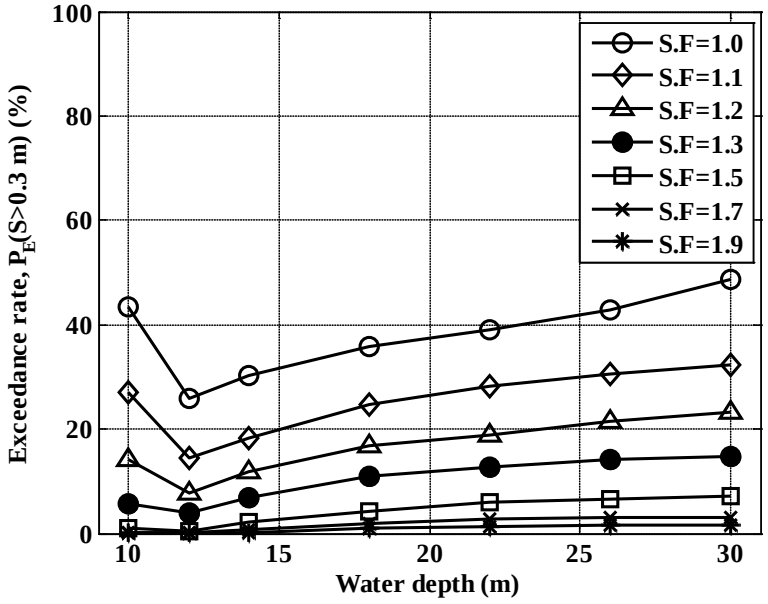

(b)

Fig 4. 7 Exceedance rate(S>0.3 m) of perforated-wall caisson breakwater in different water depths of (a) bottom slope=1/50, (b) bottom slope=1/20

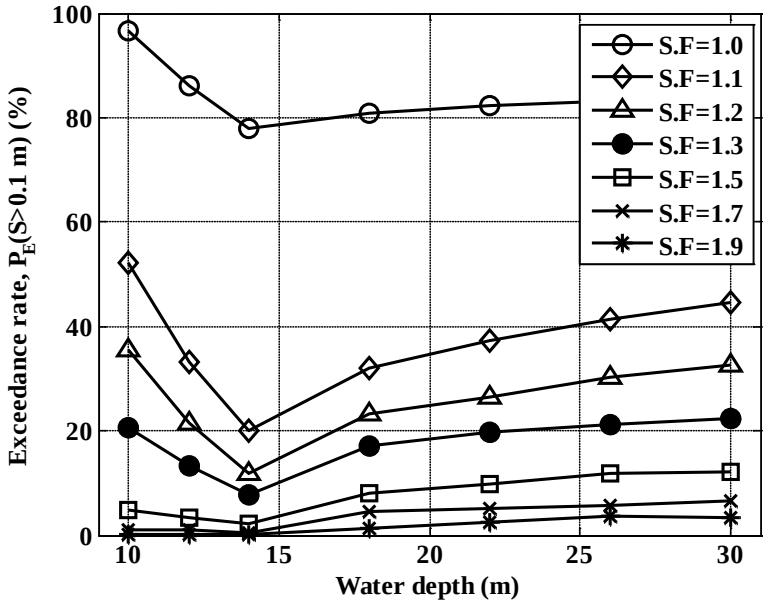

(a)

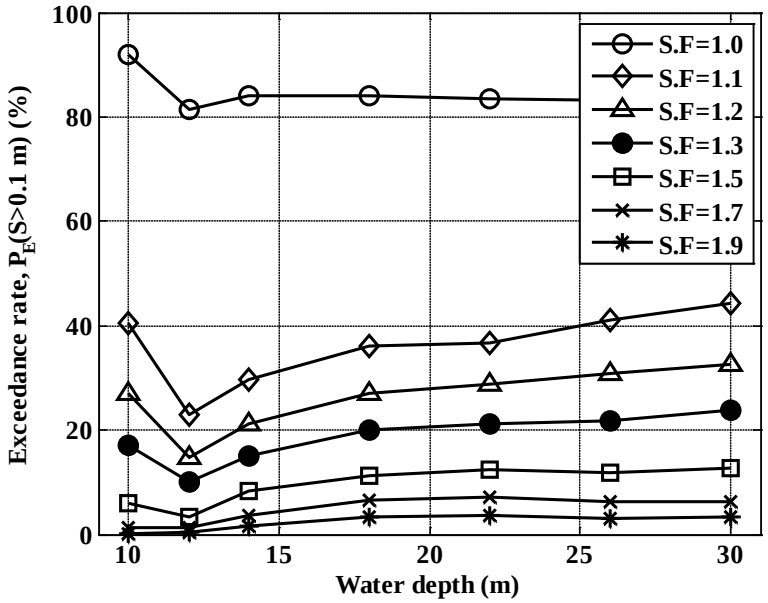

(b)

Fig 4. 8 Exceedance rate(S>0.1 m) of solid-wall caisson breakwater in different water depths of (a) bottom slope=1/50, (b) bottom slope=1/20

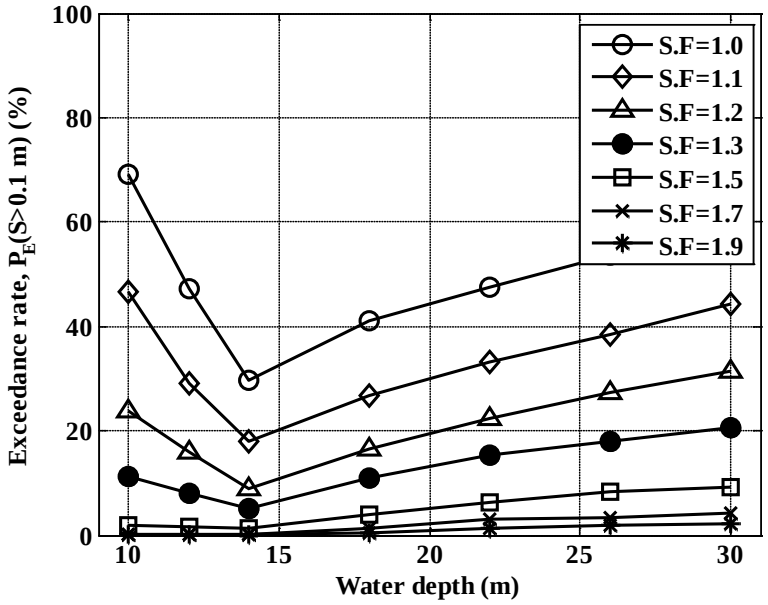

(a)

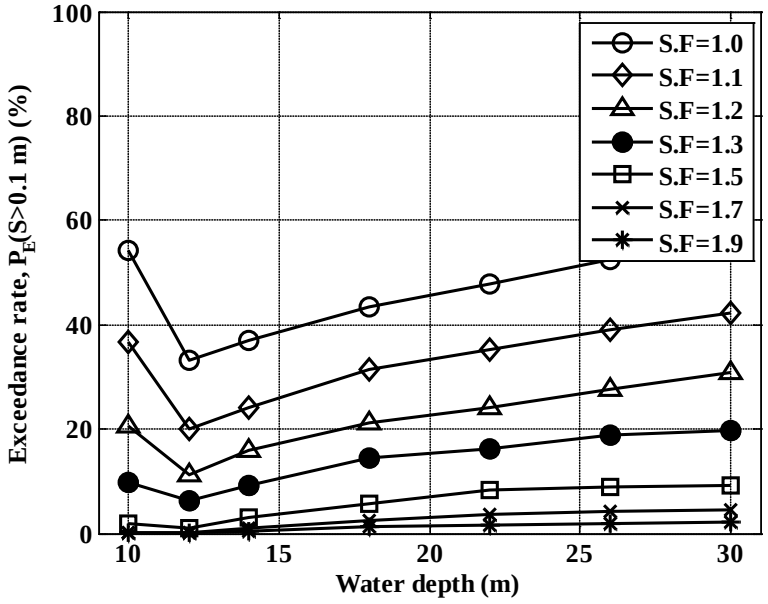

(b)

Fig 4. 9 Exceedance rate(S>0.1 m) of perforated-wall caisson breakwater in different water depths of (a) bottom slope=1/50, (b) bottom slope=1/20

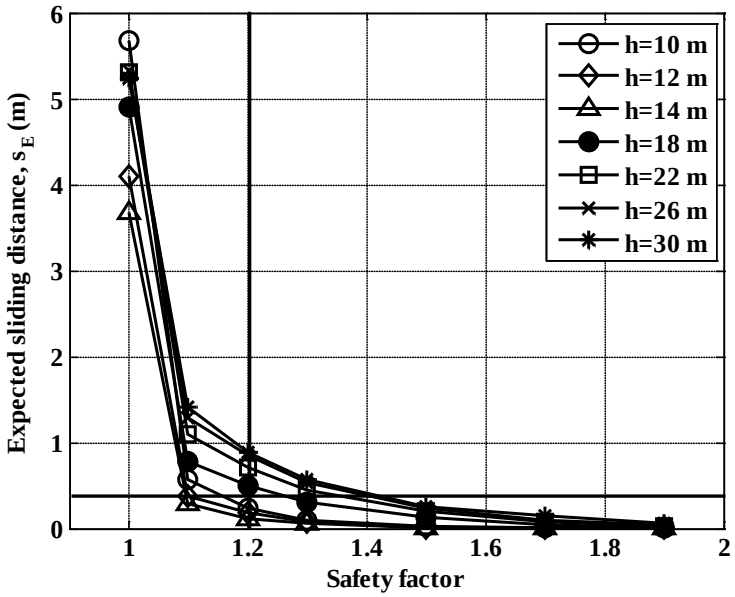

(a)

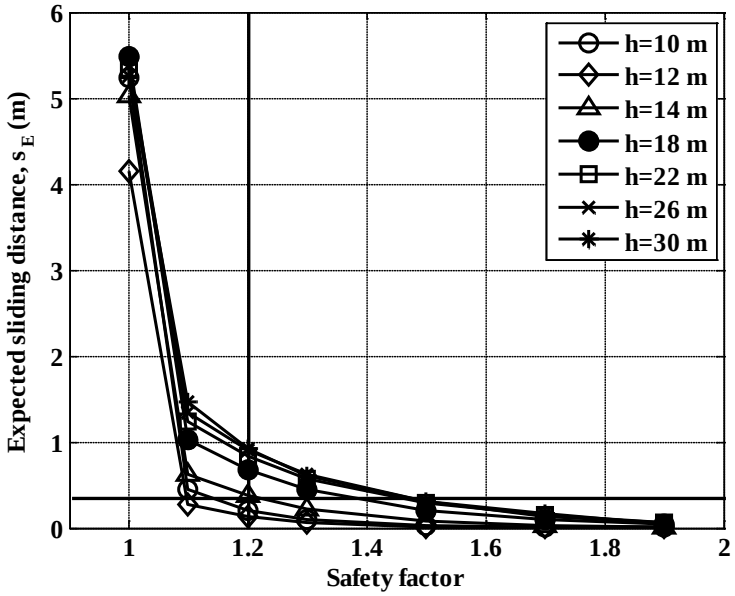

(b)

Fig 4. 10 Expected sliding distance of solid-wall caisson for different safety factors in different water depths of (a) bottom slope=1/50, (b) bottom slope=1/20

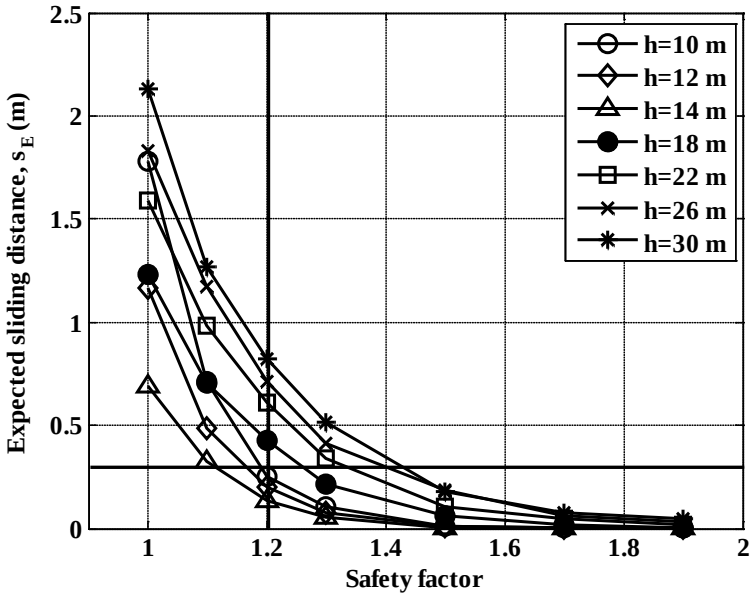

(a)

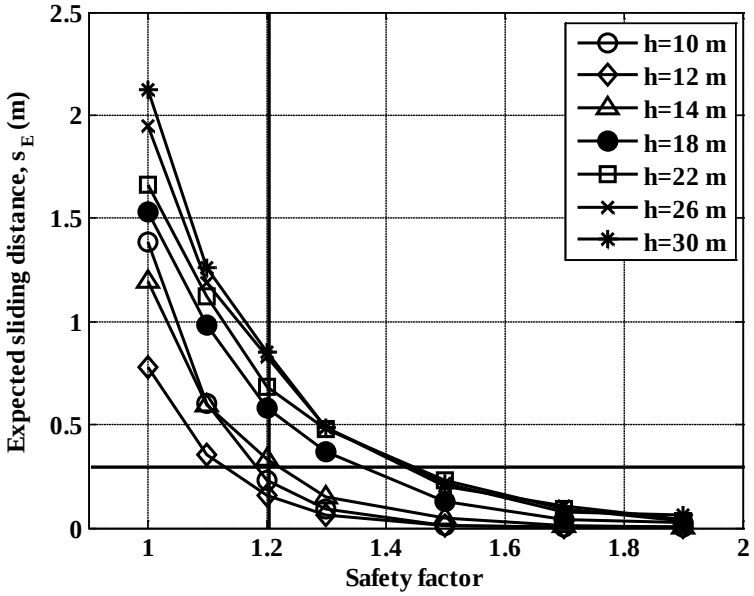

(b)

Fig 4. 11 Expected sliding distance of perforated-wall caisson for different safety factors in different water depths of (a) bottom slope=1/50, (b) bottom slope=1/20

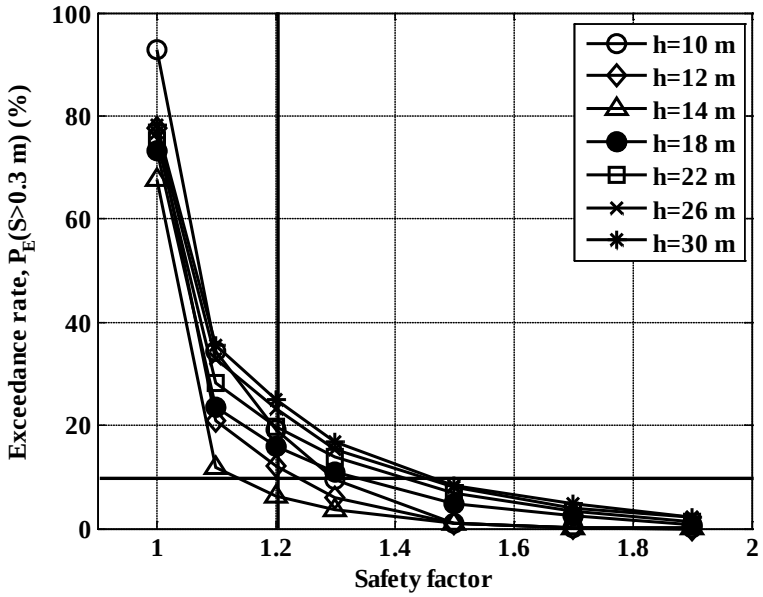

(a)

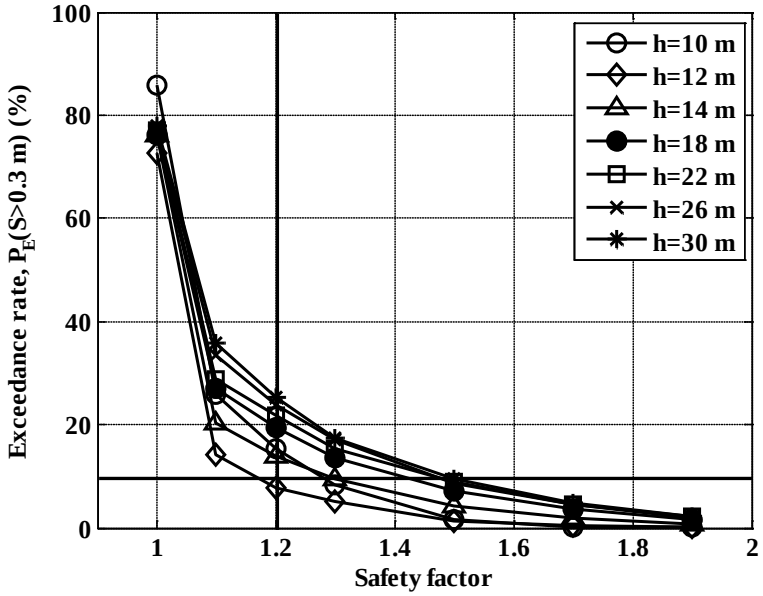

(b)

Fig 4. 12 Exceedance rate(S>0.3 m) of solid-wall caisson in different safety factors in different water depths of (a) bottom slope=1/50, (b) bottom slope=1/20

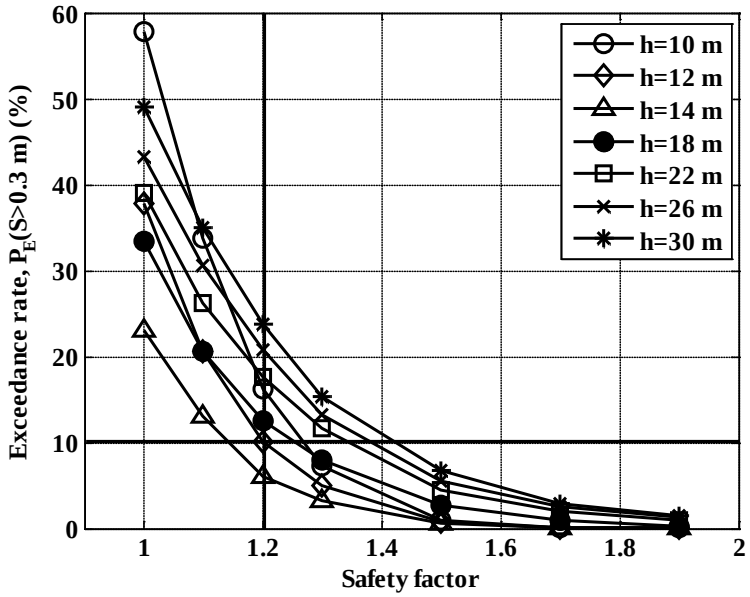

(a)

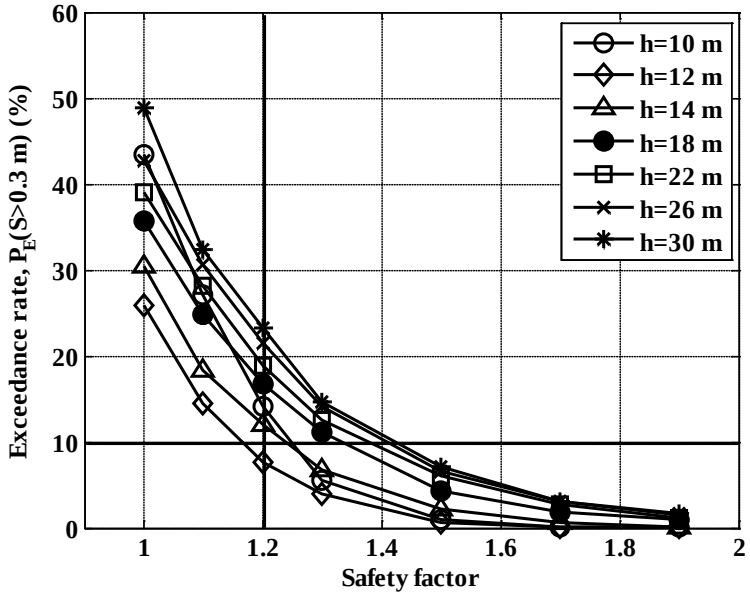

(b)

Fig 4. 13 Exceedance rate(S>0.3 m) of perforated-wall caisson for different safety factors in different water depths of (a) bottom slope=1/50, (b) bottom slope=1/20

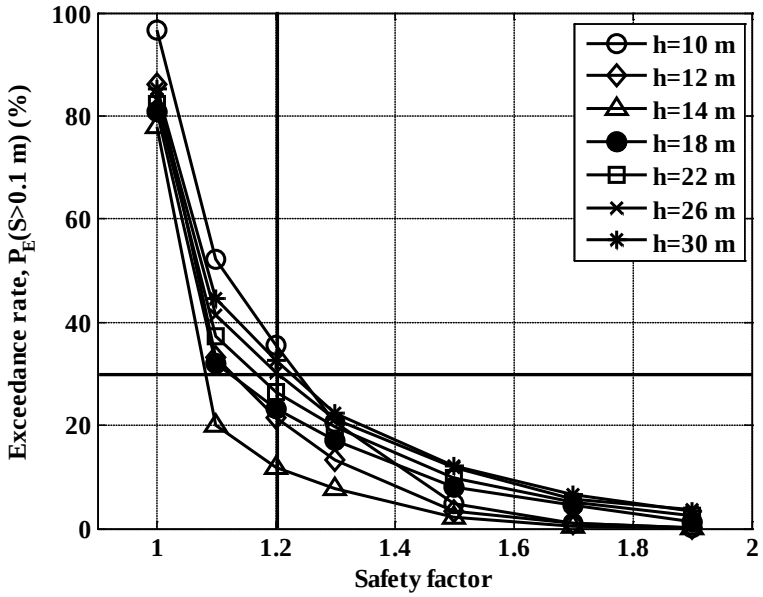

(a)

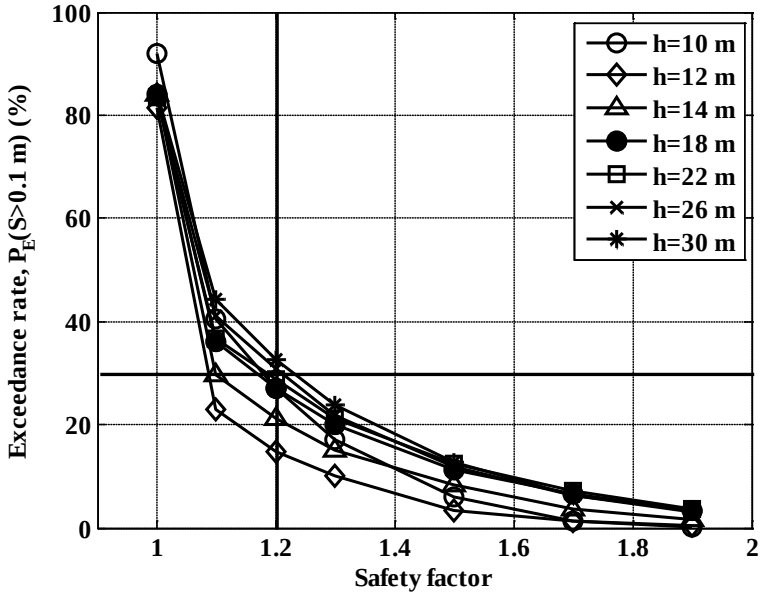

(b)

Fig 4. 14 Exceedance rate(S>0.1 m) of solid-wall caisson for different safety factors in different water depths of (a) bottom slope=1/50, (b) bottom slope=1/20

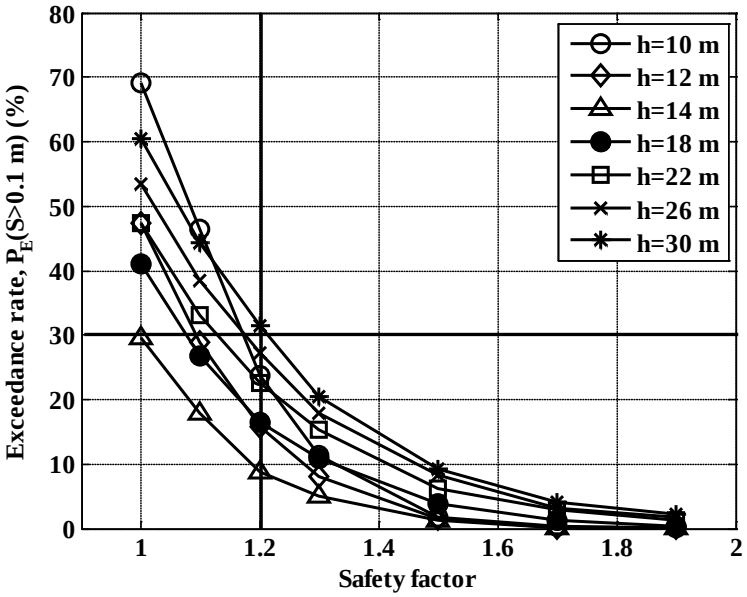

(a)

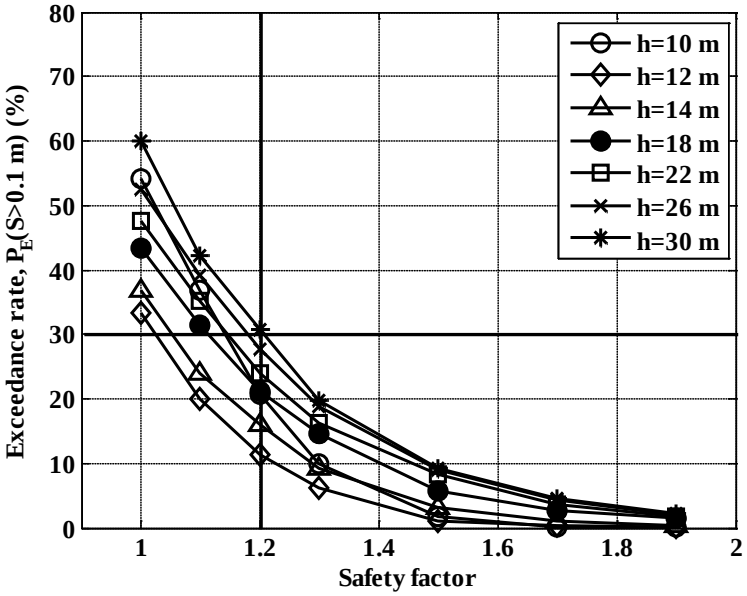

(b)

Fig 4. 15 Exceedance rate(S>0.1 m) of perforated-wall caisson for different safety factors in different water depths of (a) bottom slope=1/50, (b) bottom slope=1/20

4.4 Comparison and analysis

Fig 4. 16~Fig 4. 18 summarize and show the result of computations of the solid-wall caisson breakwater and the perforated-wall caisson breakwater.

Fig 4. 16 shows a comparison of the safety factor for sliding while satisfying the allowable expected sliding distance of 0.3m between the solid-wall caisson breakwater and the perforated-wall caisson breakwater depending on water depths. When the bottom slope is 1/50 and 1/20, both safety factors of the solid-wall caisson breakwater and the perforated-wall caisson breakwater are similar in their tendency inside the surf zone. Even though the safety factor of the solid-wall caisson breakwater is higher than the perforated-wall caisson breakwater outside the surf zone, the difference is not much.

Fig 4. 17 shows a comparison of the safety factor while satisfying the exceedance rate of 10 % of the sliding distance of 0.3 m between the solid-wall caisson breakwater and the perforated-wall caisson breakwater depending on water depths. For the bottom slope is 1/50 and 1/20, although the safety factor of the solid-wall caisson breakwater is higher than the perforated-wall caisson breakwater in all water depths, the difference is not much.

Fig 4. 18 shows a comparison of the safety factor while satisfying the exceedance rate of 30 % of the sliding distance of 0.1 m between the solid-wall caisson breakwater and the perforated-wall caisson breakwater depending on water depths. For the bottom slope is 1/50 and 1/20, although the safety factor of the solid-wall caisson breakwater is higher than the perforated-wall caisson breakwater in all water depths, the difference is not

much. In summary, the tendency of safety factor depending on water depths that satisfies the criteria for performance-based design method shows close similarity between the solid-wall caisson breakwater and the perforated-wall caisson breakwater.

Fig 4. 19~Fig 4. 21 show a comparison of caisson width between the performance-based design method and the deterministic design method depending on water depths. Here H_{0D} is the design wave height, B_p is the width of perforated-wall caisson breakwater in the performance-based design method, B_d is the width of perforated-wall caisson breakwater that satisfies the safety factor 1.2 in the deterministic design method. If the relative caisson width$\left(B_p / B_d\right)$ is less than 1, it means that the performance-based design method requires a smaller caisson width than the deterministic design method. For cases that the allowable expected sliding distance satisfies 0.3 m, the performance-based design method requires a bigger width than the deterministic design method and is non-economical in throughout the water depths, except inside the surf zone. If the exceedance rate of $S < 0.3$ m satisfies 10 % which is under the ultimate limit state, for both bottom slopes, in all water depths, except the location where the wave breaking occurs, the performance-based design method requires a bigger width and non-economical than the deterministic design method. In the repairable limit state, for both bottom slopes in all water depths, the performance-based method requires a smaller width and is economical than the deterministic design method. The tendency of the result is very similar each other for the allowable

expected sliding distance (Fig 4. 19) and the ultimate limit state (Fig 4. 20). In the repairable limit state (Fig 4. 21), there is no noticeable difference between different bottom slopes, and it shows the relative width of close to 1 when the water depth is the greatest and smallest, and it shows the value of less than 1 when it falls somewhere between. As it is shown in the researches by Kim et al. (2009), it is believed to be more reasonable to evaluate with the results of exceedance rate rather than with the allowable expected sliding distance.

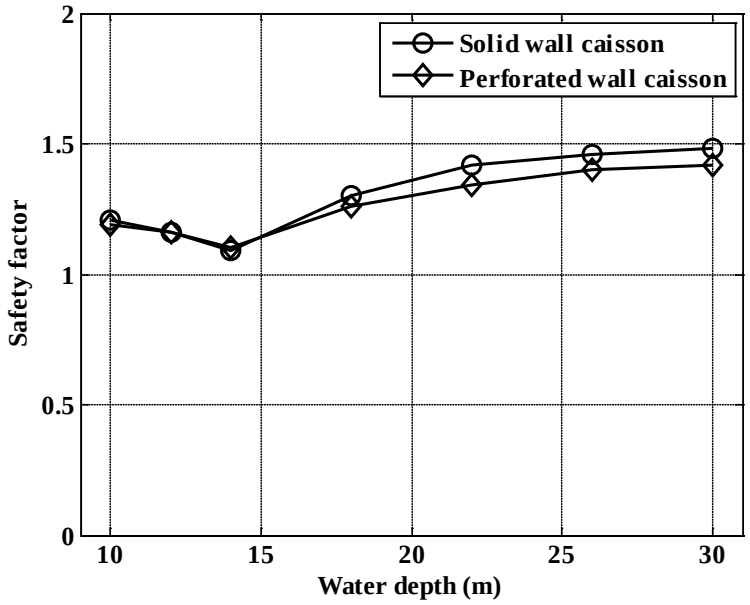

(a)

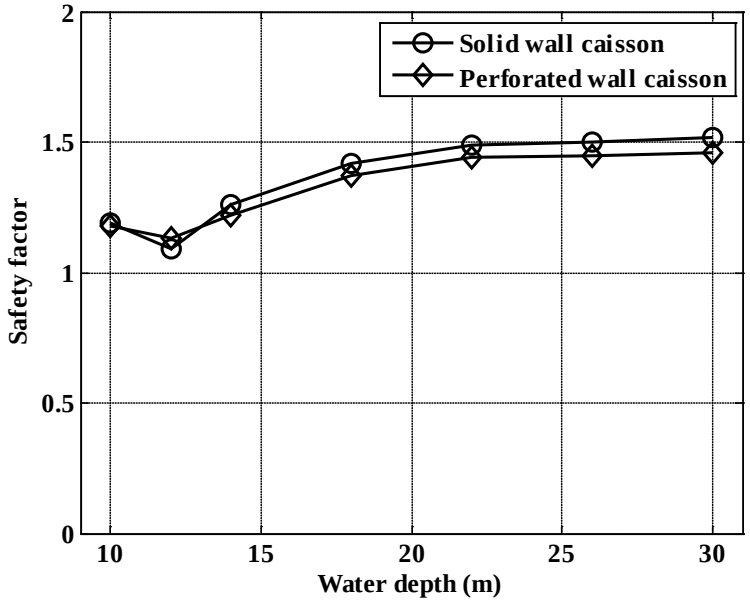

(b)

Fig 4. 16 Comparison of safety factors corresponding to allowable expected sliding distance of 0.3 m in different water depth of (a) bottom slope=1/50 (b) bottom slope=1/20

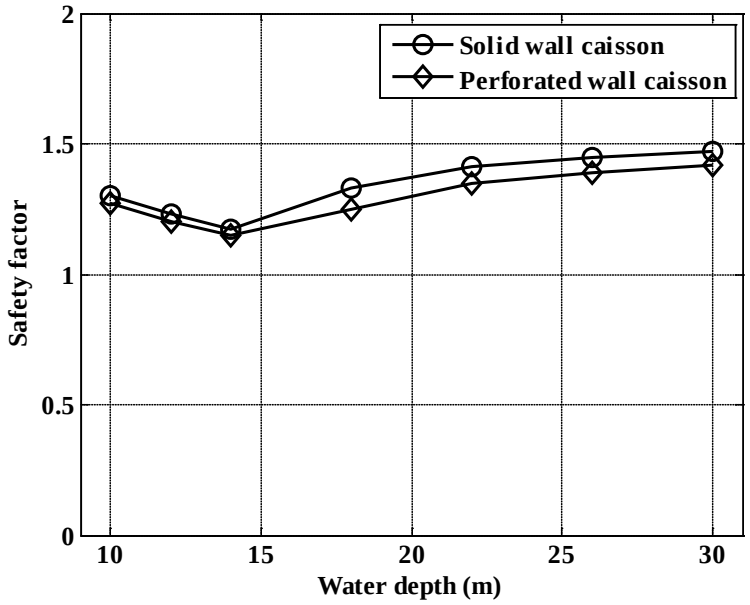

(a)

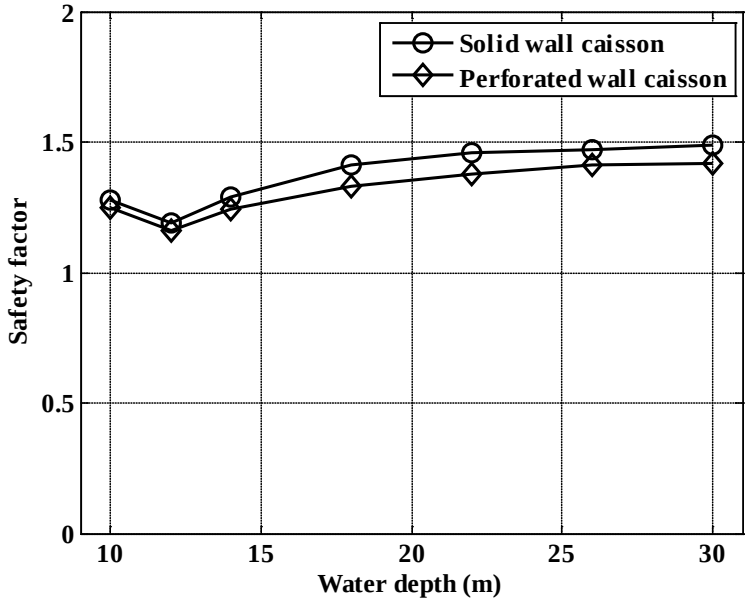

(b)

Fig 4. 17 Comparison of safety factors corresponding to exceedance rate for ultimate limit state in different water depths of (a) bottom slope=1/50 (b) bottom slope=1/20

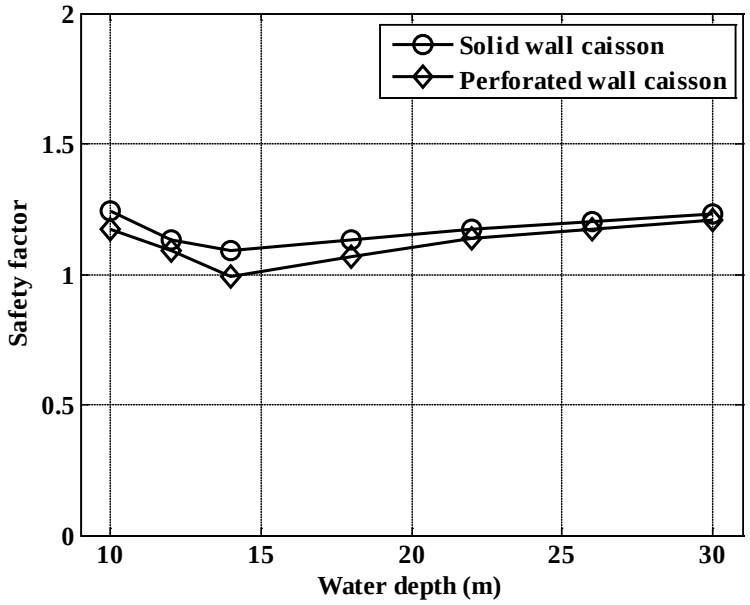

(a)

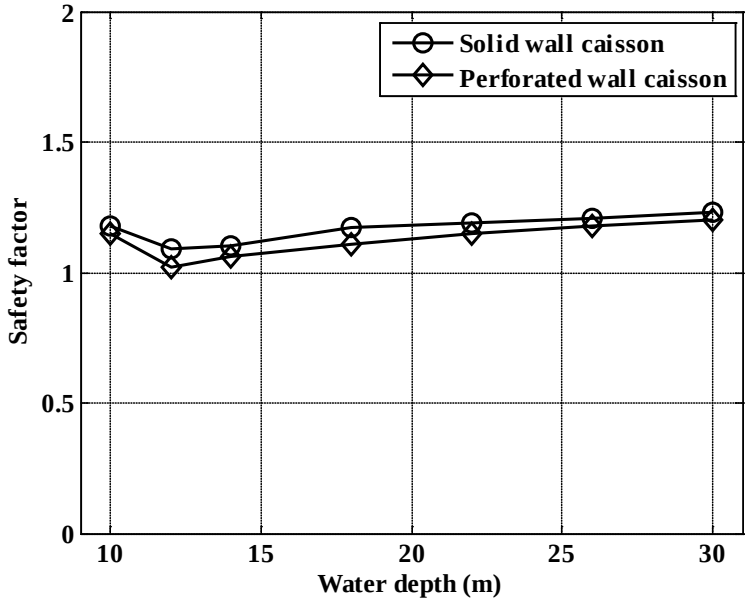

(b)

Fig 4. 18 Comparison of safety factors corresponding to exceedance rate for repairable limit state in different water depths of (a) bottom slope=1/50 (b) bottom slope=1/20

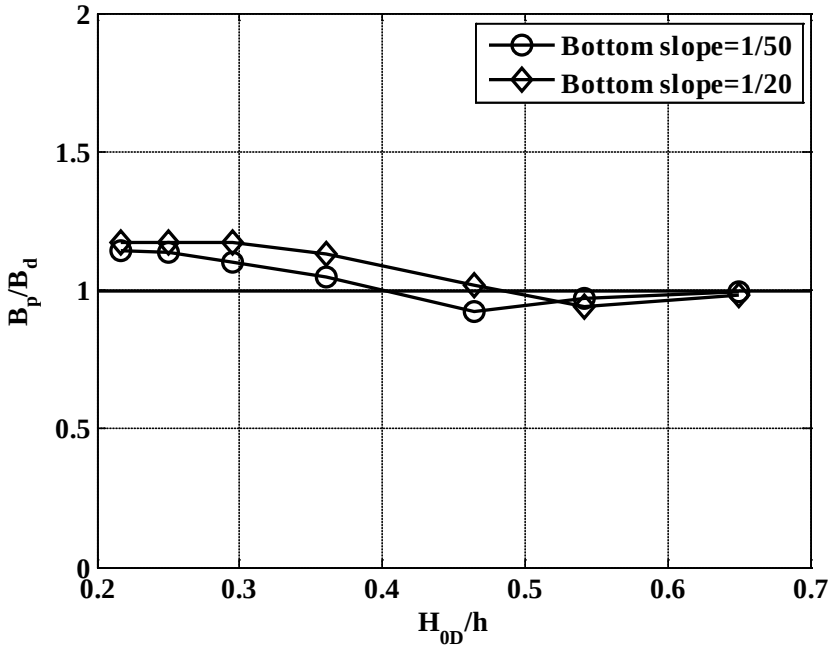

Fig 4. 19 Relative caisson width based on expected sliding distance of 0.3 m

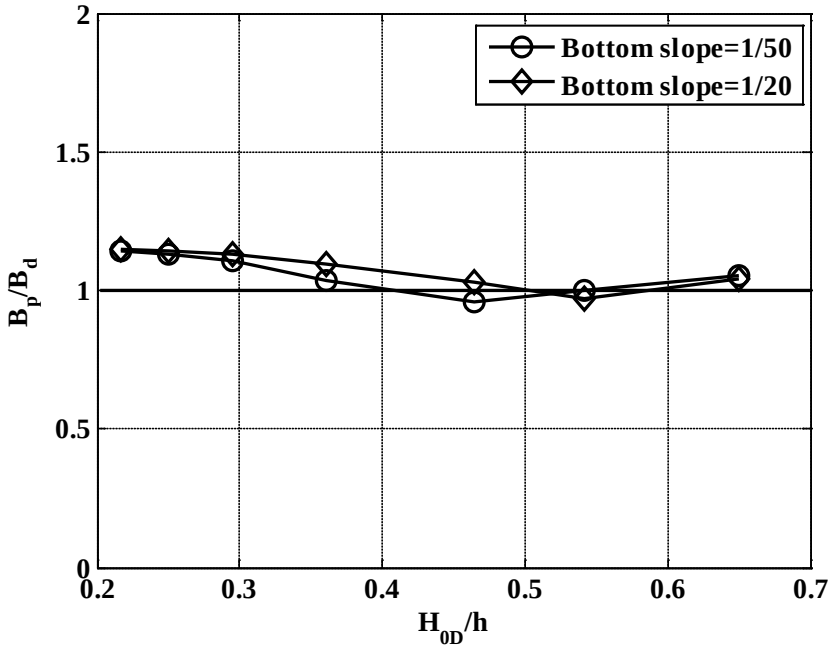

Fig 4. 20 Relative caisson width based on ultimate limit state (Exceedance rate of 10 % for total sliding distance of 0.3 m)

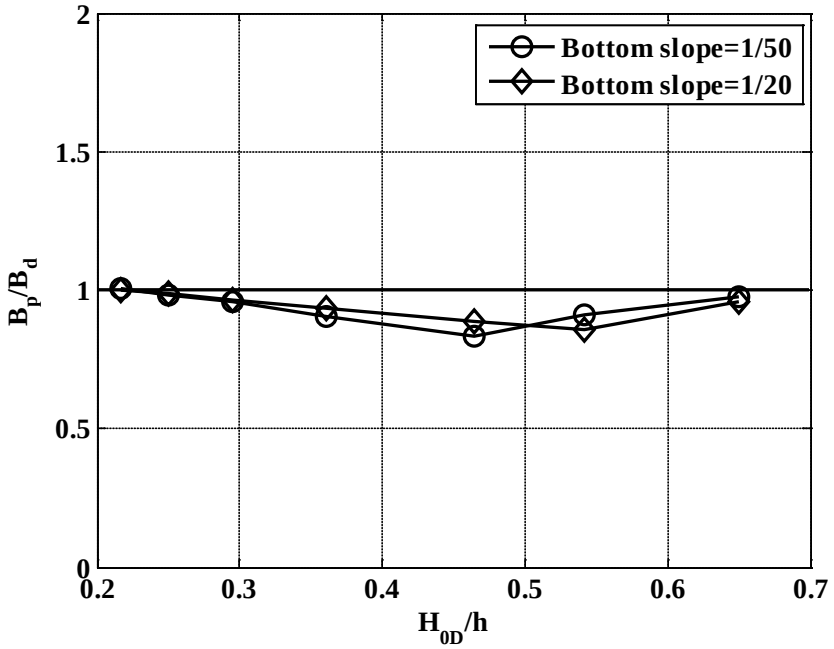

Fig 4. 21 Relative caisson width based on repairable limit state (Exceedance rate of 30 % for total sliding distance of 0.1 m)

CHAPTER 5 CONCLUSIONS AND FUTURE STUDY

5.1 Conclusions

This research was conducted by expanding and applying the performance-based design method that has been applied to the solid-wall caisson breakwater to the perforated-wall caisson breakwater. Also, after determining the cross-section by varying the safety factor, which is used in the deterministic design method, the analysis was mad by applying the cross-section to the performance-based design method. The analysis method employed the allowable expected sliding distance proposed by Takahashi et al. (2001), and the exceedance rate for an allowable sliding distance used by Kim et al. (2009) for the analysis.

The first purpose of this research is to examine the applicability of the model by comparing and analyzing the results from the performance-based design method used for the solid-wall caisson breakwater and the perforated-wall caisson breakwater. The solid-wall caisson breakwater's front wall consists of solid walls and there exists a high impulsive wave component since it absorbs the wave directly in the front. On the other hand, the perforated-wall caisson breakwater has the dissipating effect of wave force brought on by frontal perforated walls and wave chambers, there is a relatively low impulsive wave element compared to the solid-wall caisson breakwater. Therefore, the results of perforated-wall caisson breakwater (expected sliding distance, exceedance rate) show a safe result in overall compared to the solid-wall caisson breakwater, and their tendencies are

identical. Accordingly, there is little problem in applying the performance-based design method for the conventional solid-wall caisson breakwater to the perforated-wall caisson breakwater. Questions about which breakwater is more economical should be considered as a separate issue. The perforated-wall caisson breakwater has a relatively superior performance in wave reflection than the solid-wall caisson breakwater as shown in previous studies. The perforated-wall caisson requires a smaller weight since its safety factor is smaller than that for the solid-wall caisson breakwater. However, it is difficult to judge which is more economical since the reduction of weight of a perforated-wall caisson may cause an increase of caisson width compared with the solid-wall caisson. And since the perforated-wall caisson breakwater has a relatively more complexity in its configuration than the solid-wall caisson breakwater, the costs incurred in production and construction cannot be ignored. It is not possible to judge that the perforated-wall caisson breakwater is more economical than the solid-wall caisson breakwater just because the former is superior in caisson sliding.

The second purpose is to compare and analyze the results of the perforated-wall caisson breakwater between the performance-based design method and the conventional deterministic design method. Analysis of the allowable expected sliding distance and the exceedance rate under the ultimate limit state requires a bigger value than the estimated width in the deterministic design method, and therefore indicates that the performance-based design method is non-economical one. However, if it is a condition where requires a high safety factor by the judgment of an engineer, since a

bigger width can be determined even in the deterministic design method, it is not possible to simply determine that the performance-based design method to be non-economical for the allowable expected sliding distance and the ultimate limit state. Analysis of the exceedance rate under the repairable limit state requires a smaller value than the estimated width calculated by the deterministic design method, and therefore shows the performance-based design method an economical one.

Therefore, the design for sliding of the perforated-wall caisson breakwater by the performance-based design method in the repairable limit state (less than 30% of exceedance rate) is expected to be more efficient than the deterministic design method which uses the safety factor of 1.2 since it can reduce the width by 16%.

5.2 Future study

In the performance-based design for sliding of a caisson breakwater, the estimation of wave force and the distribution of time series have a strong influence on determining the sliding distance. For the solid-wall caisson breakwater, the estimation method of wave force and the time series have been proposed based on hydraulic model tests by numerous researchers. For the perforated-wall caisson breakwater, the estimation method of wave force was proposed based on hydraulic model tests under various conditions by Takahashi et al. (1991). Kim (2005) applied the wave pressure formula of Takahashi et al. (1991) to propose the times series of wave force acting on the perforated-wall caisson breakwater. This is an equation derived from the aspect of theoretical approach and is not derived from experiments. Although the calculated wave force is similar to the time series of wave force measured by the research of Takahashi et al. (1991), the wave force acting at the bottom of the wave chamber does not exists in the solid-wall caisson breakwater, so it may be unreasonable to assume the time series as a triangular distribution. Therefore, if the time series of the wave force on a perforated-wall caisson breakwater is proposed based on the experiments, more reasonable design results can be estimated in the future.

Secondly, since the reliability design method uses the probability distribution of design variables, the distribution estimation has a large influence on the design. The research on the distribution estimation of the solid-wall caisson breakwater has been actively conducted. However, the studies on the perforated-wall caisson breakwater are relatively scarce. This

study used the results of Takayama and Ikeda (1992) for the distribution of horizontal wave force acting on the perforated-wall caisson breakwater. However, since the formulae for wave force acting on the bottom of the wave chamber and uplift force have not been proposed, the formulae used for the solid-wall caisson breakwater were used. Therefore, the research on the probability distribution of the design variables applying to the perforated-wall caisson breakwater must be more actively conducted so that a more reasonable result of design can be predicted.

Third, the research for the allowable failure criteria for the sliding of a perforated-wall caisson breakwater is necessary. The allowable expected sliding distance and exceedance rate used in this research is the criteria that have been in use for the solid-wall caisson breakwater. For the perforated-wall caisson breakwater, it is believed that the allowable failure criteria for sliding is different from that of the solid-wall caisson breakwater and thereby needs a new allowable criteria.

References

Goda, Y. (1974). A new wave pressure formulae for composite breakwater, *Proc. 14th Int. Conf. Coast. Eng.*, ASCE, Copenhagen, 1702-1720.

Goda, Y. (1975). Deformation of irregular waves due to depth-controlled wave breaking. *Rep. of Port and Harbour Engineering,* 14(3), 5012-5018.

Goda, Y., and Suzuki, Y. (1975). Computation of refraction and diffraction of sea waves with Mitsuyasu's directional spectrum, *Tech. Note of Port and Harbour Res. Inst.* 230, 45.

Goda, Y., Takagi, H. (2000). A reliability design method of caisson breakwaters with optimal wave height. *Coast. Eng. J*. 42. 357-387.

Goda, Y. (2003). Revisiting Wilson's formulas for simplified wind wave prediction. *J. Waterw., Port, Coast. Ocean Eng.,* 129(2), 93-95.

Goda, Y. (2010). *Random seas and design of maritime structures, 3rd ed., World Scientific, 3rd ed,* World Scientific, Singapore.

Hong, S. Y., Suh, K.D., and Kweon, H.M. (2004). Calculation of expected sliding distance of breakwater caisson considering variability in wave direction. *Coastal Eng. J.*, 46(1), 119-140.

Huang, Z., Li, Y., Liu, Y. (2011). Hydraulic performance and wave loadings of perforated/slotted coastal structures: A review. *Ocean Eng*. 38, 1031-1053.

Iwagaki Y., and Sakai, T. (1968). On the shoaling of finite amplitude waves (2), *Proc. 15th Japanese Conf. Coastal Eng*, 59-106.

JPHA (2007). Japan Port and Habor Association, *Technical Standards and Commentaries of Port and Harbor Facilities in Japan* (in Japanese)

Kim, D.-H. (2005). Calculation of expected sliding distance of wave dissipating caisson breakwater, *J. Korea Society of Coast. Ocean Eng.*, 17(4), 213-220. (in Korean)

Kim, S.-W., Suh, K.-D., (2006). Application of reliability design methods to Donghae harbor breakwater, *Coast. Eng. J.* 48(1), 31-57.

Kim, S.-W., Suh, K.-D., Oh, Y. M., (2006). Comparative study of reliability design methods by application to Donghae harbor breakwaters: 2. Sliding of caissons, *J. Korea Society of Coast. Ocean Eng.*, 18(2), 137-146. (in Korean)

Kim, S.-W., Suh, K.-D. (2009). Exceedance probability of allowable sliding distance of caisson breakwaters in Korea, *J. Korea Society of Coast. Ocean Eng.*, 21(6), 495-507. (in Korean)

Kim, T. M., and Takayama, T. (2003). Computational improvement for expected sliding distance of a caisson-type breakwater by introduction of a doubly-truncated normal distribution. *Coast. Eng. J,* 45(3), 387-419

Korea Ocean Research and Development Institute. (1992). *Basic design study of offshore breakwater(Hydraulic model test-II).* (in Korean)

Ministry of Land, Transport and Maritime Affairs. (2011). *Standards for the breakwater reliability design.* (in Korean)

Mitsuyasu, H., Tasai, F., Suhara, T., Mizuno, S., Ohkuso, M., Honda T., and Rikiishi, K. (1977). Observations of the directional spectrum of ocean waves using a cloverleaf buoy, *J. Phys. Oceanogr.*, Vol. 5, 750-760.

Oumeraci, H., Kortenhaus, A., Allsop, W., de Groot, M., Grouch, R., Vrijling, H., Voortman, H. (2001). *Probabilistic design tools for vertical breakwater,* Sweta & Zeitlinger B.V., Lisse.

Overseas Coastal Area Development Institute of Japan (OCDI) (2009). Technical standards and commentaries for port and harbor facilities in Japan.

Shimosako, K., and Takahashi, S. (1998). Reliability design method of composite breakwater using expected sliding distance. *Rep. of Port and Harbor Res. Inst,* 47(3), 3-30. (in Japanese)

Shimosako, K., and Takahashi, S. (1999). Application of deformation-based reliability design for coastal structures, *Proc. Int. Conf. Coastal Struct., 1999,* A. A. Balkema, Spain, 363-371.

Shimosako, K., and Tada, T. (2004). Verification procedures of performance-based design on the sliding stability of composite breakwaters, *Proc. Tech-Ocean 2004.*, 53-58.

Suh, K.-D., Kweon, H.-D., Lee, D.-Y. (2008). Statistical characteristics of deepwater waves along the Korean coast, *J. Korea Society of Coast. Ocean Eng.*, 20(4), 342-354. (in Korean)

Suh, K-D., Kwon, H-D., Lee, D-Y. (2010). Some characteristics of large deepwater waves around the Korean Peninsula, *Coast. Eng.*, 57, 375-384.

Suh, K-D., Kim, S-W., Mori, N., Mase, H. (2012). Effect of climate change on performance-based design of caisson breakwaters. *J. Waterway, Port, Coast., Ocean Eng.*, 138, 215-225.

Suh, K-D., Kim, S.-W., Kim, S., Cheon, S. (2013). Effects of climate change on stability of caisson breakwaters in different water depths. *Ocean Eng.*, 71, 103-112.

Takahashi, S., Shimosako, K. and Sasaki, H. (1991). Experimental study on wave forces acting an perforated wall caisson breakwaters. *Rep. of port and harbor Res. Inst.* 30(4). 3-34 (in Japanese).

Takahashi, S., Tanimoto, K., and Shimosako, K. (1994). A proposal of impulsive pressure coefficient for the design of composite breakwaters. *Proc. Int. Conf. Hydro-Tech. Eng. Port and Harbour Const.*, Yokohama, Japan, 489-504.

Takahashi, S., Tanimoto, K., and Shimosako, K. (1994). Wave pressure on a perforated wall caisson. *Proc. Int. Conf. Hydro-Tech. Eng. Port and Harbour Const.*, Yokosuka, Japan, 747-764.

Takahashi, S., Shimosako, K., Kimura, K., Suzuki, K. (2000). Typical failure of composite breakwaters in Japan. *Proc. 27th Int. Conf. Coast. Eng.*, 1899-1910.

Takayama, T., Ikeda, N. (1992). Estimation of sliding failure probability of present breakwaters for probabilistic design. *Rep. of the Port and Hab. Res. Inst.*, 31(5), 3-32.

Tanimoto, K., and Takahashi, S. (1994). Design and construction of caisson breakwater – the Japanese experience. *Coast. Eng.*, 22, 57-77.

U.S. Army Coastal Eng. Res. Center. (1977). *Shore Protection Manual 3rd edn.*, U.S. Government Publishing Office, Washington, D.C., USA.

초 록

유공케이슨 방파제의 활동에 대한 설계법 비교 연구

서울대학교 대학원

건설환경공학부

김 남 훈

케이슨 방파제를 설계함에 있어서 방파제의 주요 파괴 모드인 활동에 대하여 안전율을 이용하는 결정론적 설계법이 사용되어 왔다. 하지만 구조물에 작용하는 하중과 구조물의 저항력 등에 대한 불확실성을 안전율이라는 간단하지만 경험적인 상수를 대신하기 때문에 활동량에 대한 정량적, 상대적인 평가가 어려워 구조물을 과대 혹은 과소 설계할 가능성을 내포하고 있다. 이러한 설계변수의 불확실성을 확률적 개념으로 고려하여 케이슨의 활동량을 계산하는 성능 설계법이 제안되고 있다. 무공케이슨 방파제의 성능 설계법은 과거 여러 연구자들에 의해 연구가 진행되어 왔으며, 현재 그 틀이 거의 잡혀져 있다 해도 과언이 아니다. 반면, 유공케이슨 방파제의 경우 전면의 유공벽 구조에 의한 파력 감쇄에 따라 구조물의 안정성이 증대되는 효과가 있음에도 불구하고 이와 관련된 연구는 국내·외적으

로 아직 많이 이루어지지 않았다.

본 연구에서는 기존의 무공케이슨 방파제의 성능 설계법 이론을 유공케이슨 방파제에 확장, 적용하여 이론의 적용 가능성 여부를 판단한다. 또한 결정론적 설계법의 결과와 비교 분석하여 합리적인 설계법을 결정 한다. 이는 유공케이슨 방파제의 성능 설계법에 대한 기준을 제시하기 위해 수행되는 기초 연구이다. 따라서 향후 유공케이슨 방파제의 성능 설계에 매우 중요한 지표가 될 것으로 예상된다.

주요어: 유공케이슨 방파제, 신뢰성 설계법, 성능 설계법, 기대활동량, 초과확률

학번: 2012-20892

공학석사 학위논문

유공케이슨 방파제의 활동에 대한 설계법 비교 연구

Comparative study of design methods for sliding of perforated wall caisson breakwater

2014년 02월

서울대학교 대학원

건설환경공학부

김 남 훈

ABSTRACT

Comparative Study of Design Methods for Sliding of Perforated Wall Caisson Breakwater

Nam-Hoon, Kim

Department of Civil and Environmental Engineering

The Graduate School

Seoul National University

In the design of a caisson breakwater against sliding, the deterministic design method has been used with consideration of certain margin of safety factor. However, it is difficult to quantitatively and comparatively evaluate the sliding distance using the safety factor because of the uncertainty of the design variables. It may cause the over- or under-design of the structure. Therefore, it is required to develop probabilistic design methods (e.g., performance-based design method) to consider the uncertainties of the design variables by computing the sliding distance of the caisson. The performance-based design method of a solid-wall caisson breakwater has been investigated by many researchers and its framework is almost completed. On the other hand, researches on a perforated-wall caisson breakwater have been scarcely made despite the fact that it has greater structural safety due to decreased impulsive wave force at the perforated-wall.

In this study, the conventional performance-based design method of the solid-wall caisson breakwater has been expanded and applied to the perforated-wall caisson breakwater in order to examine the feasibility of its application. In addition, a comparative analysis is made between the deterministic design method and performance-based design method. It will serve as a basic research to standardize the criteria of the performance-based design method of a perforated-wall caisson breakwater. Moreover, it is expected to be an important and useful tool in designing a stable perforated-wall caisson breakwater in the future.

Keywords: Perforated-wall caisson breakwater, reliability design method, performance-based design method, expected sliding distance, exceedance rate

Student number: 2012-20892

CONTENTS

LIST OF TABLES

LIST OF FIGURES

LIST OF SYMBOLS

Latin upper case

B	Caisson width
B_c	Chamber width
B_M	Berm width
F_D	Force related sliding velocity including the wave-making resistance force
F_R	Resistance force
$G(\theta \mid f)$	Directional spreading function
H	Individual wave height
H_b	Breading wave height
$H_{\max}$	Maximum wave height at breakwater site
H_0	Offshore wave height
H_0'	Equivalent deepwater wave height
$H_{1/3}$	Significant wave height
$H_{1/3e}$	Significant wave height through wave transformation
H_{0e}	Sample of extreme distribution of deepwater wave height
$(K_r)_{eff}$	Effective refraction coefficient
K_s	Nonlinear shoaling coefficient
K_{si}	Linear shoaling coefficient

L	Probabilistic variable of load component or Wave length
L'	Wave length at d'
L_0	Deep water wave length
M_a	Added mass
N	Total number of simulation
P_e	Exceedance rate
P_f	Probability of failure
P_H	Horizontal wave force
P_I	Horizontal wave force at Crest I
P_{IIa}	Horizontal wave force at Crest IIa
P_{IIaM}	Wave force acting on the chamber at Crest IIa
P_{IIb}	Horizontal wave force at Crest IIb
P_{IIbM}	Wave force acting on the chamber at Crest IIb
P_U	Uplift force
P_V	Chamber force
R	Probabilistic variable of resistance component
$S_0(f)$	Frequency spectrum
$S_0(f,\theta)$	Offshore directional wave spectrum
$T_{1/3}$	Significant wave period
U	Uplift force
U_I	Uplift force at Crest I
U_{IIa}	Uplift force at Crest IIa

U_{IIb}	Uplift force at Crest IIb
W	Caisson weight in the air
W'	Caisson weight in water
Z	Design criterion that can judge the success and failure of structure

Latin lower case

d	Water depth at the top of foot protection
d'	Water depth of the wave chamber
f	Wave frequency
f_{DTN}	Probability density function of doubly truncated normal distribution
f_p	Peak wave frequency
h	Water depth
h'	Water depth at the top of rubble mound foundation
h_c	Crest elevation
h_{c1}	Crest elevation of perforated wall
h_{c2}	Crest elevation of solid wall
m_0	Zeroth moments of the frequency spectrum
n	Number of failure state in the simulation
n_e	Number of limit state in the simulation
r	Random variables
r'	Random variables using doubly-truncated normal distribution

s	Directional spreading parameter
s_a	Allowable sliding distance
$s_{\max}$	Peak value of directional spreading parameter
t_d	Time difference of wave force between Crest I and Crest IIa
t_m	Start time of wave force acting on the wave chamber
x_G	Horizontal displacement of caisson

Greek upper case

$\Gamma(\cdot)$	Gamma function

Greek lower case

α	Scale parameter of Weibull distribution
α_1	Parameter for a standing wave force
α_2	Parameter for an impulsive wave force
α_I	Parameter for an impulsive wave force proposed by Takahashi et al. (1994)
α_{X_i}	Bias coefficient of design variables
α^*	Maximum value between α_2 and α_I
β	Wave direction
η^*	Run-up height

ε	Opening ratio of the perforated wall
ε'	Reduction rate of wave force
γ_{X_i}	Variation coefficient of design variables
ξ	Location parameter of Weibull distribution
κ	Shape parameter of Weibull distribution
$\lambda_1, \lambda_2, \lambda_3$	Correction coefficient for vertical caisson breakwater
λ_S	Correction coefficient for perforated front wall
λ_L	Correction coefficient for solid front wall
λ_R	Correction coefficient for solid rear wall
λ_M	Correction coefficient for wave chamber
λ_U	Correction coefficient for uplift
μ	Friction coefficient
μ_{X_i}	Mean of design variables
σ_{X_i}	Standard deviation of design variables
θ	Angle of the bottom slope
τ_0	Duration of impulsive wave
τ_0'	Duration of wave force at Crest IIa

CHAPTER 1 INTRODUCTION

1.1 Necessity and background of research

Existing harbor structures have been generally designed by the deterministic design method. The safety factor is calculated with the force acting on the structure during the lifetime. The safety factor is then compared against the requirement of safety factor to judge the safety of the structure. It is assumed that the uncertainty of the load on and resistance of the structure can be determined by using the safety factor as an evaluation index. However, it poses a possibility of over- or under-estimation of structure dimension since the quantitative and comparative evaluations of a structure displacement are not easy.

In order to overcome the shortcomings of the deterministic design method, a probabilistic design method has been used since 1970's, which now is known as a reliability design method. The reliability design methods for coastal structures have been studied since the mid 1980's. In place of the safety factor of the deterministic design method, reliability design method considers the probabilistic uncertainty of the design variables affecting the failure of the structure. This method is such that probability of failure is within an allowable limit to satisfy stability, functionality, and economic feasibility of the structure.

Failure modes of caisson breakwaters are sliding, overturning, and geotechnical failure of rubble mound foundation. Failure of caisson breakwaters is dominated by sliding among these modes. A concept of

expected sliding distance of caisson breakwaters has been adapted first in Japan. It uses a probability distribution of wave height and time series of wave force and makes repeated computations of cumulative sliding distances that may occur during the lifetime. The sliding distances are then averaged to determine the expected sliding distance. This has been recognized as a significant measure to evaluate performance of breakwaters. There are two typical types of caisson breakwaters: a solid-wall caisson breakwater and a perforated-wall caisson breakwater; the former consists a solid frontal wall and the latter a perforated frontal wall.

Computation models for the expected sliding distance of a solid-wall caisson breakwater have been researched in large volume and its framework is almost fully established. On the other hand, researches on the perforated-wall caisson breakwaters are scarce either at home or abroad despite the fact that it poses great structural stability due to decreased impulsive wave force with good wave dissipation at the perforated wall.

This research is done as a fundamental study to develop a performance-based design method of the perforated-wall caisson breakwater. Its main purpose is to compare and analyze the pros and cons of the perforated-wall caisson breakwater, while the performance-based design method mostly applied to the solid-wall caisson breakwater is expanded to be applied to the design of the perforated-wall caisson breakwater.

1.2 Research trends

The reliability design method which reflects uncertainties of the design variables into the structure design has become to be recognized as a major technology to proactively manage the structural risks throughout the world. A design criteria ISO 2394 of International Organization for Standardization (ISO) requires a probabilistic design of a structure. The reliability theory has already been introduced all over the world in harbor structure designs for this reason and the establishments of international standards have been centered around Japan (JPHA, 2007; OCDI, 2009) and Europe (ECS, 1991, 1992). Thus, the trend of civil engineering structure design is moving away from the deterministic design method toward the probabilistic design method. In order to come up with performance-based reliability design criteria against natural disaster in Korea to be in line with global trends, the Ministry of Land, Transport and Maritime Affairs had initiated the reliability design method studies to be applied to harbor structure designs with Korea Institute of Ocean Science and Technology (formerly the Korea Ocean Research and Development Institute) since 2006. In 2011, it published the standards for the breakwater reliability design (2011).

A performance-based design method which determines the reliability of the caisson structure with the expected sliding distance has been suggested by Shimosako and Takahashi (1999) and Goda and Takagi (2000), and has been used by numerous researchers at home and abroad. In Korea, Hong et al. (2003) expanded Shimosako and Takahashi (1999) model and computed the expected sliding distance of the solid-wall caisson breakwater considering the

variability of wave directions. While Shimosako and Takahashi (1999) had only considered the unidirectional irregular wave entering a harbor with normal incidence to an area with shore-parallel contours, Hong et al. (2003) had considered effects of shoaling, refraction and breaking of multi-directional irregular wave that are closer to actual situations. The reliability analysis shows that the variability of wave direction significantly affects the expected sliding distance of caissons and gives possibility of a cost-effective design. Kim et al. (2003) computed the expected sliding distance of the solid-wall caisson breakwater using the doubly-truncated normal distribution for the friction coefficient and wave force in order to overcome limitations of the normal distribution. Since the normal distribution of the horizontal wave force and friction coefficient may be distributed from negative infinity to positive infinity, there is a possibility to extract a design value that may not occur. To correct this, a doubly-truncated normal distribution using the upper and lower limits based on research results of Takayama and Ikeda (1992) that were closer to actual situations are used. Kim (2005) proposed to use time series of wave force based on Shimosako and Takahashi (1999) model and made computations of the expected sliding distance for the perforated-wall caisson breakwater. Kim et al. (2009) identified the limitations while evaluating the reliability with the expected sliding distance and came up with solutions to structural reliability evaluation by computing the exceedance rate of an allowable sliding distance. Suh et al. (2012) made a computation of expected sliding distance of the solid-wall caisson breakwater considering the climate change effect. They predicted increases in expected sliding distance of the

solid-wall caisson breakwater in the future due to sea level rise caused by climate change effect.

Computation of expected sliding distance has been studied by numerous researchers and Table 1. 1 demonstrates the summary. However, majority of researches were on the expected sliding distance of the solid-wall caisson breakwaters except Kim (2005). There is not much study available on the expected sliding distance of the perforated-wall caisson breakwaters until recently.

The reliability design method is being actively researched worldwide and Japan and other countries are already using the new design method. The clarified standards for domestic introduction are believed to be very important at this point. Thus, it is very critical to study the less researched perforated-wall caisson breakwaters and appropriate standards should be established.

Table 1. 1 Research trend of performance-based design of caisson breakwater

Year	Author	Contribution	Caisson type
1999	Shimosako and Takahashi	First proposal of performance-based design method	Solid wall
2000	Goda and Takagi	Improvement of the method proposed by Shimosako and Takahashi (1999)	Solid wall
2003	Hong et al.	Variability in wave direction	Solid wall
2003	Kim et al.	Doubly-truncated normal distribution	Solid wall
2005	Kim	Time series of perforated-wall caisson breakwater	Perforated wall
2009	Kim et al.	Exceedance rate of allowable sliding distance	Solid wall
2012	Suh et al.	Effect of climate change	Solid wall

1.3 Research details and methodology

This study mainly uses the performance-based design method among the probability design methods that is used in Japan. The performance-based design method uses a pre-determined acceptable expected damage to design a structure within that expected damage (Standards for the breakwater reliability design, 2011). Basic concept of the performance-based design method assumes that every load and resistance factors have different probability density functions, makes enough number of simulations in order to simulate the uncertainty of randomly fluctuating load and resistance factors and computes approximated probability of failure. It basically is the same concept as the Level III reliability design method with only difference in evaluation criteria of structural reliability which could be either a probability of failure or expected damage.

The performance-based design method of caisson breakwaters uses the expected sliding distance as the expected damage which requires wave data at the location of the breakwaters. The wave height may be the most important factor in computing the wave force of the structure in designing the caisson breakwaters and it plays a major role in determining the cross-section of the structure. To predict the structural reliability against the uncertainty of wave height in the performance-based design method, deepwater wave heights defined by the probability distribution function are used. Deepwater waves will be transformed into the waves at breakwater site by water depth, tidal level, wave direction and boundary conditions. The wave force acting on the caisson breakwater is computed using the transformed shallow water waves.

Total sliding distance during lifetime can be computed based on this and the expected sliding distance is computed with an average of the repeated simulations. But one limitation of this method is that an actual sliding distance may exceed the expected sliding distance since it is an average of simulated sliding distance within lifetime. In order to overcome this limitation, Kim et al. (2009) evaluated the stability by computing the exceedance rate for an allowable sliding distance.

The most dominant factor that affects the sliding of the caisson breakwaters is the wave force acting on the caisson. Caissons are typically either a solid-wall or perforated-wall shapes; former having solid frontal walls, latter perforated frontal walls. Sliding distance of the solid-wall caisson breakwater can be computed using the maximum wave force proposed by Goda (1974) with application of the wave force and time series model developed by Shimosako and Takahashi (1998 and 1999). However, it cannot be applied to the perforated-wall caisson breakwaters which have different maximum wave force and time series due to the wave dissipation at the perforated frontal wall. In general, the wave force acting on the perforated-wall caisson breakwaters is less than that of the solid-wall caisson breakwaters because of wave force reduction due to the wave dissipation at the perforated frontal wall. Takahashi et al. (1991) computed the wave force acting on the perforated-wall caisson breakwaters by expanding the Goda (1974) model and Kim (2005) computed the expected sliding distance by developing and applying the wave force and time series model of the perforated-wall caisson breakwaters using previous research results. In this

study, the expected sliding distance and exceedance rate is computed by applying the wave force time series model of the perforated-wall caisson breakwaters developed by Kim (2005) to the performance-based design method. This study is very important in providing information to the performance-based design of the perforated-wall caisson breakwaters in the future with its comparison analysis of the pros and cons of the existing deterministic design method and performance-based design method of the solid-wall caisson breakwaters.

CHAPTER 2 THEORITICAL BACKGROUND

2.1 Deterministic design method

In the deterministic design method, the caisson is considered to be safe against sliding if the safety factor does not exceed 1.2 (Goda, 2010).

$$S.F = \frac{\mu\left[\left(W' + P_V\right) - P_U\right]}{P_H} \tag{2.1}$$

The Eq. (2.1) represents a safety factor of a caisson sliding used in the deterministic design method, where μ is a friction coefficient between the caisson and rubble mound foundation, W' the caisson weight in water, P_U the uplift force, P_H the horizontal wave force acting on the caisson, and P_V is the wave force acting on the lower part of the wave chamber. In the deterministic design method, sliding of caisson will occur if the S.F. exceeds 1.2 and the caisson will be unstable.

S.F. of the caisson breakwater can be computed according to Fig 2. 1, and the stability can be determined by changing the structure dimension in comparison with allowed safety factor of 1.2.

In the perforated-wall caisson breakwaters, there is a phase difference between the forces acting on the perforated frontal wall and solid rear wall. To cope with this situation, Takahashi et al. (1991) had distinguished the phase by Crest I, Crest IIa and Crest IIb in terms of the acting states of wave force. In addition, there are wave chambers in the perforated-wall caisson breakwaters to dissipate the wave energy. Thus, the horizontal wave force,

wave force acting on the lower part of the wave chamber and the uplift force can be computed for different phases to determine different S.F's. The minimum S.F. will be used in the design. In the solid-wall caisson breakwater, S.F. is computed with the horizontal wave force and uplift force from the wave force formula of Goda (1975). Since there is no wave chamber in the solid-wall caisson breakwaters, the wave force acting on the lower part of the wave chamber should be 0 in Eq. (2.1).

2.2 Reliability design method

2.2.1 Overview of reliability design method

The reliability design method uses a pre-determined design standard Z and analyzes the relationship between structural load L and resistance R to validate the structural safety.

$$Z = R - L \tag{2.2}$$

where the structure is safe if $Z > 0$, there is sliding if $Z < 0$, and it is on safety boundary if $Z = 0$. Eq. (2.2) is an equation derived depending on the form of failure of the target structure and defined as a failure function, limit state function or safety margin.

In the existing deterministic design method, the structural safety was determined by the safety factor in consideration of representative $\overline{R}$ and $\overline{L}$ without considering the statistical characteristics of R and L: where there is a safety margin if $\overline{R} > \overline{L}$ to maintain a proper safety factor. However, the concept of the reliability design method takes into consideration the statistical properties of the design variables with changing characteristics of R and L, even if the same safety factor is maintained with consistent representative values.

Therefore, considering the probability of failure depending on the statistical characteristics of the design variables is a much better alternative than the safety factor method considering only the representative values of the design variables in evaluating the structural stability.

2.2.2 Level III reliability design method

The reliability design method is classified as Level I, II and III depending on the degree of probabilistic concepts. Level III reliability design method directly assigns the randomly generated probabilistic variables that follow certain distribution functions into the limit state function by considering every design variables as probabilistic variables. Level III reliability design method mostly used the Monte-Carlo Simulation (MCS) which is one of the most common ways to estimate the probability of failure. In the MCS, uniformly distributed random number between 0 and 1 is extracted and changed to a random number that best reflects the distribution characteristic of the probability variables, to generate samples of sufficient size. Generated probabilistic variables will be assigned into the limit state function to determine the structural safety. The probability of failure for $Z \le 0$ in the limit state function of Eq. (2.2) is expressed as the following.

$$P_f = P\left(Z \le 0\right) = \lim_{x \to \infty} \frac{n}{N} \tag{2.3}$$

where, N is the number of total simulations, and n is the number of simulations for $Z \le 0$ in the limit state function. The accuracy of the probability of failure estimated by Eq. (2.3) depends on the number of simulations. n / N is a statistical variable of the extracted distribution and is dependent on the number of simulations N, especially for a variance. In case of small N or a low probability of failure, the probability of failure given by n / N has considerable uncertainty. Thus, the number of total simulations N

has to be determined depending on the probability of failure.

2.2.3 Performance-based design method

The performance-based design method designs a structure such that the expected failure is within a pre-determined allowable expected failure by assuming that a structure will maintain its function within the pre-determined allowable expected failure. The performance-based design method has basically the same concept as the Level III reliability design method. In other words, the breakwater is designed to maintain its function during its lifetime without any problems. But the two methods have a slightly different interpretation. Level III reliability design method computes the probability of failure of the load that might exceed the resistance considering the uncertainty of randomly changing load and resistance factors with an assumption that all load and resistance factors have different probability density functions. On the other hand, the performance-based design method predicts the sliding distance kinetically per each wave conditions to keep the expected values of the sliding distance below the allowable value (Standards for the breakwater reliability design, 2011).

In the performance-based design method, the sliding distance of the caisson is considered as the criterion of the structural functionality so that the expected sliding distance during the lifetime of the structure is calculated to determine the stability of the caisson breakwater. However, the expected sliding distance of the caisson breakwater possesses a limitation to be an

evaluation standard of the stability of the caisson. Since the expected sliding distance is an average of a number of simulations, sometimes the actual sliding distance can exceed the average. In order to overcome such shortcoming, Kim et al. (2009) identified the limitations that might occur in evaluating the stability with the expected sliding distance and computed the exceedance rate for an allowable sliding distance and evaluated the structural stability.

The expected sliding distance and the exceedance rate of the caisson breakwaters can be computed following the procedure in Fig 2. 2 and the structural reliability can be determined by comparing with the allowable values.

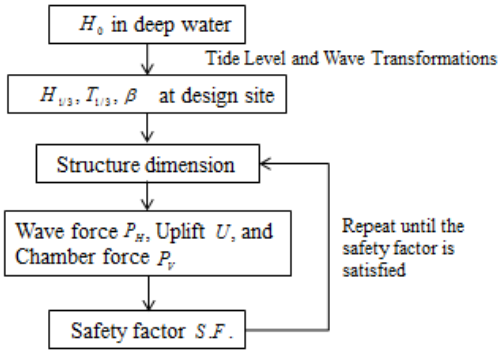

Fig 2. 1 Schematic flow chart for computation of safety factor

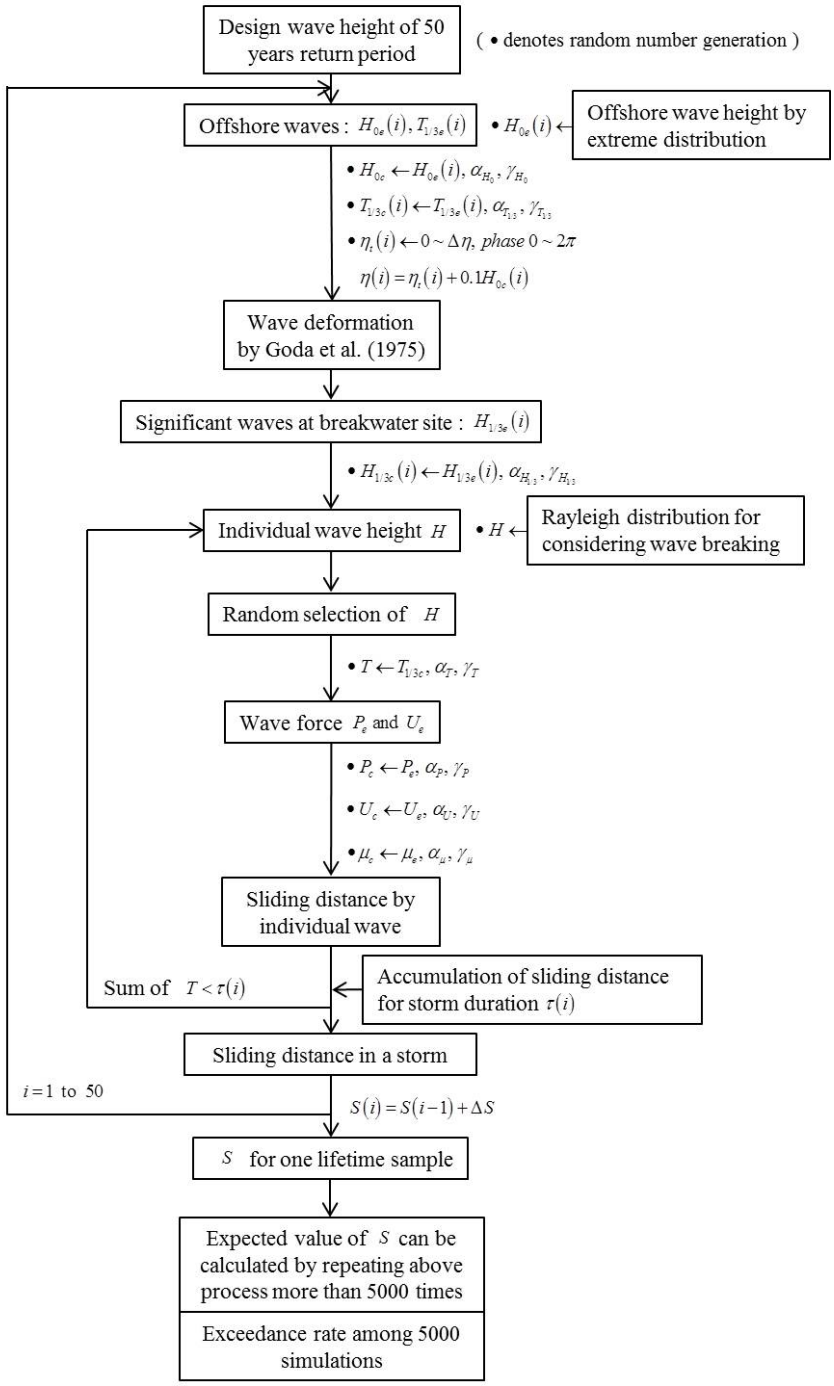

Fig 2. 2 Schematic flow chart for computation of expected sliding distance and exceedance rate given by Hong et al. (2004)

CHAPTER 3 DESIGN VARIABLES

3.1 Deepwater wave

In general, failures of the caisson breakwaters are caused by high waves corresponding to the design waves. Thus, it should be allowed to use the annual maximum deepwater wave in the computation. Deepwater wave height used in the performance-based design method is generally determined by the extreme wave height distribution from the wave data of a long-term observation or hindcasts.

$$F_{Weibull}(X) = 1 - \left[\exp\left(-\left(\frac{X - \xi}{\alpha} \right) \right)^{\kappa} \right] \tag{3.1}$$

The weibull distribution for deepwater wave height given by Eq. (3.1) is used in this study, where X is an annual maximum deepwater wave height and, α, ξ and κ are scale, location and shape parameter, respectively. The probabilistic wave is the 50-year lifetime used by Kim (2005) of 6.5m significant wave height whose scale, location and shape parameters are 2.005, 1.595 and 1.525, respectively. H_{0e} is a randomly extracted annual maximum significant wave height from extreme distribution of given deepwater wave height. Since these wave heights have uncertainty due to finite characteristic of parameter of extreme wave data or inaccuracy of the hindcasts data, probabilistic changes of the normal distribution which has an average μ_{H_0} and a standard deviation σ_{H_0} proposed by Takayama and Ikeda (1992) have

to be considered.

$$\mu_{H_0} = \left(1+\alpha_{H_0}\right) H_{0e}, \quad \sigma_{H_0} = \gamma_{H_0} H_{0e} \tag{3.2}$$

where α_{H_0} and γ_{H_0} are bias coefficient and coefficient of variation, respectively. Shimosako and Takahashi (1999) have suggested 0.0 and 0.1 for the bias coefficient and coefficient of variation of the deepwater wave height. As a result, the normal distribution of Eq. (3.2) determines the deepwater wave height H_{0c} to be used in the computation of wave force. Fig 3. 1 demonstrates an example of 50-year deepwater wave height generated using the parameters of the distribution function.

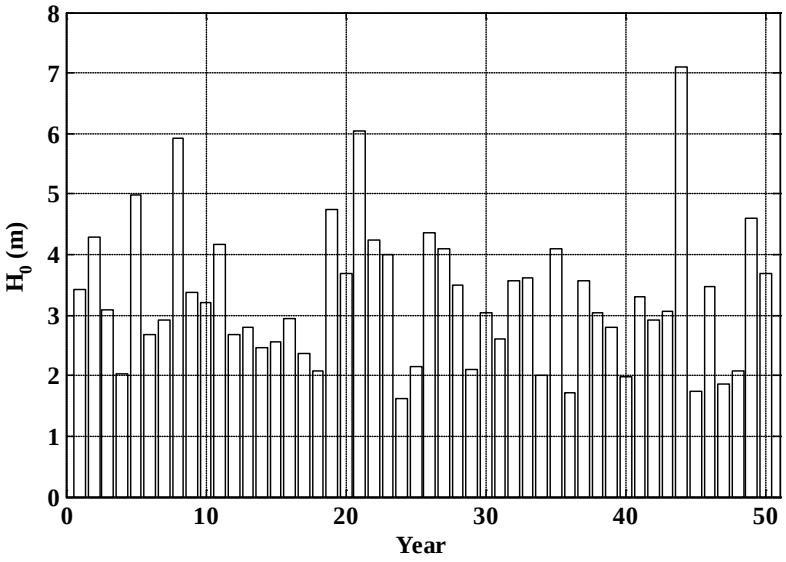

Fig 3. 1 Sample of offshore wave height for one lifetime of structure

3.2 Significant wave period

Goda (2003) and Wilson (1965) analyzed the significant wave height and significant wave period of fully developed wind wave with varied wind speed under an assumption that their equation used long enough fetch length, to come up with the following equation to express the relation between significant wave height and significant wave period.

$$T_{1/3} \cong 3.3 H_{1/3}{}^{0.63} \tag{3.3}$$

Shore Protection Manual (1977) published by Coastal Engineering Research Center of U.S. proposed the following equation to express the relation between significant wave height and significant wave period.

$$T_{1/3} \cong 3.85 H_{1/3}{}^{0.5} \tag{3.4}$$

On the other hand, Suh at al. (2010) used data and hindcasts observed in Korean coast and an actual long-term observation data of Japan to analyze; Eq. (3.3) of Goda (2003) and Eq. (3.4) of U.S. Army (Shore Protection Manual, 1977) were averaged into Eq. (3.5); both are used to express the relationship between the significant wave height and significant wave period for a high wave that close to the designed wave.

$$T_{1/3e} = \frac{1}{2}\left(3.3 H_{1/3}{}^{0.63} + 3.85 H_{1/3}{}^{0.5}\right) \tag{3.5}$$

The sample significant wave period $T_{1/3c}$ is determined by assigning the

probabilistic change of normal distribution with the average $\mu_{T_{1/3}}$ and standard deviation $\sigma_{T_{1/3}}$, i.e.

$$\mu_{T_{1/3}} = (1+\alpha_T)T_{1/3e}, \quad \sigma_{T_{1/3}} = \gamma_T T_{1/3e} \tag{3.6}$$

where α_T and γ_T are bias coefficient and coefficient of variation of the wave period, respectively. Fig 3. 2 demonstrates a sample significant wave period generated with a probabilistic change of the normal distribution showing relationship between the significant wave height and significant wave period in Eq. (3.5) whose bias coefficient and coefficient of variation are 0.0 and 0.1, respectively.

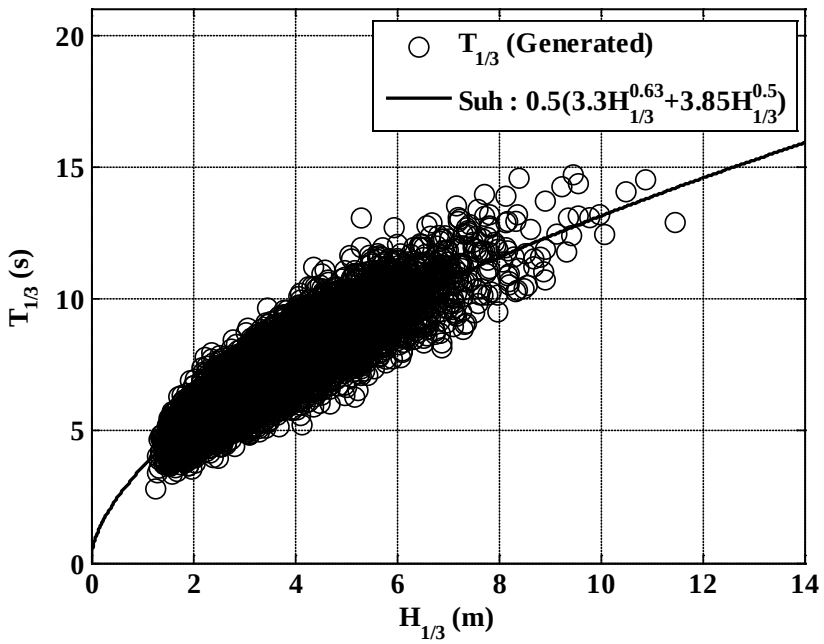

Fig 3. 2 Relation between significant wave height and significant wave period

3.3 Significant wave height at breakwater site

The wave height at the location of the breakwater is computed using a wave transformation model which considered wave breaking effect. To overcome the long computation time in the performance-based design method due to large number of simulations, a simplified equation proposed by Goda (1975) is used. As in Shimosako and Takahashi (1999), irregular waves propagating to the coast with parallel contours are used. Tidal levels were assumed to possess a sinusoidal wave type change between low water level (LWL) and high water level (HWL). Thus, a random number uniformly distributed between 0 and 2π is extracted as the phase of the sinusoidal curve and a sample tidal level with respect to the mean sea level η is determined.

3.3.1 Directional spreading function

The directional spreading function indicates how the wave energy is distributed around the principal wave direction when the wave propagates to the coast. Mitsuyasu et al. (1977) suggested the directional spreading function as shown in Eq. (3.7) based on the observation data of the clover-leaf buoy. It is called the Mitsuyasu-type directional spreading function.

$$G(\theta \mid f) = G_0 \cos^{2s}\left(\frac{\theta - \theta_0}{2}\right) \tag{3.7}$$

where f is frequency of the wave, θ the direction of the wave, θ_0 the

principal wave direction, and s the parameter indicating the directional spreading of the energy which is also called a directional spreading parameter. The larger the directional spreading parameter, more wave energy concentrated near the principal wave direction. If wave direction is spread from $-\pi$ to π in reference to the principal wave $(\theta = 0°)$, G_0 is defined as follows:

$$G_0 = \frac{1}{\pi} 2^{2s-1} \frac{\Gamma^2(s+1)}{\Gamma(2s+1)} \tag{3.8}$$

where Γ is a Gamma function. Goda and Suzuki (1975) proposed the following directional spreading parameter.

$$s = \begin{cases} (f / f_p)^5 s_{\max} & : f \le f_p \\ (f / f_p)^{-2.5} s_{\max} & : f > f_p \end{cases} \tag{3.9}$$

where f_p is a peak frequency which has a relationship of $f_p = 1/(1.05T_{1/3})$ with the significant wave period for the Bretschneider-Mitsuyasu spectrum. $s_{\max}$ is a peak value at $f = f_p$. $s_{\max}$ uses the following values in engineering terms.

$$s_{\max} = \begin{cases} 10 & \text{for wind waves} \\ 25 & \text{for swell with short decay distance} \\ 75 & \text{for swell with long decay distance} \end{cases} \tag{3.10}$$

3.3.2 Frequency spectrum

The frequency spectrum of wave indicates how the wave energy is distributed for each frequency. Directional spectrum considering the directional spreading function is as follows:

$$S(f,\theta) = S(f)G(\theta \mid f) \tag{3.11}$$

where $S(f)$ is the frequency spectrum. Various frequency spectra have been proposed. Eqs. (3.12), (3.13), (3.14) and (3.15) are Bretschneider-Mitsuyasu spectrum, Modified Bretschneider-Mitsuyasu spectrum modified by Goda, JONSWAP (Joint North Sea Wave Project) spectrum, and TMA spectrum, respectively.

$$S_{BM}(f) = 0.257 H_{1/3}{}^2 T_{1/3}{}^{-4} f^{-5} \exp\left[-1.03\left(T_{1/3} f\right)^{-4}\right] \tag{3.12}$$

$$S_{MBM}(f) = 0.205 H_{1/3}{}^2 T_{1/3}{}^{-4} f^{-5} \exp\left[-0.75\left(T_{1/3} f\right)^{-4}\right] \tag{3.13}$$

$$S_J(f) = \beta_J H_{1/3}{}^2 T_p{}^{-4} f^{-5} \exp\left[-1.25\left(T_p f\right)^{-4}\right] \gamma^{\exp\left[-\left(T_p f - 1\right)^2 / 2\sigma^2\right]} \tag{3.14}$$

$$S_{TMA}(f) = S_J(f) \cdot \phi(kh) \;:\; \phi(kh) = \frac{\tanh^2 kh}{1 + 2kh / \sinh 2kh} \tag{3.15}$$

The Bretschneider-Mitsuyasu spectrum is a spectrum for fully developed wind waves, which was modified by Goda to come up with the Modified Bretschneider-Mitsuyasu spectrum. The JONSWAP spectrum is a spectrum for developing wind waves in a fetch-limited state. The TMA spectrum is an

expanded version of the JONSWAP spectrum which expressed wave height changes by the depth-limited breaking in $\phi(kh)$ format in terms of the relative depth (kh). Variables in Eq. (3.14) are as follows:

$$\beta_J = \frac{0.0624}{0.230 + 0.0336\gamma - 0.185(1.9+\gamma)^{-1}}\left[1.094 - 0.01915\ln\gamma\right] \tag{3.16}$$

$$T_p \cong T_{1/3} / \left[1 - 0.132(\gamma + 0.2)^{-0.559}\right] \tag{3.17}$$

$$\sigma = \begin{cases} \sigma_a \ : \ f \le f_p \\ \sigma_b \ : \ f \ge f_p \end{cases} \tag{3.18}$$

$$\gamma = 1 \sim 7(\text{mean of } 3.3), \ \sigma_a \cong 0.07, \ \sigma_b \cong 0.09 \tag{3.19}$$

3.3.3 Wave transformation

Goda (1975) proposed the following equations to compute the wave transformation on the coast including the surf zone.

$$H_s = \begin{cases} K_s H_0' & : h / L_0 \ge 0.2 \\ \min\left\{(\beta_0 H_0' + \beta_1 h),\ \beta_{\max} H_0',\ K_s H_0'\right\} & : h / L_0 < 0.2 \end{cases} \tag{3.20}$$

$$H_{\max} = \begin{cases} 1.8 K_s H_0' & : h / L_0 \ge 0.2 \\ \min\left\{(\beta_0^* H_0' + \beta_1^* h),\ \beta_{\max}^* H_0',\ 1.8 K_s H_0'\right\} & : h / L_0 < 0.2 \end{cases} \tag{3.21}$$

where H_s is a significant wave height at the location of the breakwater, $H_{\max}$ the maximum wave height, H_0' an equivalent deepwater wave height

corresponding to the significant wave height, K_s the shoaling coefficient, h water depth and L_0 is the deepwater wave length. β_0, β_1, $\beta_{\max}$, β_0^*, β_1^*, and $\beta_{\max}^*$ are the coefficients depending on deepwater wave steepness and bottom slope, which are expressed as follows:

$$\beta_0 = 0.028\left(H_0'/L_0\right)^{-0.38}\exp\left[20\tan^{1.5}\theta\right] \tag{3.22}$$

$$\beta_1 = 0.52\exp\left[4.2\tan\theta\right] \tag{3.23}$$

$$\beta_{\max} = \max\left\{0.92, 0.32\left(H_0'/L_0\right)^{-0.29}\times\exp\left[2.4\tan\theta\right]\right\} \tag{3.24}$$

$$\beta_0^* = 0.052\left(H_0'/L_0\right)^{-0.38}\exp\left[20\tan^{1.5}\theta\right] \tag{3.25}$$

$$\beta_1^* = 0.63\exp\left[3.8\tan\theta\right] \tag{3.26}$$

$$\beta_{\max} = \max\left\{1.65, 0.53\left(H_0'/L_0\right)^{-0.29}\times\exp\left[2.4\tan\theta\right]\right\} \tag{3.27}$$

where $\tan\theta$ is the bottom slope. To compute the equivalent deepwater wave height H_0', a computation of the refraction coefficient has to be preceded. Refraction coefficient computations of irregular wave are as follows:

$$\left(K_r\right)_{eff} = \left(\frac{m_0}{m_{s0}}\right)^{1/2} \tag{3.28}$$

$$m_0 = \int_0^\infty S(f)\,df = \int_0^\infty\int_{\theta_{\min}}^{\theta_{\max}} S_0(f,\theta_0)K_s^{\,2}(f,h)K_r^{\,2}(f,h,\theta_0)\,d\theta_0\,df \tag{3.29}$$

$$m_{s0} = \int_0^{\infty} \int_{\theta_{\min}}^{\theta_{\max}} S_0(f,\theta_0) K_s^{\,2}(f,h)\, d\theta_0 df \tag{3.30}$$

where m_0 is the zeroth moment considering both shoaling coefficient and refraction coefficient, and m_{s0} is the zeroth moment considering only the shoaling coefficient. From the ratio of the two zeroth moments, the effective refraction coefficient $(K_r)_{eff}$ is determined. $K_s(f,h)$ is a linear shoaling coefficient for the regular wave, f is a frequency, θ_0 is a wave direction of the deepwater wave, and h is water depth.

Goda (1975) used a non-linear shoaling coefficient in his equation which was proposed by Iwagaki et al. (1981).

$$K_s = K_{si} + 0.0015\left(\frac{h}{L_0}\right)^{-2.87}\left(\frac{H_0'}{L_0}\right)^{1.27} \tag{3.31}$$

where K_s, K_{si} are non-linear and linear shoaling coefficients, respectively. Fig 3. 3 shows the refraction coefficient derived by the Modified BM spectrum and directional spreading function. As the principal direction increases, the refraction coefficient tends to decrease. The refraction coefficient is the greatest when the wave normally propagates to the coast. The breaking wave height can be computed using the equation for breaking wave height in shallow water region proposed by Goda (1974).

$$\frac{H_b}{L_0} = A\left\{1 - \exp\left[-1.5\frac{\pi h}{L_0}\left(1 + 15\tan^{4/3}\theta\right)\right]\right\} \tag{3.32}$$

A is 0.18 and 0.12, respectively, for the upper and lower limits of the breaking wave height. This study used 0.18 to satisfy the condition that the individual wave height cannot be greater than the upper limit of the breaking wave height. Fig 3. 4 and Fig 3. 5 represent the wave height with respect to water depth using Eqs. (3.20), (3.21) and (3.32) with bottom slope of 1/50 and 1/20. It is found that a surf zone forms at 14m when the bottom slope is 1/50, and at 12m when the bottom slope is 1/20.

The wave height $H_{1/3e}$ at the location of the breakwater is assumed to have a computational uncertainty, and the probabilistic change is given according to the normal distribution with an average μ_{H_s} and a standard deviation σ_{H_s}.

$$\mu_{H_{1/3}} = \left(1+\alpha_{H_{1/3}}\right) H_{1/3e}, \quad \sigma_{H_{1/3}} = \gamma_{H_{1/3}} H_{1/3e} \tag{3.33}$$

where $\alpha_{H_{1/3}}$ and $\gamma_{H_{1/3}}$ are the bias coefficient and coefficient of variation, respectively. Shimosako and Takahashi (1999) proposed 0.0 and 0.1 for the bias coefficient and coefficient of variation of the significant wave height, respectively. A normal distribution of Eq. (3.33) determines the sample significant wave height $H_{1/3c}$ to be used in the computation. Fig 3. 6 demonstrates an example of the significant wave height at the location of the breakwater generated in 50-year lifetime.

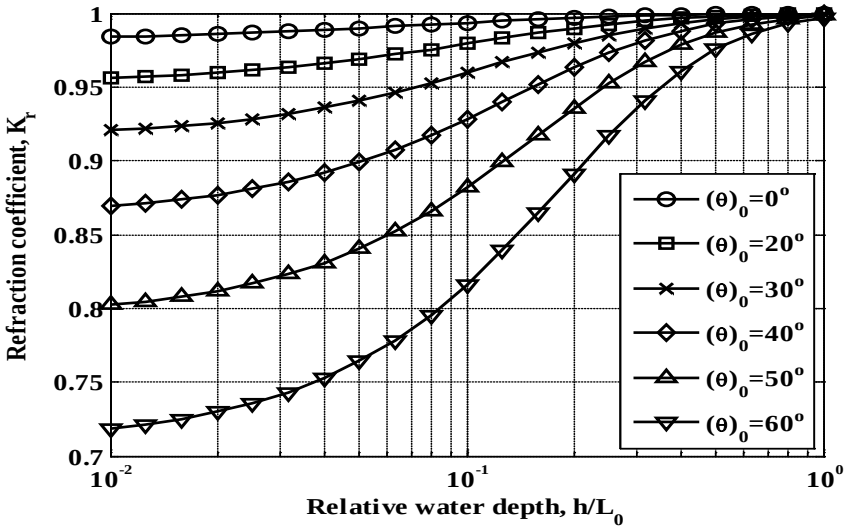

Fig 3. 3 Refraction coefficient of random sea waves with $s_{max} = 25$ on a coast with straight and parallel depth-contours

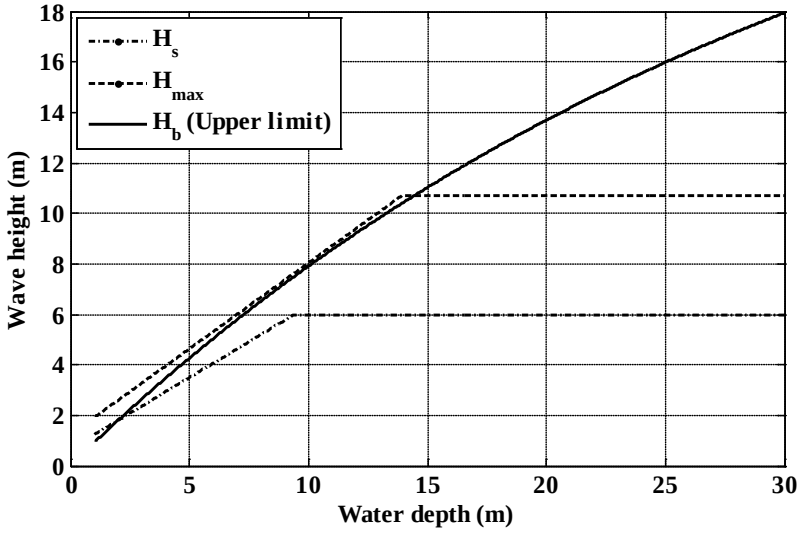

Fig 3. 4 Wave heights in different water depths on a coast with bottom slope of 1/50

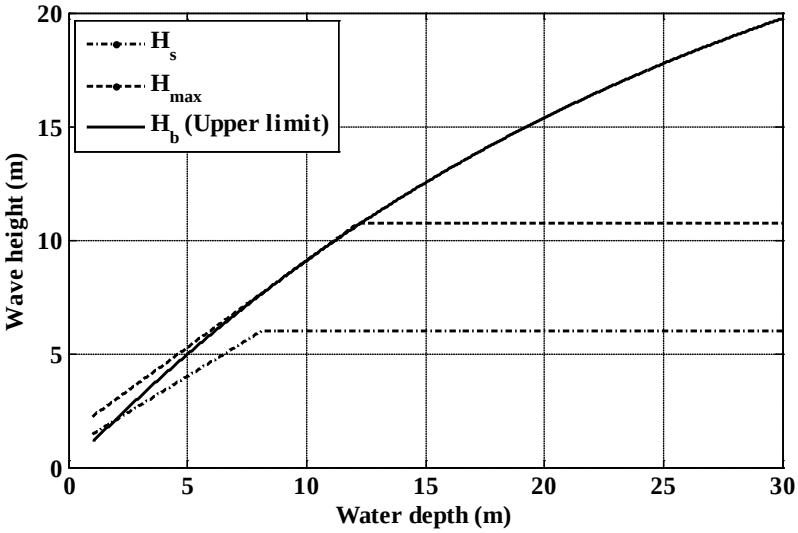

Fig 3. 5 Wave heights in different water depths on a coast with bottom slope of 1/20

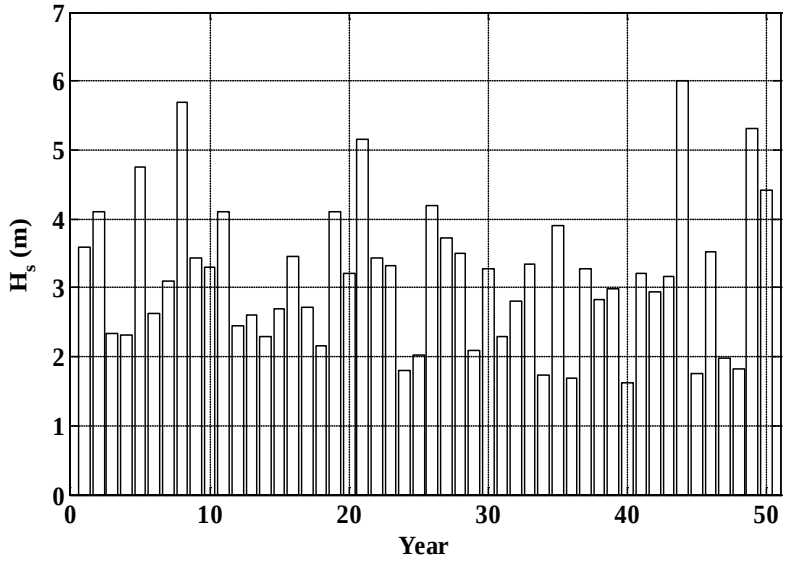

Fig 3. 6 Sample of design wave height at the breakwater for one lifetime of structure

3.4 Individual wave

After the significant wave height at the location of the breakwater is computed, the individual wave during a storm can be extracted by the Rayleigh distribution.

$$P_{Rayleigh}\left(H\right)=e^{-\left(H/H_{rms}\right)^2} \tag{3.34}$$

$$H_{rms}=\frac{H_s}{1.416} \tag{3.35}$$

If the extracted individual wave height is greater than the breaking wave height computed by Eq. (3.32), then the breaking wave height should be used instead of the extracted individual wave height.

In the case of the individual wave period, the wave period T to be used in the computation is determined by giving the probabilistic change of the normal distribution in a same manner as in the significant wave period.

$$\mu_T=\left(1+\alpha_{T_{1/3}}\right)T_{1/3c},\quad \sigma_T=\gamma_{T_{1/3}}T_{1/3c} \tag{3.36}$$

where $\alpha_{T_{1/3}}$ and $\gamma_{T_{1/3}}$ are bias coefficient and coefficient of variation, respectively. Their values use the same values for the significant wave period. Fig 3. 7 shows the occurrence frequency of the individual wave height when the significant wave height is 6.28m. The Rayleigh distribution is also presented in the same figure.

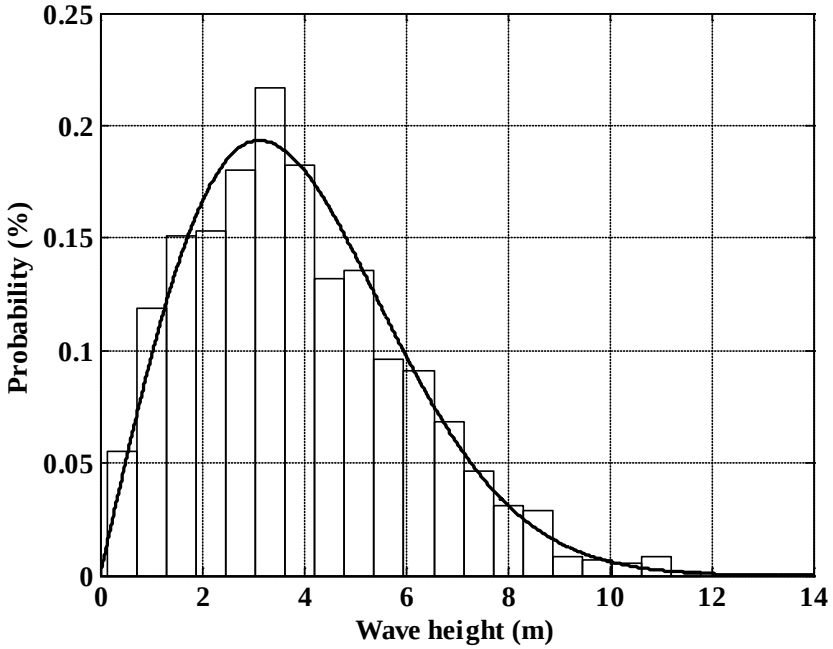

Fig 3. 7 Frequency of individual wave heights in a storm event of significant wave height of 6.28 m

3.5 Calculation of wave force acting on solid-wall caisson breakwater

For the computation of the wave force acting on the solid-wall caisson breakwater, the Goda (1974) formula expanded by Takahashi et al. (1991) and Takahashi and Tanimoto (1994) is used. This equation assumes that the wave pressure is distributed in a trapezoidal shape on the front of the caisson wall as illustrated in Fig 3. 8.

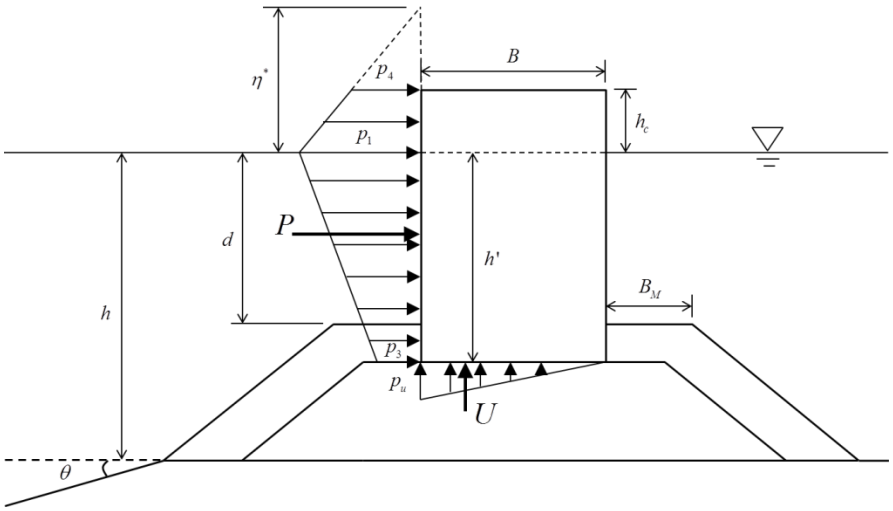

Fig 3. 8 Pressure distribution for solid-wall caisson breakwater

However, it is not much different from the Goda (1974) formula since the correction coefficients λ_1, λ_2, and λ_3 for a typical solid-wall caisson breakwater are 1. The wave force computation by Goda (1974) is as follows:

$$P = \frac{1}{2}\left(p_1 + p_3\right)h' + \frac{1}{2}\left(p_1 + p_4\right)h_c^* \tag{3.37}$$

$$U = \frac{1}{2}p_u B \tag{3.38}$$

where P is a horizontal wave force and U is an uplift force, with each terms in Eqs. (3.37) and (3.38) are computed as follows:

$$p_1 = \frac{1}{2}\left(1+\cos\beta\right)\left(\alpha_1\lambda_1 + \alpha_2\lambda_2\cos^2\beta\right)w_0 H_{\max} \tag{3.39}$$

$$p_2 = \frac{p_1}{\cosh\left(2\pi h / L\right)} \tag{3.40}$$

$$p_3 = \alpha_3 p_1 \tag{3.41}$$

$$p_4 = \alpha_4 p_1 \tag{3.42}$$

$$p_u = \frac{1}{2}\left(1+\cos\beta\right)\alpha_1\alpha_3\lambda_3 w_0 H_{\max} \tag{3.43}$$

$$h_c^* = \min\left\{\eta^*, h_c\right\} \tag{3.44}$$

$$\eta^* = 0.75\left(1+\lambda_1\cos\beta\right)H_{\max} \tag{3.45}$$

where β is an angle between the direction of wave approach and a line normal to the breakwater. w_0 is the unit weight of sea water, $H_{\max}$ is the maximum wave height at the location of the breakwater, h is a depth in front of the breakwater, h_c is the crest elevation of upright section, and η^* is a run-up parameter. Coefficients of Eqs. (3.39) to (3.45) are computed as follows:

$$\alpha_1 = 0.6 + \frac{1}{2}\left[\frac{4\pi h / L}{\sinh\left(4\pi h / L\right)}\right]^2 \tag{3.46}$$

$$\alpha_2 = \min\left\{\frac{h_b - d}{3h_b}\left(\frac{H_{\max}}{d}\right)^2, \frac{2d}{H_{\max}}\right\} \tag{3.47}$$

$$\alpha_3 = 1 - \frac{h'}{h}\left[1 - \frac{1}{\cosh(2\pi h / L)}\right] \tag{3.48}$$

$$\alpha_4 = 1 - \frac{h_c^*}{\eta^*} \tag{3.49}$$

where α_1, α_2, α_3, and α_4 are the correction factors of wave pressure, and h_b is the water depth at $5H_{1/3}$ away from the breakwater. α_2 is a coefficient to consider the effect of the rubble mound. Since this coefficient is not sufficient to express the impulsive wave pressure, Takahashi and Shimosako (1994) had introduced a correction coefficient of impulsive wave α_I for the cases that impulsive wave breaking occurs easily such as relatively high and wide mound or very steep bottom slope. A relation between α_2 and α_I are as follows:

$$\delta_{11} = 0.93\left(\frac{B_M}{L} - 0.12\right) + 0.36\left(0.4 - \frac{d}{h}\right) \tag{3.50}$$

$$\delta_{22} = -0.36\left(\frac{B_M}{L} - 0.12\right) + 0.93\left(0.4 - \frac{d}{h}\right) \tag{3.51}$$

$$\delta_1 = \begin{cases} 20\delta_{11} & \text{when } \delta_{11} \le 0 \\ 15\delta_{11} & \text{when } \delta_{11} > 0 \end{cases} \tag{3.52}$$

$$\delta_2 = \begin{cases} 4.9\delta_{22} & \text{when } \delta_{22} \le 0 \\ 3.0\delta_{22} & \text{when } \delta_{22} > 0 \end{cases} \tag{3.53}$$

$$\alpha_{IH} = \min\left\{H_{\max} / d,\ 2.0\right\} \tag{3.54}$$

$$\alpha_{IB} = \begin{cases} \cos\delta_2 / \cosh\delta_1 & \text{when } \delta_2 \le 0 \\ 1/\left(\cosh\delta_1 \cosh^{1/2}\delta_2\right) & \text{when } \delta_2 > 0 \end{cases} \tag{3.55}$$

$$\alpha_I = \alpha_{IH}\alpha_{IB} \tag{3.56}$$

$$\alpha^* = \max\left\{\alpha_2,\ \alpha_I\right\} \tag{3.57}$$

To consider the effect of the impulsive wave pressure in the existing wave force equation, α^* is used in place of α_2 through the above computation processes.

3.6 Calculation of wave force acting on perforated-wall caisson breakwater

Takahashi et al. (1991) had performed hydraulic experiments under various conditions to come up with a computation of wave force acting on the perforated-wall caisson breakwaters. He had classified waves into Crest I, Crest IIa, and Crest IIb as shown in Fig 3. 9. Crest I occurs at the moment when the wave makes a first contact with the front of the perforated wall; horizontal wave pressure acts on both perforated wall and solid-wall on the front face of the caisson and the uplift force acts on the bottom of the caisson. Crest IIa occurs at the moment when the wave passes through the perforated front wall and makes a contact with the solid-wall at the rear; horizontal wave pressure acts not only on the front wall but also on the rear wall and wave pressure increases at the bottom of the wave chamber due to raised water level. Crest IIb occurs at the moment when the previous Crest IIa becomes the standing waves. The computation of the wave force is the same as that for the solid-wall caisson breakwater by Takahashi et al. (1991) and Takahashi and Tanimoto (1994). Correction coefficients $\lambda_1, \lambda_2,$ and λ_3, however, should be applied according to the phase of wave pressure as shown in Table 3.1 by Takahashi et al. (1991); where B' is the width of the wave chamber plus a thickness of the front wall, and L' is the wave length at a depth d' within the wave chamber. When calculating the correction coefficient of the impulsive wave α^* for the rear wall which is required in computing the correction coefficient of λ_{R2} for Crest IIa, the water depth within the wave

chamber d', wave length within the wave chamber L', and $B'-(d-d')$ should be used in place of the water depth d, wave length L, and B_M. Fig 3. 10, Fig 3. 11, and Fig 3. 12 demonstrate the wave pressure distribution and example of applied correction coefficients of Crest I, Crest IIa and Crest IIb, respectively. It is assumed that the wave pressure is distributed in a trapezoidal shape along the front and rear wall of the wave chamber and the pressure at the bottom of the wave chamber is assumed to be hydrostatic. Computations of the front-wall wave pressure for the perforated and solid parts are done separately using an interpolation, and the same for the computation for the wave pressure at the rear wall. The pressure acting on the bottom of the wave chamber is computed with the correction coefficient λ_M, the same as the computation for the pressure acting on the rear wall. Since the perforated-wall caisson breakwater has a wave absorbing structure, unlike the solid-wall caisson breakwater, it effectively decreases the maximum wave force. Thus the wave force decrease according to the porosity of the front wall is as follows, when the wave force is computed.

$$\varepsilon = \frac{\ell \times h \times N}{L \times H} \tag{3.58}$$

$$\varepsilon' = 1 - \varepsilon \tag{3.59}$$

where ε and ε' are the porosity and dissipation rate of the wave force, respectively, and ℓ, h, N, L and H are the width, height and the number of the slit, the length of a caisson (in a parallel direction with the

breakwater) and the height from crest to bottom of the slit, respectively. The correction coefficient of the wave force computed above is only applied to the perforated part of the front wall.

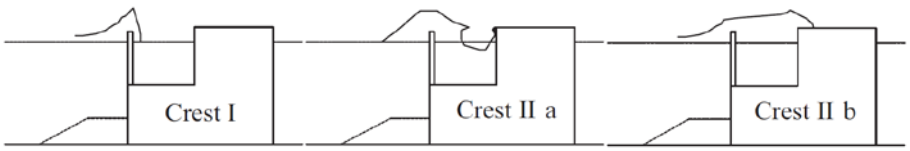

Fig 3. 9 Phase difference for wave action on a perforated caisson defined by Takahashi et al. (1991)

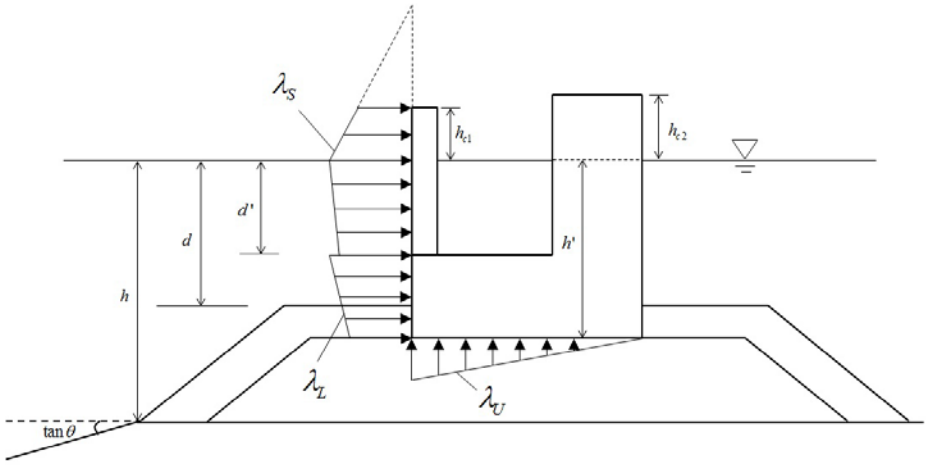

Fig 3. 10 Pressure distributions on a perforated caisson at Crest I given by Takahashi et al. (1991)

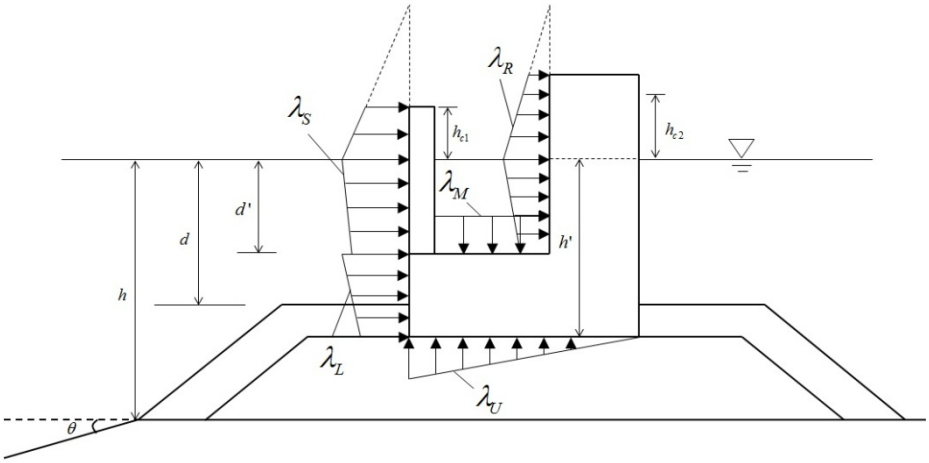

Fig 3. 11 Pressure distributions on a perforated caisson at Crest IIa given by Takahashi et al. (1991)

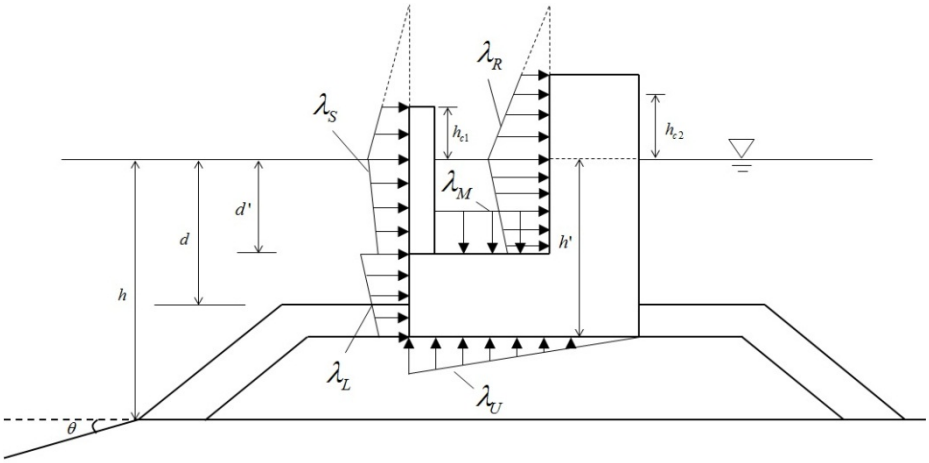

Fig 3. 12 Pressure distributions on a perforated caisson at Crest IIb given by Takahashi et al. (1991)

Table 3.1 Correction coefficients for perforated caissons given by Takahashi et al. (1991)

		Crest I	Crest IIa	Crest IIb
Perforated part of the front wall	λ_{S1}	0.85	0.7	0.3
	λ_{S2}	$0.4 \quad (\alpha^* \le 0.75)$ $0.3/\alpha^* \quad (\alpha^* > 0.75)$	0.0	0.0
Solid part of the front wall	λ_{L1}	1.0	0.75	0.65
	λ_{L2}	$0.4 \quad (\alpha^* \le 0.75)$ $0.2/\alpha^* \quad (\alpha^* > 0.75)$	0.0	0.0
Wave chamber rear wall	λ_{R1}	0.0	$20B'/3L' \quad (B'/L' \le 0.15)$ $1.0 \quad (B'/L' > 0.15)$	$1.4 \quad (H_d/d \le 0.1)$ $1.6-2H_d/d \quad (0.1 < H_d/d < 0.3)$ $1.0 \quad (H_d/d \ge 0.3)$
	λ_{R2}	0.0	$0.56 \quad (\alpha^* \le 25/28)$ $0.5/\alpha^* \quad (\alpha^* > 25/28)$	0.0
Wave chamber bottom slab	λ_{M1}	0.0	$20B'/3L' \quad (B'/L' \le 0.15)$ $1.0 \quad (B'/L' > 0.15)$	$1.4 \quad (H_d/d \le 0.1)$ $1.6-2H_d/d \quad (0.1 < H_d/d < 0.3)$ $1.0 \quad (H_d/d \ge 0.3)$
	λ_{M2}	0.0	0.0	0.0
Uplift	λ_{U3}	1.0	0.75	0.65

3.7 Doubly-truncated normal distribution

The stochastic variability of most design variables can be expressed in a normal distribution. Since the design variables are randomly extracted from negative infinity to positive infinity, some extracted variable may not be realistic. In order to overcome such shortcoming, Kim et al. (2003) used a doubly-truncated normal distribution, using the upper limit x_1 and lower limit x_2 for the wave force and friction coefficient based on the experiment data of Takayama and Ikeda (1992). This study also used his method. Other design variables use the assumption of the normal distribution due to lack of available data.

$$\int_{x_1}^{x_2} f_{DTN}(x)\,dx = 1 \tag{3.60}$$

$$f_{DTN}(x) = \frac{1}{p_{12}} f(x) \tag{3.61}$$

$$p_{12} = \int_{x_1}^{x_2} f(x)\,dx \tag{3.62}$$

The doubly-truncated normal distribution $f_{DTN}(x)$ in Eq. (3.60) is related to the normal distribution $f(x)$ as in Eq. (3.61). The cumulative distribution function $F_{DTN}(x)$ of the doubly-truncated normal distribution is the same as the cumulative distribution function $F(x)$ of the normal distribution and expressed as follows:

$$F_{DTN}(x)=\frac{1}{p_{12}}\left[\int_{-\infty}^{x} f(x)dx-\int_{-\infty}^{x_1} f(x)dx\right]=\frac{F(x)-F(x_1)}{p_{12}} \tag{3.63}$$

$F(x_1)$ and p_{12} can be computed once the upper and lower limits are determined. The random number $r(0\le r\le 1)$ of the doubly-truncated normal distribution has the following relation with the random number r' of the normal distribution.

$$r=F_{DTN}(x)=\frac{r'-F(x_1)}{p_{12}} \tag{3.64}$$

Thus, the random variable X of the doubly-truncated normal distribution can be computed as follows:

$$X=\begin{cases}\mu_X+\sqrt{2}\sigma_X\sqrt{-\dfrac{\pi}{4}\ln\left(4r'-4r'^2\right)} & r'\ge 0.5\\ \mu_X-\sqrt{2}\sigma_X\sqrt{-\dfrac{\pi}{4}\ln\left(4r'-4r'^2\right)} & r'<0.5\end{cases} \tag{3.65}$$

Fig 3. 13, Fig 3. 14, and Fig 3. 15 represent randomly extracted wave force acting on the perforated-wall caisson breakwater, wave force acting on the solid-wall caisson breakwater, and friction coefficients, respectively. Takayama and Ikeda (1992) had suggested the following upper and lower limits of the wave force; 1.28 and 0.57 for the perforated-wall caisson breakwater, 1.42 and 0.48 for the solid-wall caisson breakwater; and 1.43 and 0.71 for the friction coefficients. This indicates that the values outside the upper and lower limits that are not likely in the normal distribution are

eliminated so that reasonable wave forces and friction coefficients will be generated.

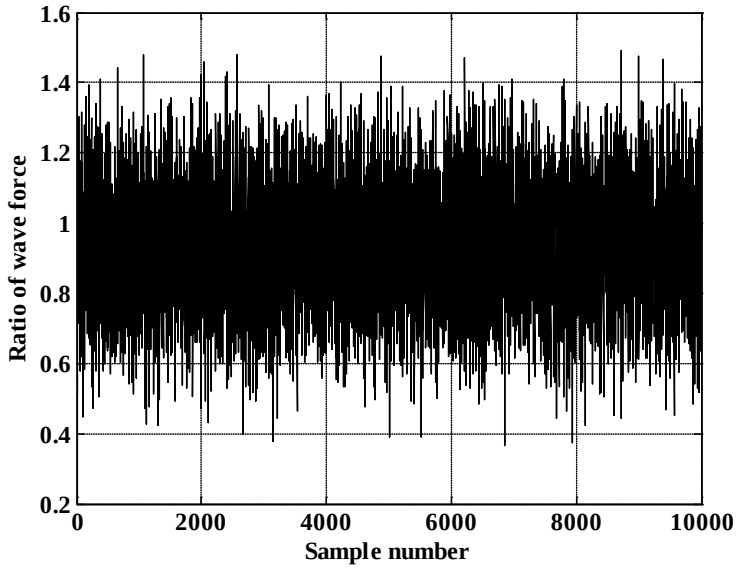

(a)

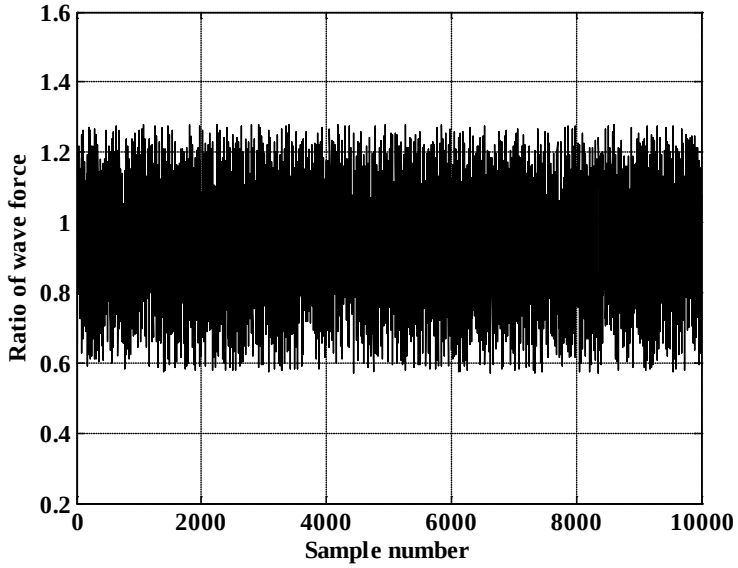

(b)

Fig 3. 13 Random sample of wave force from (a) normal distribution and (b) doubly-truncated normal distribution (Perforated-wall caisson)

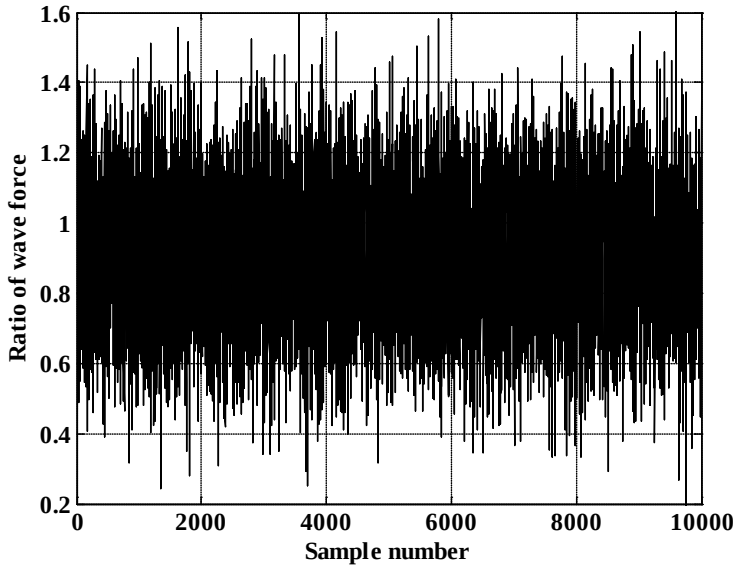

(a)

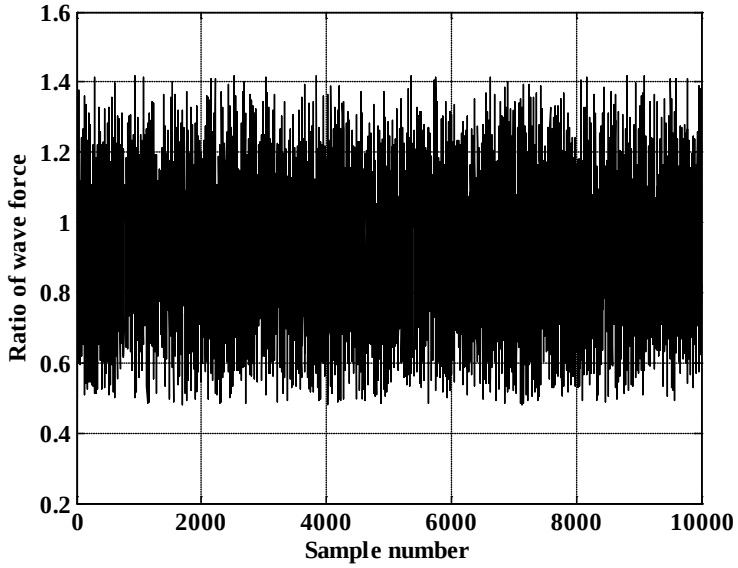

(b)

Fig 3. 14 Random sample of wave force from (a) normal distribution and (b) doubly-truncated normal distribution (Solid-wall caisson)

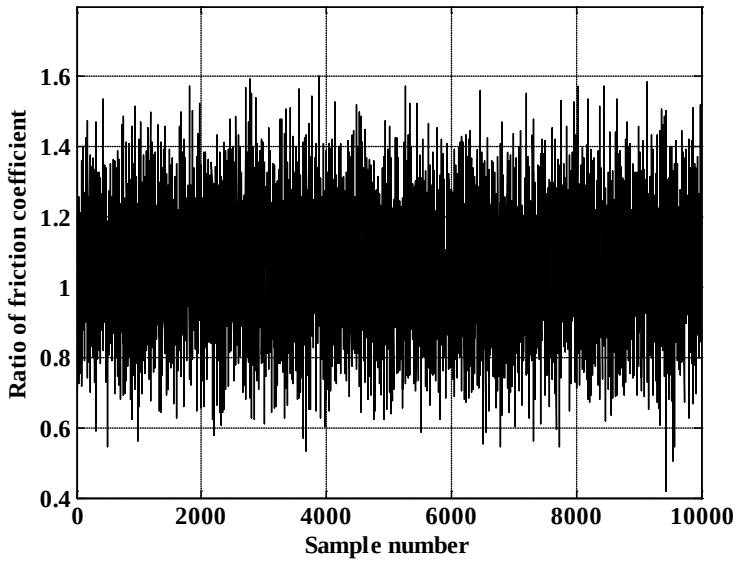

(a)

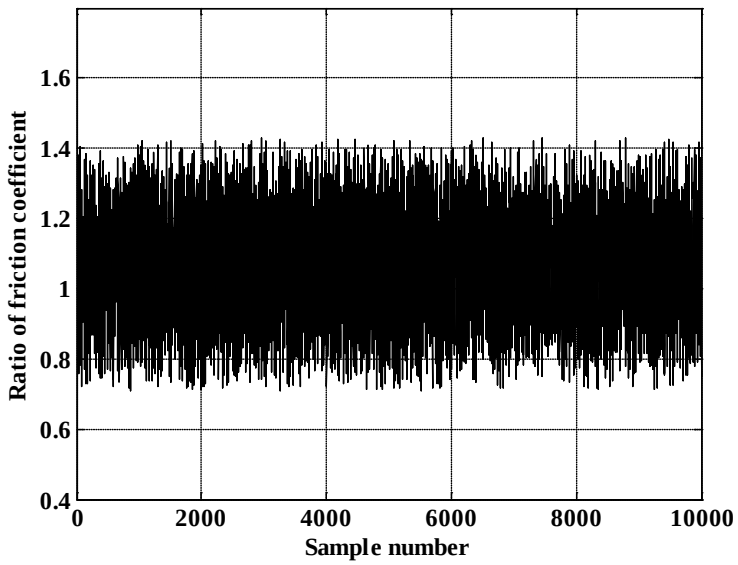

(b)

Fig 3. 15 Random sample of friction coefficient from (a) normal distribution and (b) doubly-truncated normal distribution

3.8 Uncertainty of design variables

The uncertainty of the design variables can be expressed as Eq. (3.66), and statistical characteristics of each variable are presented in Table 3.2.

$$\mu_{X_i} = \left(1+\alpha_{X_i}\right) X_i, \quad \sigma_{X_i} = \gamma_{X_i} X_i \tag{3.66}$$

where X_i, α_{X_i}, and γ_{X_i} are design variables, bias coefficient, and coefficient of variation, respectively.

Table 3.2 Statistical characteristics of design variables

Description	X_i	α_{X_i}	γ_{X_i}	References
Offshore wave height	Various	0.0	0.1	Shimosako and Takahashi (1999)
Significant wave period	Various	0.0	0.1	Suh et al. (2010)
Wave transformation	Various	0.0	0.1	Shimosako and Takahashi (1999)
Horizontal wave force (Solid)	Various	-0.09	0.19	Takayama and Ikeda (1992) Kim and Takayama (2003)
Horizontal wave force (Perforated)	Various	-0.10	0.17	Takayama and Ikeda (1992)
Vertical wave force	Various	-0.23	0.20	Oumeraci et al. (2001)
Friction coefficient	0.6	0.06	0.16	Takayama and Ikeda (1992) Kim and Takayama (2003)

3.9 Time series of wave force

3.9.1 Time series of wave force acting on solid-wall caisson

Shimosako and Takahashi (1998) proposed that the time series of the wave force used in the computation of the expected sliding distance of the solid-wall caisson breakwater is a combined form of the impulsive wave force and standing wave force; and thus expressed as follow:

$$P(t) = \max\left\{P_1(t), P_2(t)\right\} \tag{3.67}$$

$$P_1(t) = \gamma_P P_{1\max} \sin\frac{2\pi t}{T} \tag{3.68}$$

$$P_2(t) = \begin{cases} \left(\dfrac{2t}{\tau_0}\right) P_{2\max} & 0 \le t \le \tau_0 / 2 \\ 2\left(\dfrac{1-t}{\tau_0}\right) P_{2\max} & \tau_0 / 2 \le t \le \tau_0 \\ 0 & t \ge \tau_0 \end{cases} \tag{3.69}$$

$$\gamma_P = 1 - \frac{\pi}{P_{1\max}} \int_{t_1}^{t_2} \left[P_2(t) - P_{1\max} \sin\frac{2\pi t}{T} \right] dt \tag{3.70}$$

$$P_2(t) - P_{1\max} \sin\frac{2\pi t}{T} \ge 0 \tag{3.71}$$

where $P_{1\max}$ is the horizontal wave force of Goda (1974) considering only α_1, $P_{2\max}$ the wave force considering α^*, and $P_1(t)$ and $P_2(t)$ are the standing wave component and impulsive wave component, respectively. τ_0

is the duration of $P_2(t)$, T is the wave period, γ_P is the modification factor which indicates the reduction of standing wave force due to the occurrence of the impulsive wave force. The range of integration of Eq. (3.70) is the range of $P_2(t)-P_1(t)\geq 0$. The uplift force $U(t)$ may also be computed by using the following time series.

$$U(t)=\max\left\{U_1(t),U_2(t)\right\} \tag{3.72}$$

$$U_1(t)=\gamma_U U_{\max}\sin\frac{2\pi t}{T} \tag{3.73}$$

$$U_2(t)=\begin{cases}\left(\dfrac{2t}{\tau_0}\right)U_{\max} & 0\leq t\leq \tau_0/2\\ 2\left(\dfrac{1-t}{\tau_0}\right)U_{\max} & \tau_0/2\leq t\leq \tau_0\\ 0 & t\geq \tau_0\end{cases} \tag{3.74}$$

$$\gamma_U=1-\frac{\pi}{U_{\max}}\int_{t_1}^{t_2}\left[U_2(t)-U_{\max}\sin\frac{2\pi t}{T}\right]dt \tag{3.75}$$

$$U_2(t)-U_{\max}\sin\frac{2\pi t}{T}\geq 0 \tag{3.76}$$

τ_0 is the duration of the impulsive wave force and is defined as follows:

$$\tau_0=k\tau_{0F} \tag{3.77}$$

$$\tau_{0F}=\begin{cases}\left(0.5-\dfrac{H}{8h}\right) & 0\leq\dfrac{H}{h}\leq 0.8\\ 0.4T & \dfrac{H}{h}>0.8\end{cases} \tag{3.78}$$

$$k = \left(\frac{1}{\left(\alpha^*\right)^{0.3} + 1} \right)^2 \tag{3.79}$$

where τ_{0F} is the time when the water level is positive in the finite-amplitude standing wave theory, H wave height, h water depth, and α^* is an impulsive wave pressure coefficient.

Fig 3. 16 shows the time series of the wave force of combined impulsive wave and standing wave components acting on the solid-wall caisson breakwater.

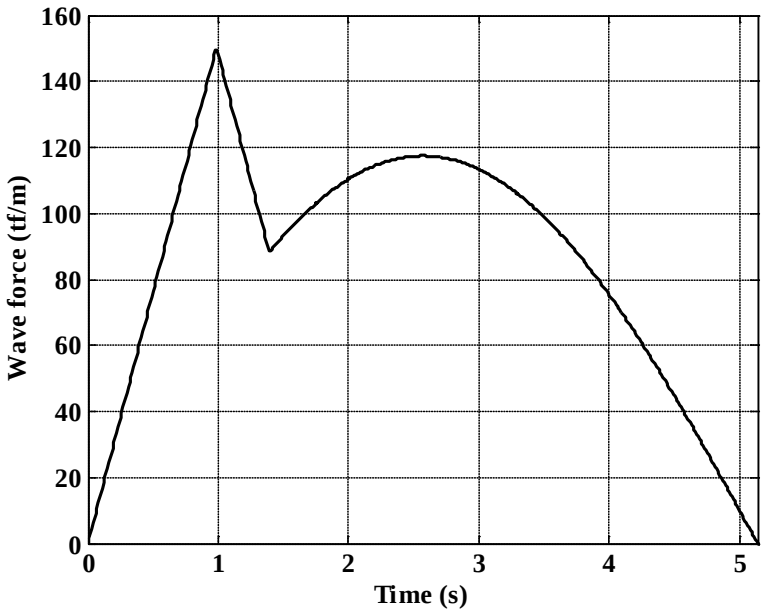

Fig 3. 16 Time series for horizontal wave force acting on solid-wall caisson breakwater

3.9.2 Time series of wave force acting on perforated-wall caisson

Kim (2005) proposed the method to compute the time series of the wave force acting on the perforated-wall caisson breakwater by combining the time series of solid-wall caisson breakwater described in the previous section with the formula proposed by Takahashi et al. (1991) to compute the wave pressure computation acting on the perforated-wall caisson breakwater. In other words, the wave forces of Crest I, Crest IIa and Crest IIb that act on the perforated-wall caisson breakwater with phase difference are expressed by two impulsive waves and one standing wave as follow:

$$P(t) = \max\left\{P_1(t), P_2(t), P_3(t)\right\} \tag{3.80}$$

$$P_1(t) = \begin{cases} \left(\dfrac{2t}{\tau_0}\right)P_I & 0 \le t < \dfrac{\tau_0}{2} \\ 2\left(\dfrac{1-t}{\tau_0}\right)P_I & \dfrac{\tau_0}{2} \le t < \tau_0 \\ 0 & t \ge \tau_0 \end{cases} \tag{3.81}$$

$$P_2(t) = \begin{cases} 0 & 0 \le t < t_d \\ \left(\dfrac{2(t-t_d)}{\tau_0'}\right)P_{IIa} & t_d \le t < \dfrac{\tau_0'}{2} + t_d \\ 2\left(\dfrac{1-(t-t_d)}{\tau_0'}\right)P_{IIa} & \dfrac{\tau_0'}{2} + t_d \le t < \tau_0' + t_d \\ 0 & t \ge \tau_0' + t_d \end{cases} \tag{3.82}$$

$$P_3(t) = \begin{cases} 0 & 0 \le t < t_d \\ P_{IIb}\sin\dfrac{2\pi(t-t_d)}{T} & t \ge t_d \end{cases} \tag{3.83}$$

where P_I, P_{IIa} and P_{IIb} are the maximum wave forces obtained using the correction coefficients in Table 3.1. The uplift force $U(t)$ for the perforated-wall caisson breakwater can be obtained by the same method of horizontal wave force.

$$U(t) = \max\left\{U_1(t), U_2(t), U_3(t)\right\} \tag{3.84}$$

$$U_1(t) = \begin{cases} \left(\dfrac{2t}{\tau_0}\right)U_I & 0 \le t < \dfrac{\tau_0}{2} \\ 2\left(\dfrac{1-t}{\tau_0}\right)U_I & \dfrac{\tau_0}{2} \le t < \tau_0 \\ 0 & t \ge \tau_0 \end{cases} \tag{3.85}$$

$$U_2(t) = \begin{cases} 0 & 0 \le t < t_d \\ \left(\dfrac{2(t-t_d)}{\tau_0'}\right)U_{IIa} & t_d \le t < \dfrac{\tau_0'}{2} + t_d \\ 2\left(\dfrac{1-(t-t_d)}{\tau_0'}\right)U_{IIa} & \dfrac{\tau_0'}{2} + t_d \le t < \tau_0' + t_d \\ 0 & t \ge \tau_0' + t_d \end{cases} \tag{3.86}$$

$$U_3(t) = \begin{cases} 0 & 0 \le t < t_d \\ U_{IIb} \sin\dfrac{2\pi(t-t_d)}{T} & t \ge t_d \end{cases} \tag{3.87}$$

where U_I, U_{IIa} and U_{IIb} are the uplift forces obtained using the correction coefficients in Table 3.1. t_d is the time difference between the wave forces $P_1(t)$ and $P_2(t)$, and τ_0' is the duration of Crest IIa, and these can be obtained as follows:

$$t_d = \frac{\tau_0}{2} + \frac{B'}{\sqrt{gd}} - \frac{\tau_0'}{2} \tag{3.88}$$

$$\tau_0' = k'\tau_{0F}' \tag{3.89}$$

$$k' = \left(\frac{1}{\left(\alpha^*\right)^{0.3} + 1} \right)^2 \tag{3.90}$$

$$\tau_{0F}' = \begin{cases} \left(0.5 - \frac{H_{\max}}{8d}\right)T & 0 < \frac{H_{\max}}{d} \le 0.8 \\ 0.4T & \frac{H_{\max}}{d} > 0.8 \end{cases} \tag{3.91}$$

Eqs. (3.89) to (3.91) use the water depth inside the wave chamber d' instead of h. In Eq. (3.91), the wave height must be the value on the rubble mound, but the wave height in front of the breakwater is used by assuming that the wave height change on the mound is small enough to be ignored (Kim, 2005).

Unlike the solid-wall caisson breakwater, the perforated-wall caisson breakwater has a wave chamber that can dissipate the wave force acting on the caisson. The force acting at the bottom of the wave chamber is caused by the increase of water level in the wave chamber and it will increase the caisson stability. The force of at the bottom of the wave chamber was calculated by assuming a triangular distribution; by using the maximum value $\left(P_{IIaM}\right)$ at the moment $\left(t_d + \tau_0'/2\right)$ when the impulsive wave impacts the rear wall and the maximum value $\left(P_{IIbM}\right)$ at the moment $\left(t_d + T/4\right)$ when the wave becomes a standing wave. (Kim, 2005).

$$P_V = \begin{cases} 0 & 0 \le t < t_m \\ \dfrac{4\left(P_{IIbM} - P_{IIaM}\right)}{T - 2\tau_0'}\left[t - \left(t_d + \dfrac{\tau_0'}{2}\right)\right] + P_{IIaM} & t_m \le t < t_d + \dfrac{T}{4} \\ -\dfrac{4\left(P_{IIbM} - P_{IIaM}\right)}{T - 2\tau_0'}\left[t - \left(t_d + \dfrac{\tau_0'}{2}\right)\right] + 2P_{IIbM} - P_{IIaM} & t_d + \dfrac{T}{4} \le t < t_d + \dfrac{T}{2} \\ 0 & t \ge t_d + \dfrac{T}{2} \end{cases}$$

(3.92)

$$t_m = \frac{-P_{IIa}\left(T - 2\tau_0'\right)}{4\left(P_{IIb} - P_{IIa}\right)} + t_d + \frac{\tau_0'}{2} \tag{3.93}$$

where t_m is the time then the vertical pressure starts occurring at the bottom of the wave chamber due to the increase of water level in the wave chamber.

Fig 3. 17 shows the time series of the perforated-wall caisson breakwater which is the combination of two impulsive wave components and one standing wave component. Fig 3. 18 shows a comparison of the time series between the perforated-wall caisson breakwater and the solid-wall caisson breakwater under the same wave condition. The perforated-wall caisson breakwater has the perforated structure that causes the reduction of wave force, and shows a smaller wave force than the solid-wall caisson breakwater, and it can be confirmed that the influence of the impulsive wave has reduced unlike the solid-wall caisson breakwater. From the shape of time series, depending on the configuration of structure, one can find out if the impulsive wave is dominant or the standing wave is dominant.

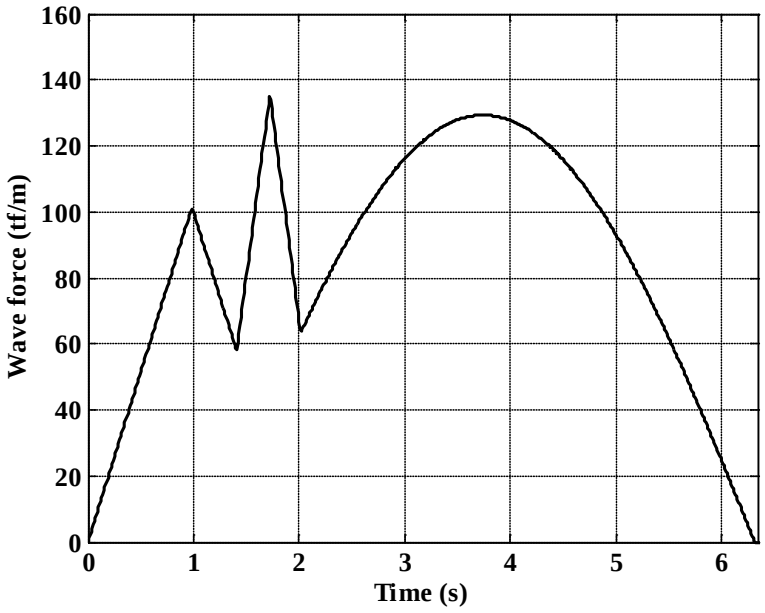

Fig 3. 17 Time series for horizontal wave force acting on perforated-wall caisson breakwater

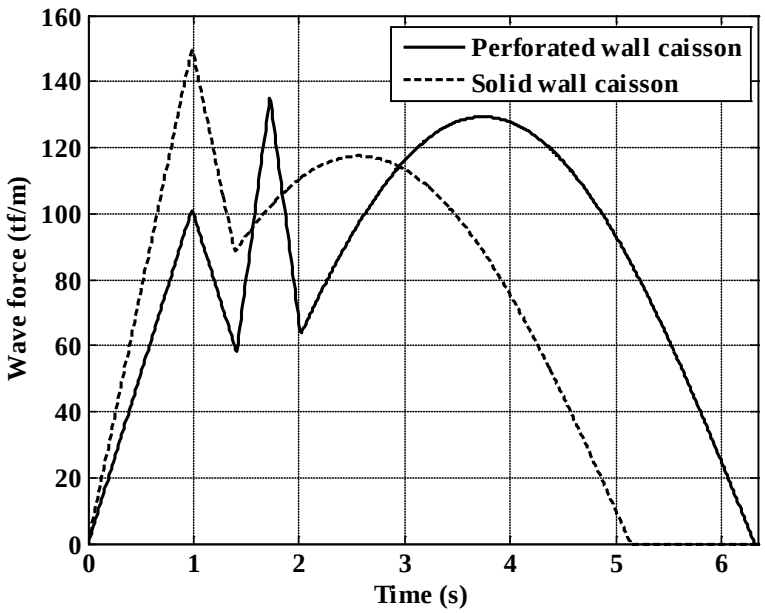

Fig 3. 18 Comparison of time series for horizontal wave force between perforated-wall caisson and solid-wall caisson

3.10 Expected sliding distance

The sliding distance of a caisson can be calculated by accumulating for the lifetime of the breakwater and by assuming the following: the storm that can cause high waves for caisson sliding landed once a year, and 1000 waves occur during the storm. For the calculation of the expected sliding distance, in order to consider the distribution of wave transformation or wave force, the accumulated sliding distance must be calculated repeatedly by changing the random numbers. These processes repeat a number of times and the average value of accumulated sliding distance calculated in each process is defined as the expected sliding distance. In other words, the expected sliding distance means the expected value of total sliding distance obtained by using the high wave that is possible to occur during the lifetime. Monte-carlo simulation was used to generate the random processes of caisson sliding. This is appropriate to the calculation of the process with complexity and many steps, and is sufficiently practical using a personal computer. In the performance-base design method, the caisson can maintain its function even if some sliding occurs. This has the possibility of producing different results than with the conventional deterministic design method. The caisson sliding can be calculated from the time series of wave force.

$$\left(\frac{W}{g}+M_a\right)\frac{d^2x_G}{dt^2}=P_H-F_R-F_D \tag{3.94}$$

$$F_R=\mu\left(W'-U\right) \tag{3.95}$$

Eq. (3.94) is the equation of motion of caisson for sliding. W is the caisson weight in the air, g is gravitational acceleration, M_a is added mass $\left(=1.0855\rho_0 h'^2\right)$, ρ_0 is density of sea water, h' is water depth in front of the caisson, x_G is the horizontal displacement of the caisson, P_H is horizontal wave force, F_R is the frictional resistance, W' is the caisson weight in water, U is the uplift force, and F_D is the wave resistance force.

In general, wave resistance force is not considered because the sliding speed is small enough to ignore. Based on the time series of wave force, if the wave force is smaller than the friction resistance, no sliding occurs, and if the wave force exceeds the friction resistance, sliding occurs and can be calculated by performing the numerical integration of Eq. (3.94) twice with respect to time. Total sliding distance can be calculated by accumulating the sliding distance during the lifetime of the breakwater. In order to estimate the expected sliding distance, the calculation of total sliding distance was repeated for 5000 times and the averaged value was obtained.

Shimosako and Takahashi (1999) proposed the allowable sliding distance of 0.3 m, but Goda and Takagi (2000) thought that 0.3 m was too large and proposed 0.1 m instead. Takahashi et al. (2001) proposed the stability criteria for the expected sliding distance as shown in Table 3.3. If only the expected sliding distance is chosen as the criteria for stability without considering the probability as shown in Table 3.3, the allowable expected sliding distance of the structure having a medium importance is less than 0.3 m.

3.11 Exceedance rate

Since the expected sliding distance is calculated as the average of the simulated sliding distances over the lifetime of the structure, the actual sliding distance can exceed the average. To overcome this, Kim et al. (2009) pointed out the limitation that can occur in evaluating the stability with the expected sliding distance, and evaluated the stability of structure by calculating the exeedance probability of an allowable sliding distance. Exceedance rate can be calculated as shown in Eq. (3.96), which can solve the problem of the structure stability evaluation.

$$P_e = \lim_{N\to\infty} \frac{n_e}{N} \tag{3.96}$$

where n_e is the number of simulations in which the total sliding distance has exceeded the allowable sliding distance, and N is the total number of simulation.

Shimosako and Tada (2004) proposed the exceedance rate criteria of an allowable sliding distance depending on the importance of structure and limit state as shown in Table 3.4 based on the observed damage of caisson breakwater for sliding. This is being used as the criteria for JPHA (2007) in Japan and standards for the breakwater reliability design (2011) in Korea. If the criteria of Table 3.4 are used, the same stability can be maintained even under any design conditions that the sliding distance changes by the environmental conditions such as the occurrence frequency of high waves. The probability exceeding an allowable sliding distance(0.1, 0.3, and 1.0 m)

during the lifetime of a medium-importance structure is proposed as 30%, 10%, and 5% for repairable limit state, extreme limit state, and collapse limit state, respectively, as shown in Table 3.4.

Table 3.3 Allowable expected sliding distance by Takahashi et al. (2001)

	Importance of structure		
	High	Medium	Low
Expected sliding distance (m)	0.03	0.3	1.0

Table 3.4 Acceptable exceedance rate of total sliding distance for breakwaters of different levels of importance, as proposed by Shimosako and Tada (2004)

Limit state (allowable sliding distance)	Importance of structure		
	High	Medium	Low
Repairable(0.1 m)	15%	30%	50%
Ultimate(0.3 m)	5%	10%	20%
Collapse(1.0 m)	2.5%	5%	10%

CHAPTER 4 RESULTS AND ANALYSIS

4.1 Validation of model

In order to validate the model which is used in this study, the experimental results of the hydraulic model tests conducted by the Korea Ocean Research and Development Institute (1992). Fig 4. 1 shows a standard cross-section which was used in the experiment, and is the perforated-wall caisson with vertical slits. Irregular waves were used in the experiment, with the significant wave height of 100-year return period is 9.5m, significant wave period 15 s, and the storm duration is 380 times the significant wave period. The conditions used in validating the model are identical to the conditions in hydraulic experiments. The wave periods of individual waves were calculated by using the coefficient of variation of 0.1 to the significant wave period, 15 s. The expected sliding distance was estimated by averaging the total sliding distances simulated 5000 times. The wave chamber in the hydraulic model test has two wave chambers, each having 4.6-m width as shown in Fig 4. 1. The calculation in this study was conducted for one narrow chamber with 4.6-m width and one wide chamber with 9.6-m width. Fig 4. 2 shows a comparison between the results of hydraulic model test and the calculation in this study.

The sliding distance calculated in this study is greater than the experimental results. The caisson used in the experiment has two wave chambers that dissipate the wave energy twice. However, the caisson used in the calculation has one wave chamber with different widths.

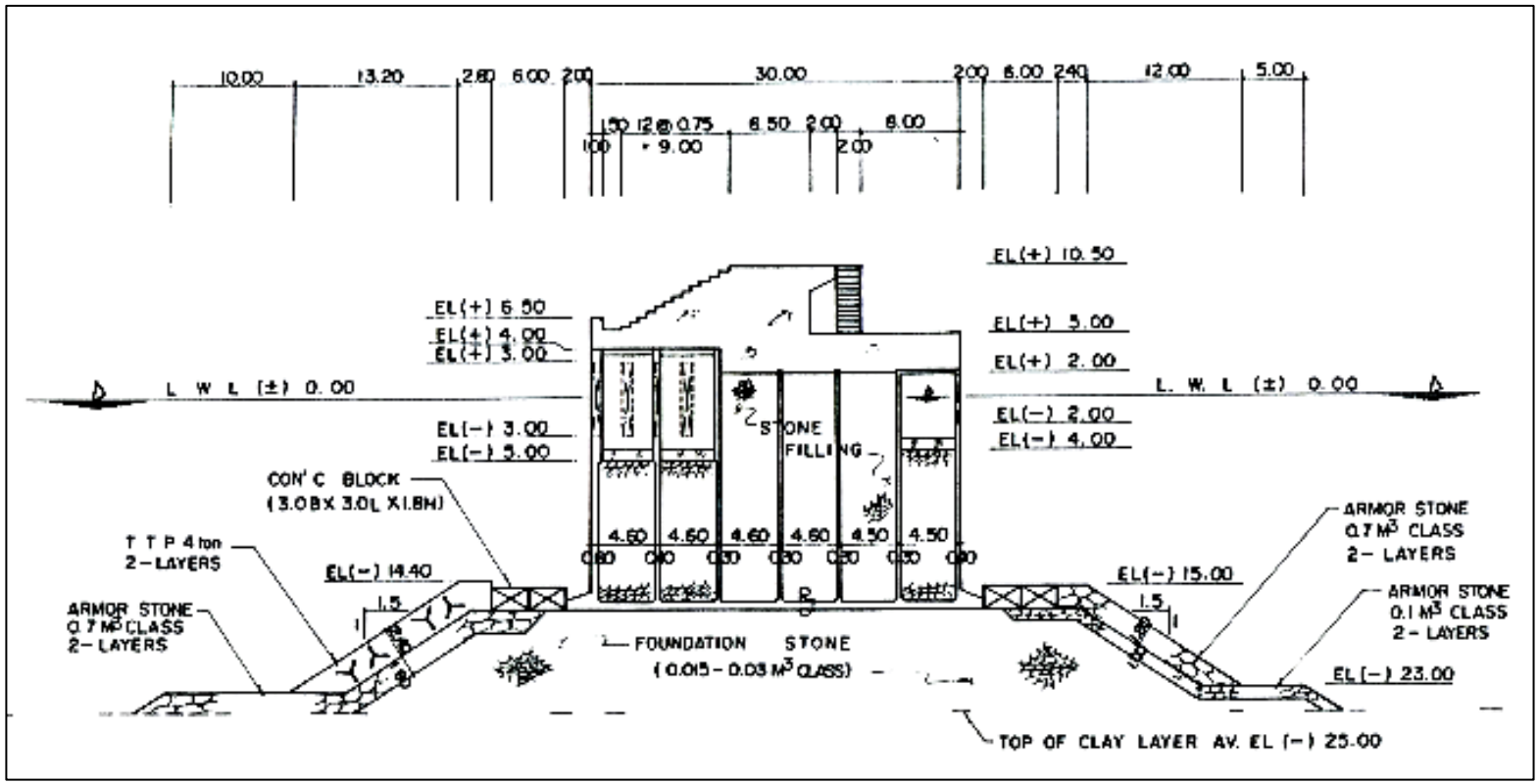

Fig 4. 1 Cross-section II of vertical slit caisson breakwater

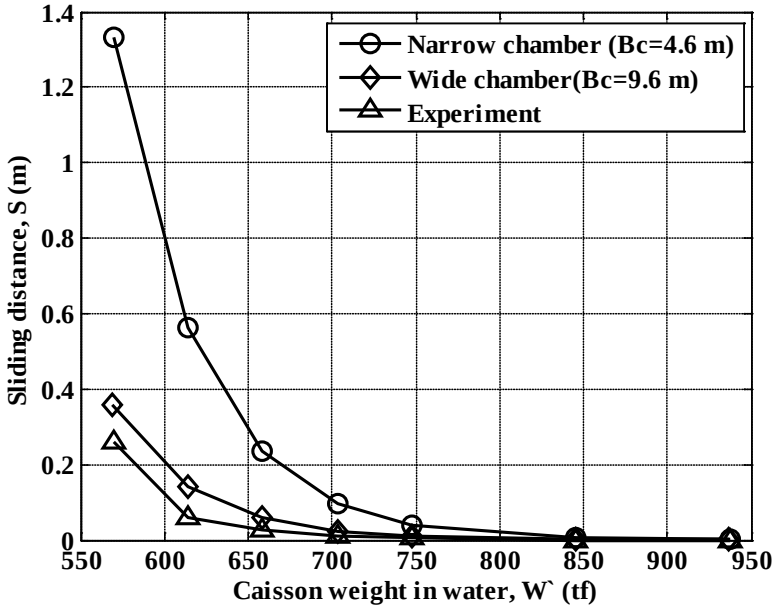

Fig 4. 2 Comparison of sliding distance versus caisson weight in water between experiment and calculation

The narrow-chamber caisson has a relatively large sliding distance since the phase difference of the wave forces acting on the front and rear wall is smaller than that of wider chamber. The caisson used in the experiment has two wave chambers, while the wide chamber in the calculation has one wave chamber. Since the wave dissipating effect by two wave chambers is greater than that in one wide chamber, the sliding distance in the calculation is estimated to be a little larger than the experimental value. The result of the calculation in this study shows the same tendency as the experimental result, although its value is slightly larger than the experimental results. Therefore, the performance-based design method used in this study seems to give a reasonable result.

4.2 Design conditions of caisson breakwater

The typical cross-section of a perforated-wall caisson breakwater is shown in Fig 4. 3, and the design conditions used in estimating the sliding distance of the perforated-wall caisson breakwater is shown in Table 4. 1.

In order to compare the deterministic design method and performance-based design method, the safety factor of sliding was changed at intervals of 0.1 from 1.0 to 1.3, and at intervals of 0.2 from 1.3 to 1.9 to determine the width of caisson that satisfies each safety factor, and the performance-based design was also performed. Water depths at the breakwater site were set at intervals of 4 m from DL(-)14 m to DL(-)30 m, and at intervals of 2 m from DL(-)10 m to DL(-)14 m. Two bottom slopes were used: 1/50 and 1/20. The ratio of the depth on top of mound to total water depth (h'/h) is set at 0.7, the ratio of the water depth inside wave chamber to the depth on top of mound (d'/h') is set at 0.5. The ratio of the wave chamber width to wave length (B_c/L) is set to be 0.12, which can significantly reduce wave reflection without significantly increasing the wave chamber width. The ratio of berm width on the mound to wave length (B_M/L) used the value of 0.05. The high water level is assume to be DL(+)0.66 m. The crest elevation of the front perforated wall is set at $0.5H_{1/3}$, and the crest elevation of the rear wall is set at $0.6H_{1/3}$. The porosity (ε) of the perforated wall is set to be 30%, which gives a minimum reflection.

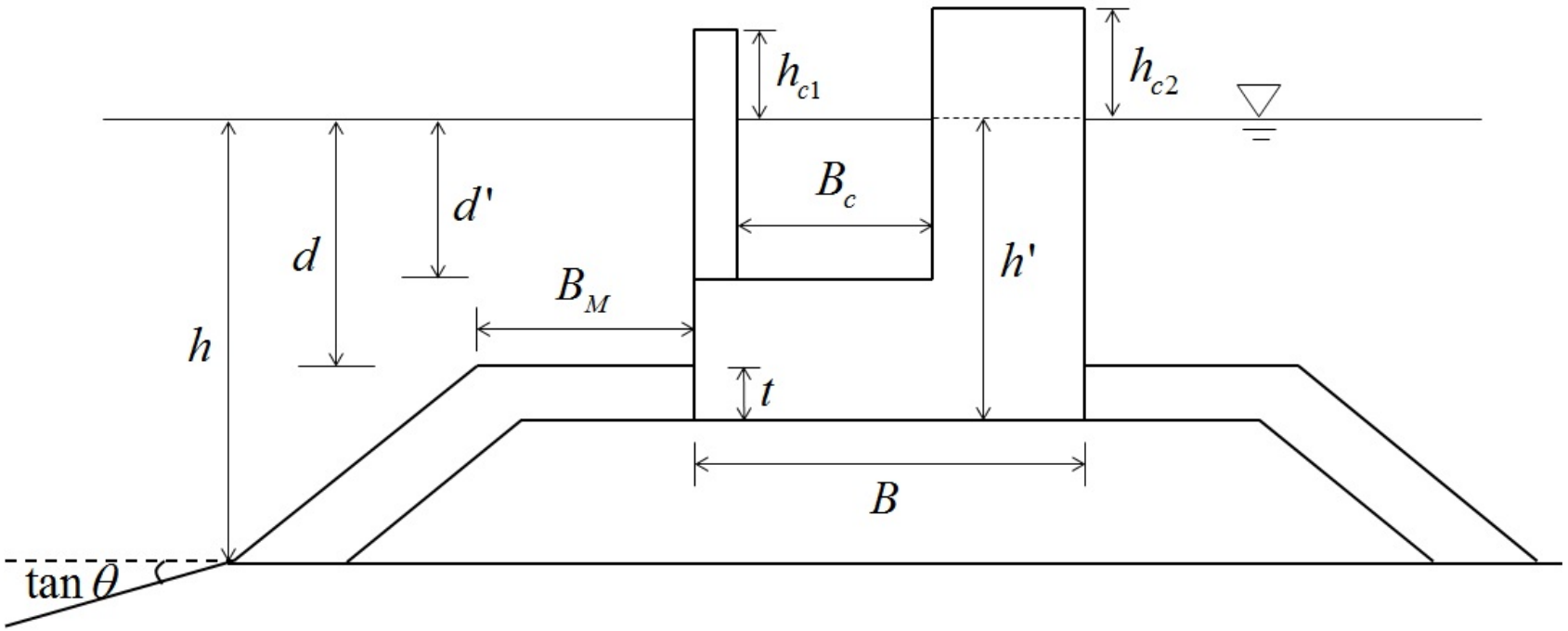

Fig 4. 3 Typical cross-section of perforated-wall caisson breakwater

Table 4. 1 Design condition

	Variable	Condition
Incident wave condition	$H_{1/3}(m)$	Weibull distribution
	$T_s(\mathrm{s})$	Suh et al. (2010b)
	$\beta(\mathrm{deg})$	0
Geometries of caisson breakwater	B	1.0, 1.1, 1.2, 1.3, 1.5, 1.7, 1.9
	h	10, 12, 14, 18, 22, 26, 30 m
	$\tan\theta$	1/50, 1/20
	h'/h	0.7
	Height of armor layer, t	$AH_{1/3}(h'/h)^{-0.787}$, $A=0.21$
	d	$h'-t$
	d'/h'	0.5
	B_c/L	0.12
	B_M/L	0.05
	HWL	0.66 m
	h_{c1}	$0.5H_{1/3}$
	h_{c2}	$0.6H_{1/3}$
	Porosity, ε	0.3

4.3 Computation results

This study was conducted by expanding the performance-based design method for a solid-wall caisson breakwater to the perforated-wall caisson breakwater.

Fig 4. 4~Fig 4. 9 show the computation results of the solid-wall caisson breakwater and perforated-wall caisson breakwater in different water depths designed by using different safety factors. Both expected sliding distance and exceedance rate decreases with decreasing water depth outside the surf zone, but they increase inside the surf zone, i.e. from 14 m for the case of bottom slope of 1/50, and from 12 m for the case of 1/20. The water depths of 14 m and 12 m are the points where wave breaking starts for the bottom slope of 1/50 and 1/20, respectively (see Fig 3. 4 and Fig 3. 5). Both expected sliding distance and exceedance rate reduce as the water depth decreases on the outside of surf zone. As shown in Fig 3. 4 and Fig 3. 5, it is because the limiting breaker height increases with the water depth so that the number of individual waves of larger wave height increases. This result has also been demonstrated for the solid-wall caisson breakwater in Suh et al. (2013). Both expected sliding distance and exceedance rate increase with decreasing water depth inside the surf zone. It is believed that inside the surf zone, as the water depth decreases, the range of wave heights that can cause caisson sliding becomes narrower so that the relative occurrence frequency of large waves close to the limiting breaker height becomes higher.

Fig 4. 10~Fig 4. 15 compare the result of computation between the deterministic design method and the performance-based design method. The

computation result shows the solid-wall caisson breakwater and the perforated-wall caisson breakwater separately.

Fig 4. 10 and Fig 4. 11 show the computation results of expected sliding distance of the solid-wall caisson breakwater and the perforated-wall caisson breakwater installed in various water depths. For both solid-wall and perforated-wall caissons, and in the case of bottom slope of 1/50, if the caisson is designed to satisfy the criterion for the expected sliding distance of the structure of medium importance (i.e. $s_E = 0.3$ m), the corresponding safety factor is smaller than 1.2 inside the surf zone $(h \le 14 \text{ m})$, while it is greater than 1.2 outside the surf zone. This implies that the caisson designed by the performance-based design method satisfies the design criterion of the deterministic design method (i.e. $S.F. = 1.2$) outside the surf zone, but it does not satisfy the criterion inside the surf zone. Also, the safety factor corresponding to $s_E = 0.3$ m increases with water depth outside the surf zone. The same is true for the case of bottom slope of 1/20, in which the boundary of the surf zone is $h = 12$ m .

This can be looked at the other way round. If the caisson is designed to satisfy the criterion of the deterministic design method (i.e. $S.F. = 1.2$), the expected sliding distance is smaller than 0.3 m inside the surf zone, while it is greater than 0.3 m outside the surf zone. Therefore, the caisson trends to be over-designed inside the surf zone and under-designed outside the surf zone from the point of view of the performance-based design method using $s_E = 0.3$ m .

Fig 4. 12 and Fig 4. 13 show the exeedance rate of solid-wall caisson breakwater and perforated-wall caisson breakwater for the ultimate limit state for the structure of medium importance. For both solid-wall and perforated-wall caissons, and for both bottom slopes of 1/20 and 1/20, if the caisson is designed to satisfy the criterion for the exceedance rate for the structure of medium importance in the ultimate limit state (i.e. $P_E\left(S > 0.3\,E\right) = 10\ \%$), the corresponding safety factor is smaller than 1.2 only at the incipient wave breaking point (i.e. $h = 14$ m for 1/50 slope and $h = 12$ m for 1/20 slope), while it is greater than 1.2 in other water depths. This implies that the caisson designed by the performance-based design method satisfies the design criterion of the deterministic design method (i.e. $S.F. = 1.2$) in all water depths except the incipient wave breaking point. On the other hand, if the caisson is designed to satisfy the criterion of the deterministic design method (i.e. $S.F. = 1.2$), the exceedance rate is smaller than 10 % only at the incipient wave breaking point, while it is greater than 10 % in other water depths. This implies that the caisson is under-designed except at the incipient wave breaking point from the view point of the performance-based design method using $P_E\left(S > 0.3\ \mathrm{m}\right) = 10\ \%$.

Fig 4. 14 and Fig 4. 15 show the exceedance rate of solid-wall caisson and perforated-wall caisson breakwater for the repairable limit state for the structure of medium importance. If the caisson is designed by the performance-based design method (i.e. $P_E\left(S > 0.1\ \mathrm{m}\right) = 30\ \%$), the safety factor is smaller than 1.2 in most cases except $h = 30$ m. This implies that

the caisson designed by the performance-based design method to satisfy the criterion of $P_E\left(S > 0.1\ \mathrm{m}\right) = 30\ \%$ does not satisfy the criterion of $S.F. = 1.2$ except at the large water depth of $h = 30\ \mathrm{m}$. On the other hand, if the caisson is designed by the deterministic design method to satisfy the criterion of $S.F. = 1.2$, the exceedance rate, $P_E\left(S > 0.1\ \mathrm{m}\right)$, is smaller than 30 % in most water depths except $h = 30\ \mathrm{m}$. This implies that the caisson in over-designed in most cases from the view point of the performance-based design method using $P_E\left(S > 0.1\ \mathrm{m}\right) = 30\ \%$.

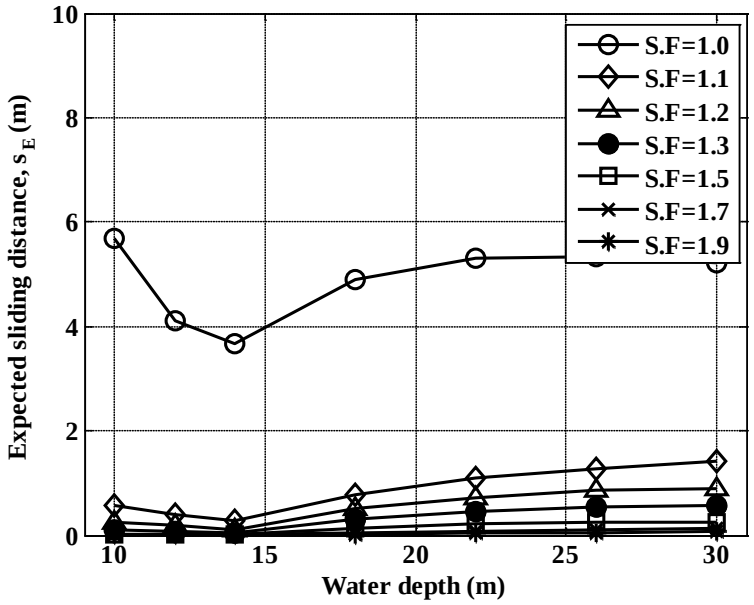

(a)

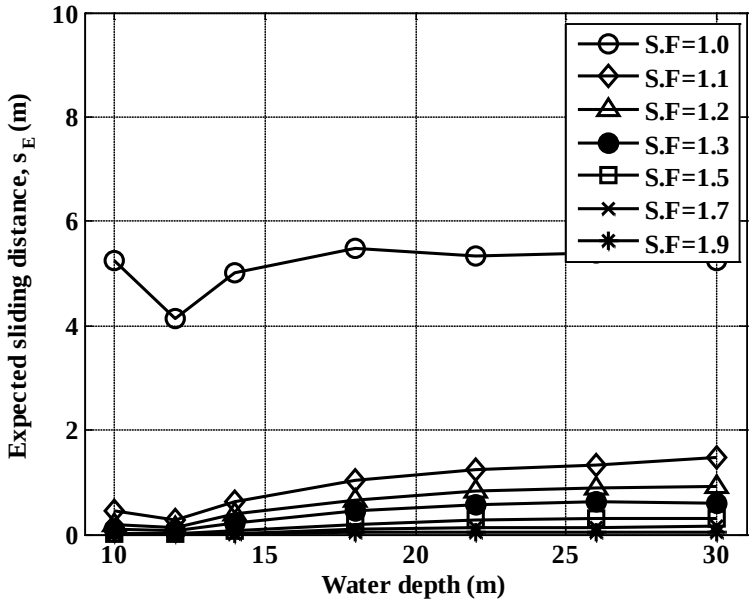

(b)

Fig 4. 4 Expected sliding distance of solid-wall caisson breakwater in different water depths of (a) bottom slope=1/50, (b) bottom slope=1/20

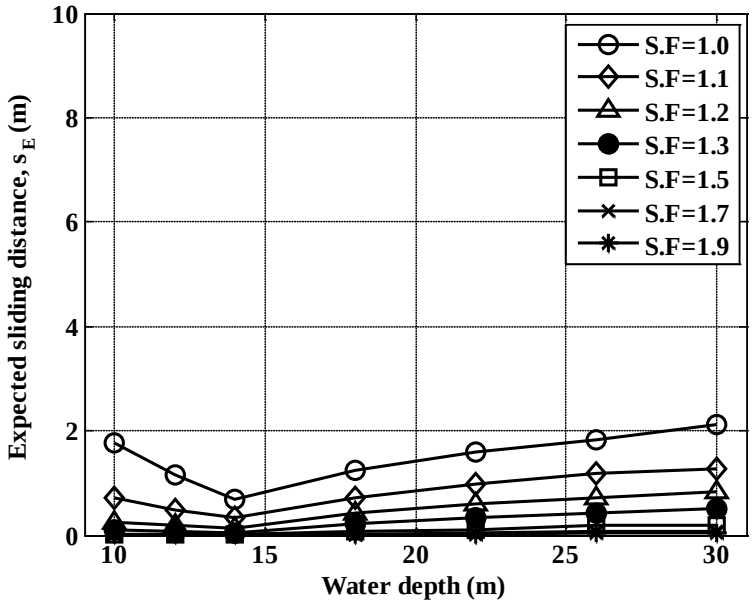

(a)

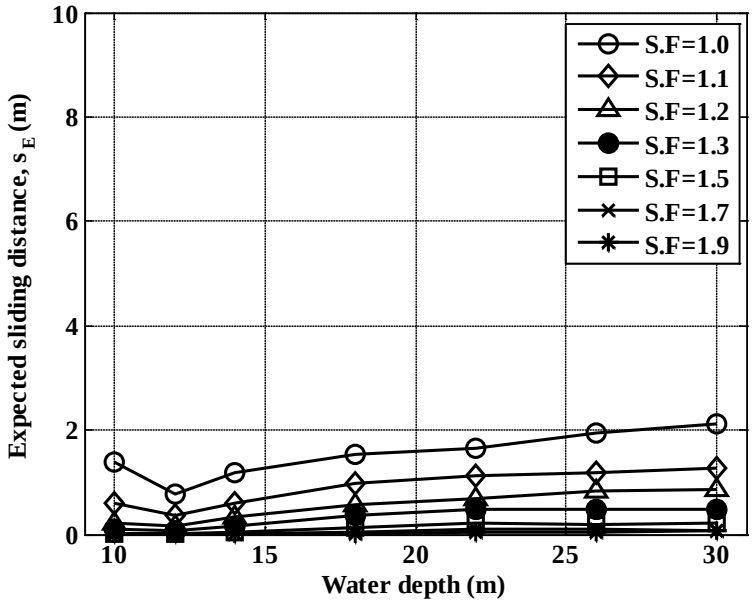

(b)

Fig 4. 5 Expected sliding distance of perforated-wall caisson breakwater in different water depths of (a) bottom slope=1/50, (b) bottom slope=1/20

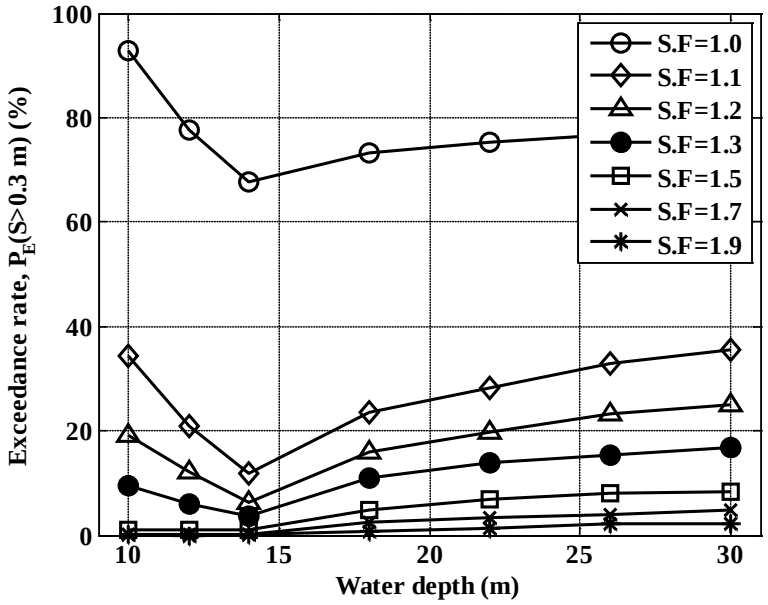

(a)

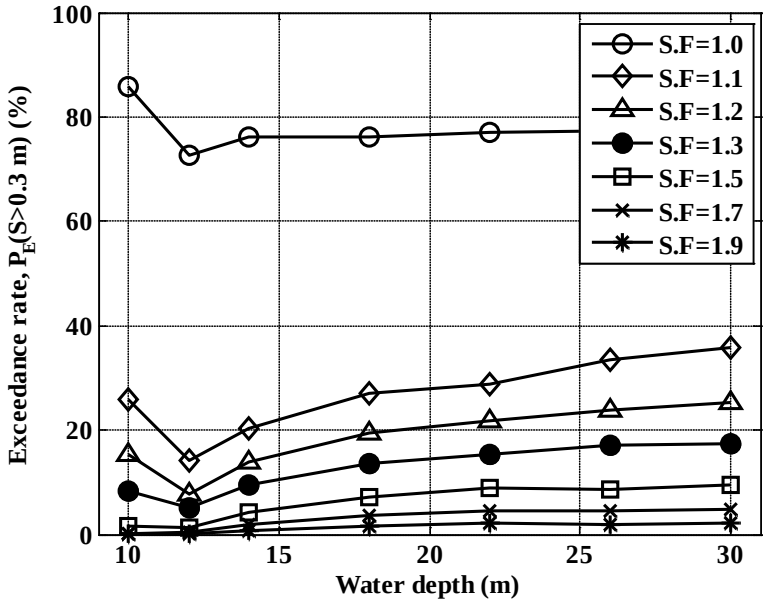

(b)

Fig 4. 6 Exceedance rate(S>0.3 m) of solid-wall caisson breakwater in different water depths of (a) bottom slope=1/50, (b) bottom slope=1/20

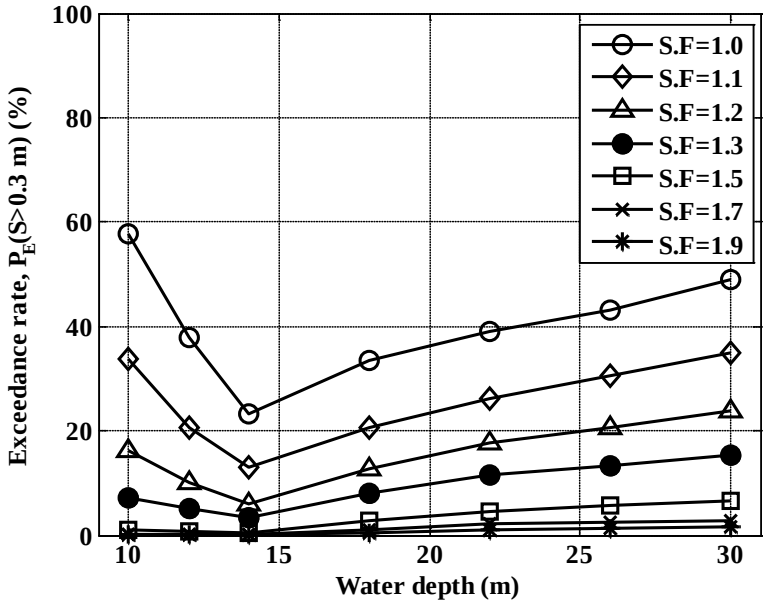

(a)

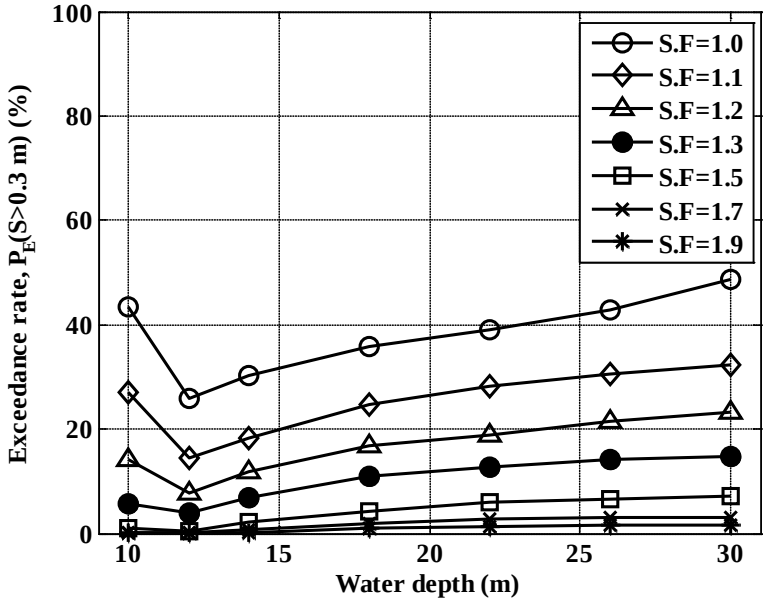

(b)

Fig 4. 7 Exceedance rate(S>0.3 m) of perforated-wall caisson breakwater in different water depths of (a) bottom slope=1/50, (b) bottom slope=1/20

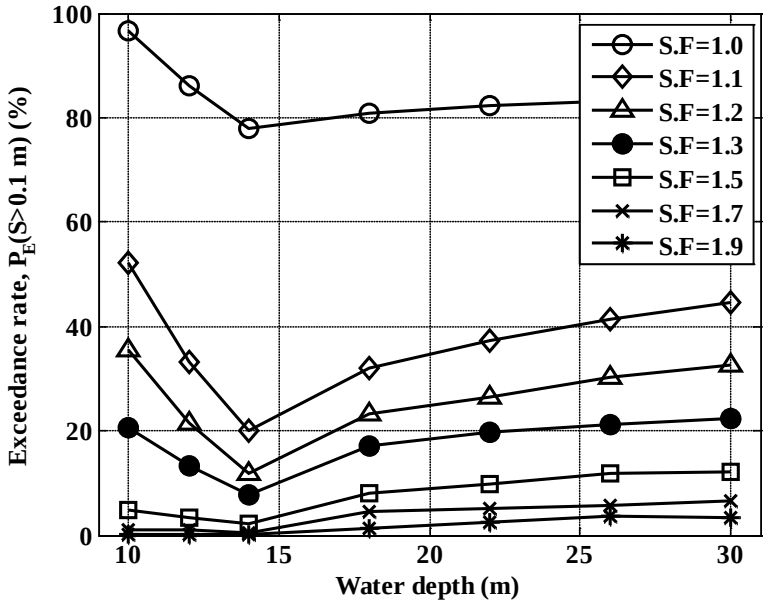

(a)

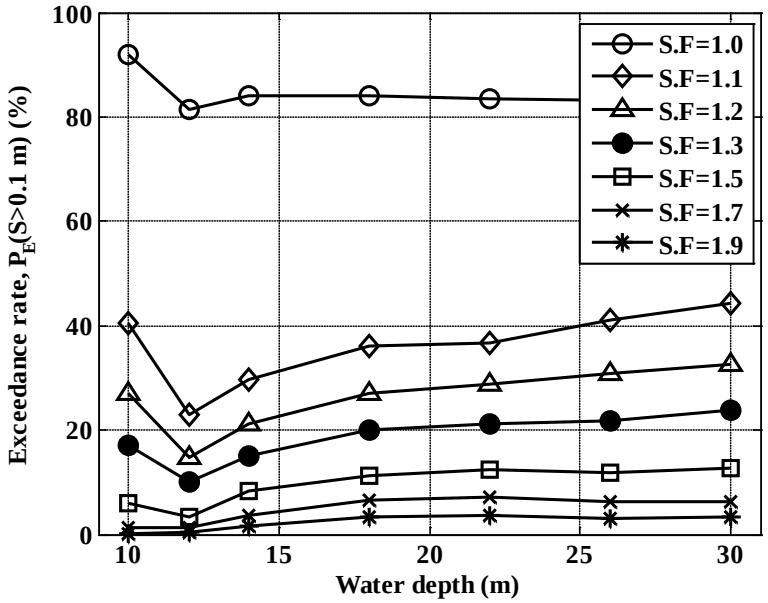

(b)

Fig 4. 8 Exceedance rate(S>0.1 m) of solid-wall caisson breakwater in different water depths of (a) bottom slope=1/50, (b) bottom slope=1/20

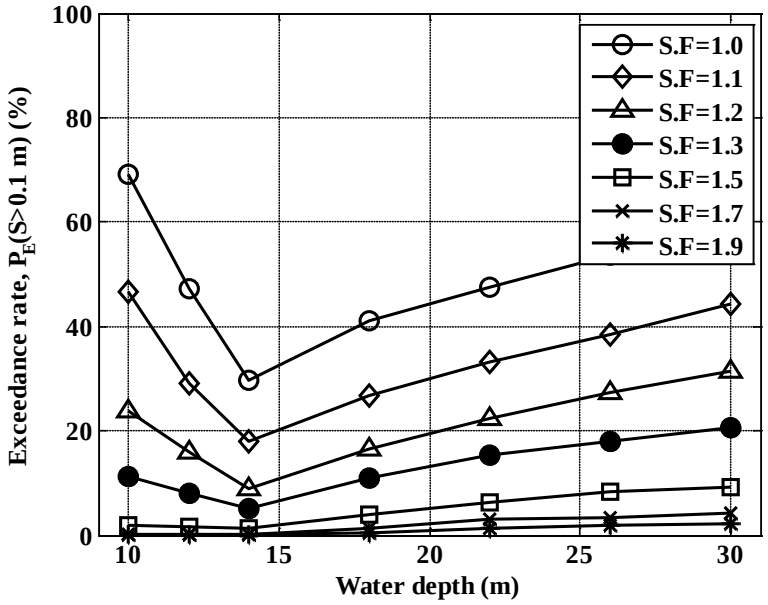

(a)

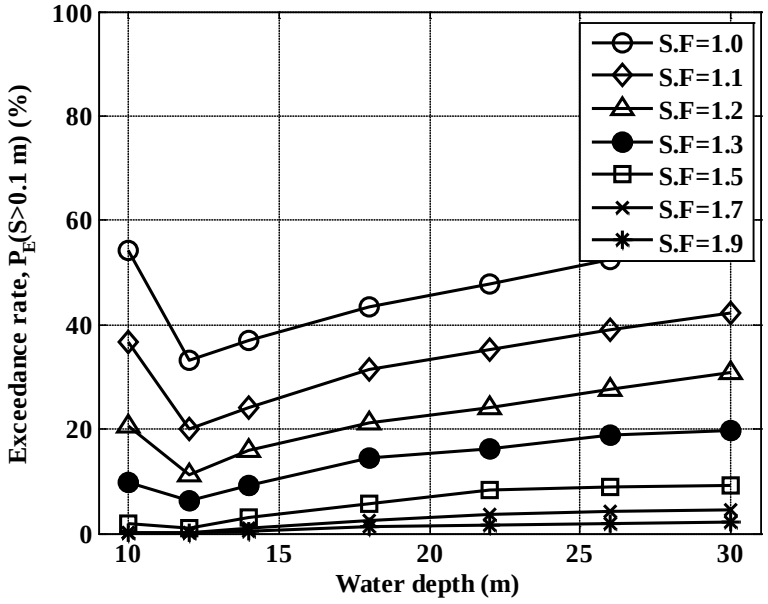

(b)

Fig 4. 9 Exceedance rate(S>0.1 m) of perforated-wall caisson breakwater in different water depths of (a) bottom slope=1/50, (b) bottom slope=1/20

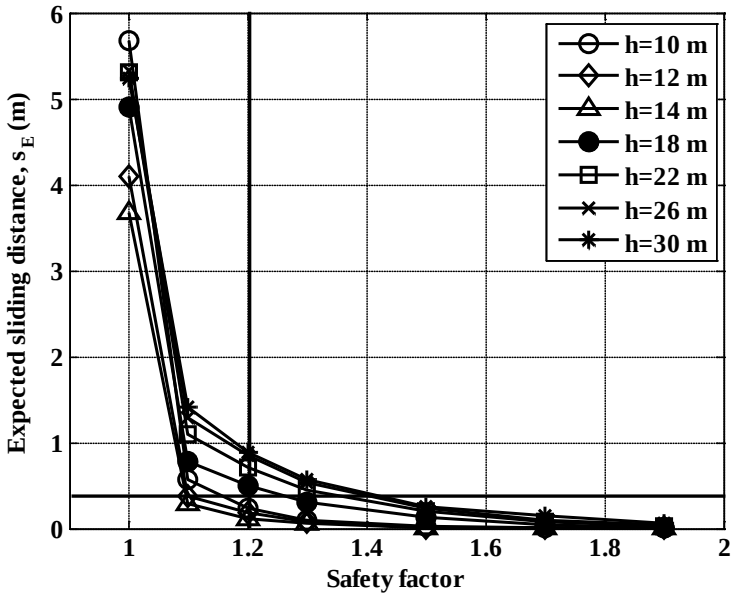

(a)

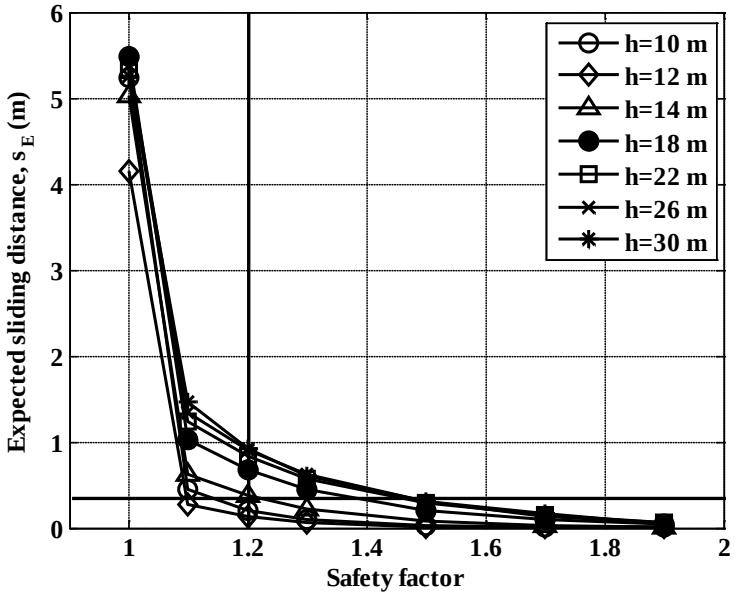

(b)

Fig 4. 10 Expected sliding distance of solid-wall caisson for different safety factors in different water depths of (a) bottom slope=1/50, (b) bottom slope=1/20

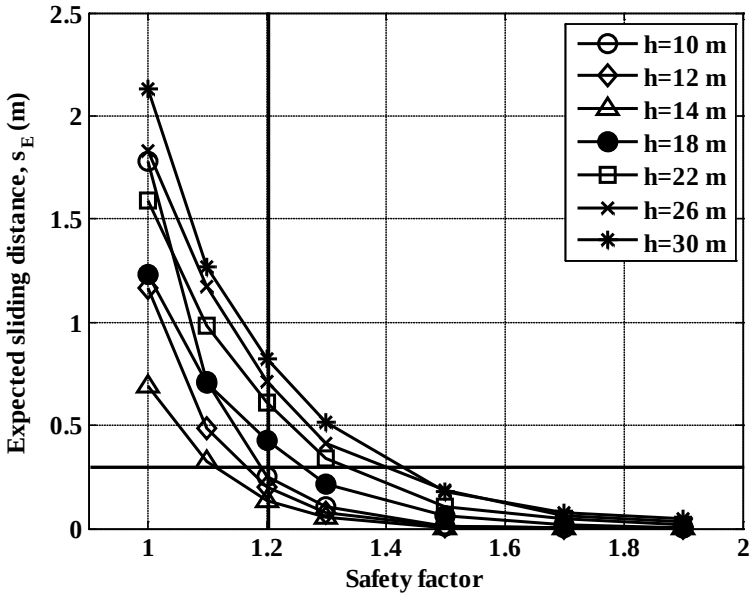

(a)

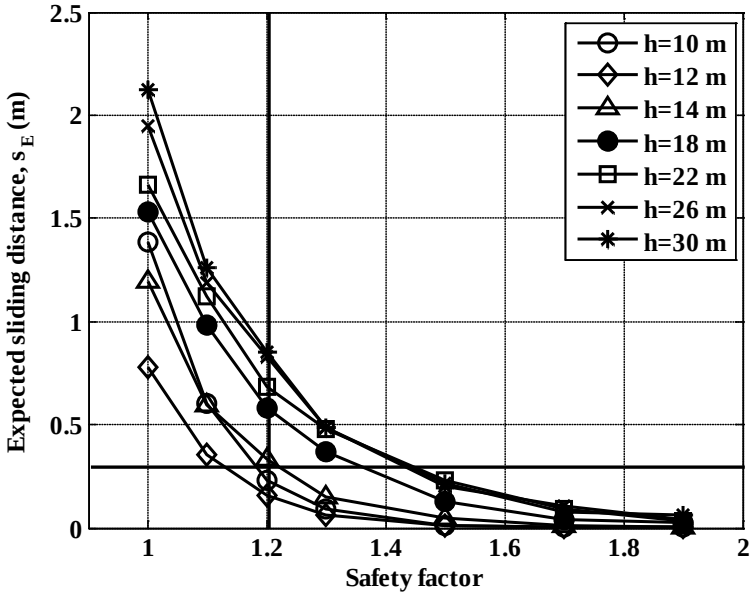

(b)

Fig 4. 11 Expected sliding distance of perforated-wall caisson for different safety factors in different water depths of (a) bottom slope=1/50, (b) bottom slope=1/20

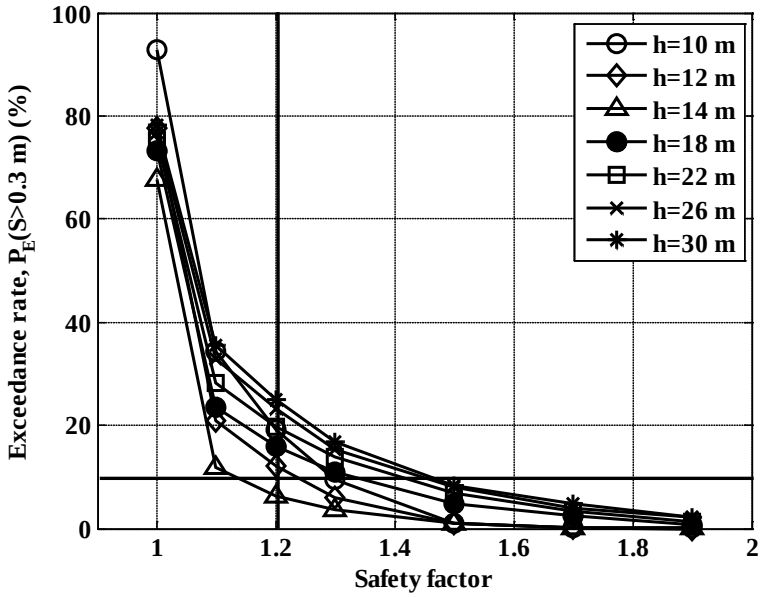

(a)

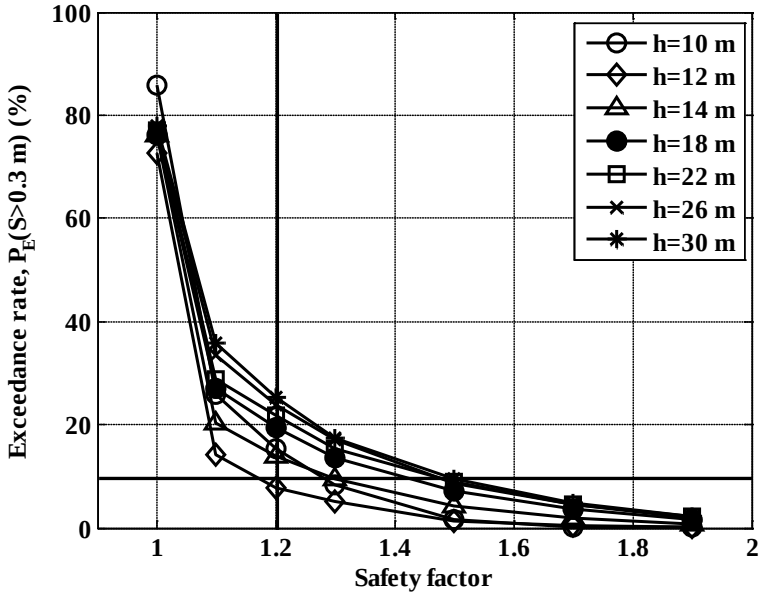

(b)

Fig 4. 12 Exceedance rate(S>0.3 m) of solid-wall caisson in different safety factors in different water depths of (a) bottom slope=1/50, (b) bottom slope=1/20

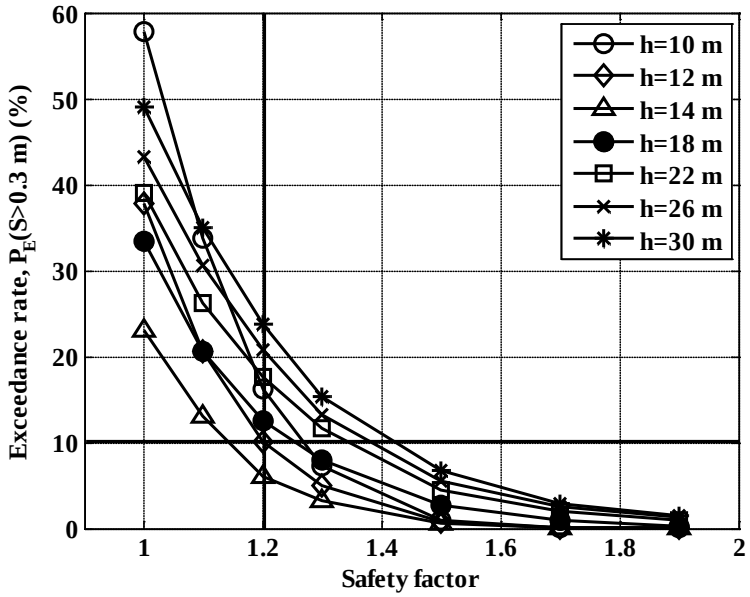

(a)

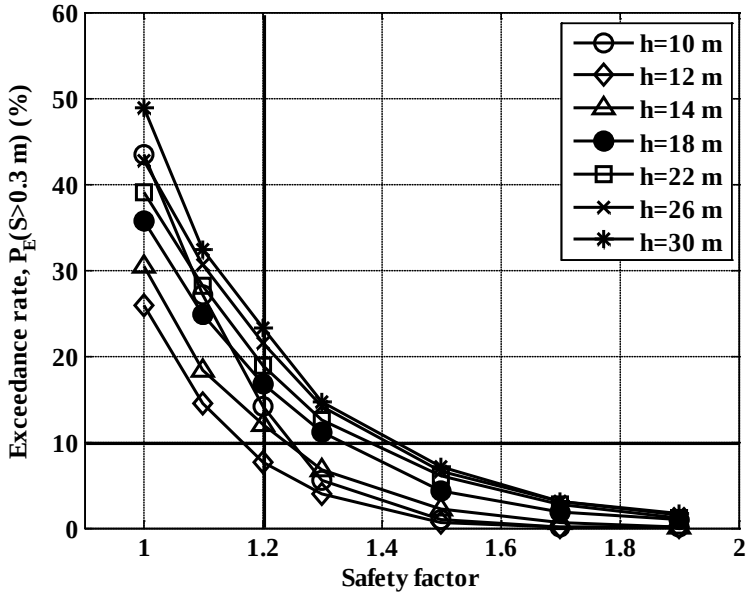

(b)

Fig 4. 13 Exceedance rate(S>0.3 m) of perforated-wall caisson for different safety factors in different water depths of (a) bottom slope=1/50, (b) bottom slope=1/20

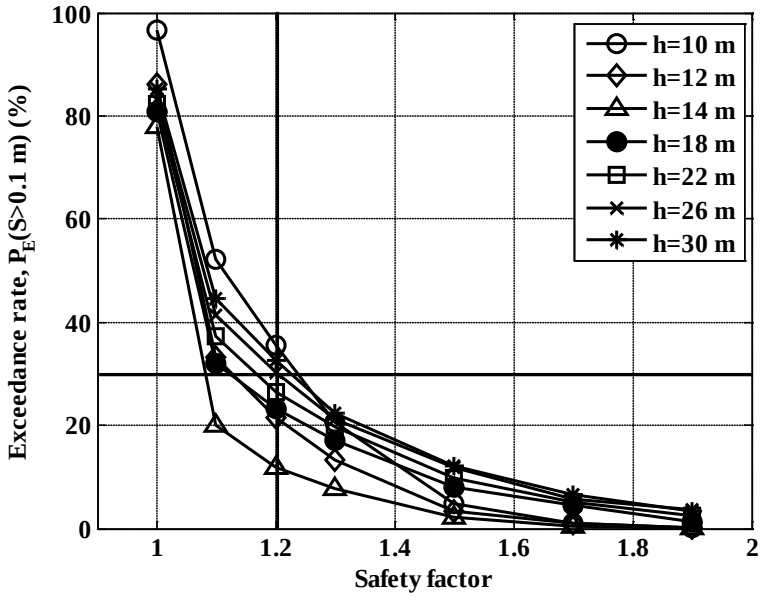

(a)

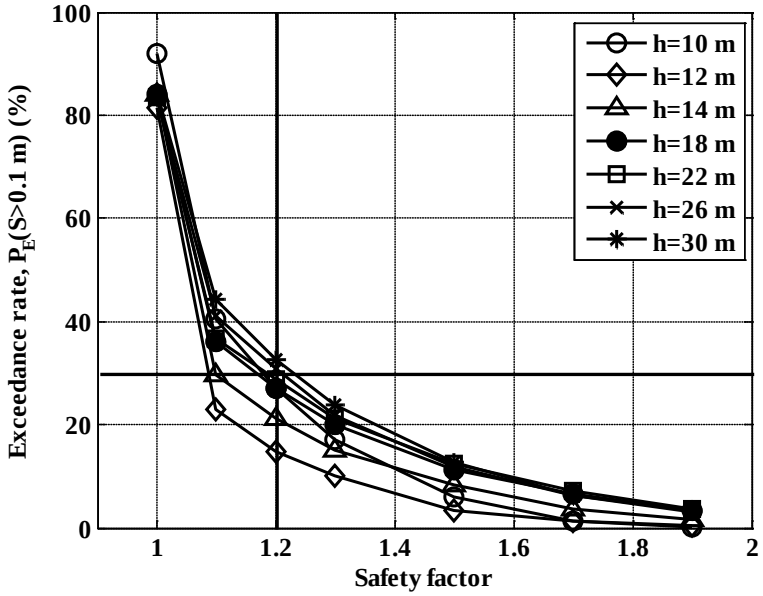

(b)

Fig 4. 14 Exceedance rate(S>0.1 m) of solid-wall caisson for different safety factors in different water depths of (a) bottom slope=1/50, (b) bottom slope=1/20

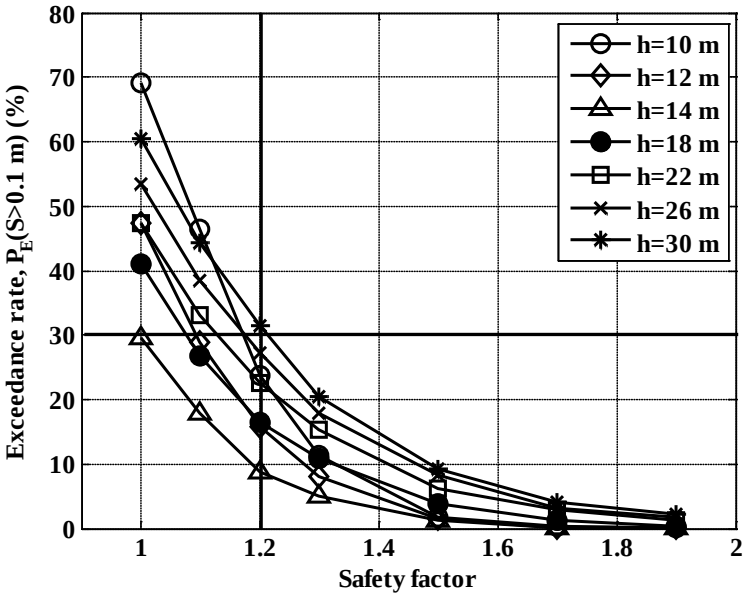

(a)

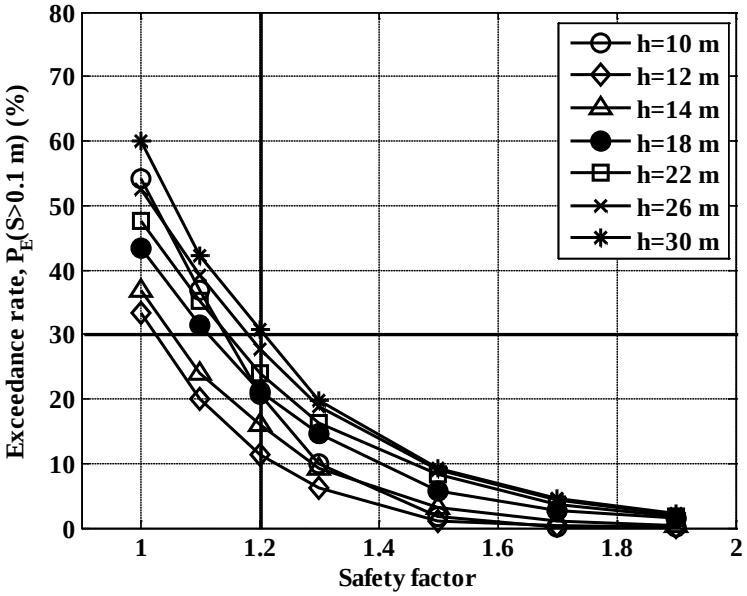

(b)

Fig 4. 15 Exceedance rate(S>0.1 m) of perforated-wall caisson for different safety factors in different water depths of (a) bottom slope=1/50, (b) bottom slope=1/20

4.4 Comparison and analysis

Fig 4. 16~Fig 4. 18 summarize and show the result of computations of the solid-wall caisson breakwater and the perforated-wall caisson breakwater.

Fig 4. 16 shows a comparison of the safety factor for sliding while satisfying the allowable expected sliding distance of 0.3m between the solid-wall caisson breakwater and the perforated-wall caisson breakwater depending on water depths. When the bottom slope is 1/50 and 1/20, both safety factors of the solid-wall caisson breakwater and the perforated-wall caisson breakwater are similar in their tendency inside the surf zone. Even though the safety factor of the solid-wall caisson breakwater is higher than the perforated-wall caisson breakwater outside the surf zone, the difference is not much.

Fig 4. 17 shows a comparison of the safety factor while satisfying the exceedance rate of 10 % of the sliding distance of 0.3 m between the solid-wall caisson breakwater and the perforated-wall caisson breakwater depending on water depths. For the bottom slope is 1/50 and 1/20, although the safety factor of the solid-wall caisson breakwater is higher than the perforated-wall caisson breakwater in all water depths, the difference is not much.

Fig 4. 18 shows a comparison of the safety factor while satisfying the exceedance rate of 30 % of the sliding distance of 0.1 m between the solid-wall caisson breakwater and the perforated-wall caisson breakwater depending on water depths. For the bottom slope is 1/50 and 1/20, although the safety factor of the solid-wall caisson breakwater is higher than the perforated-wall caisson breakwater in all water depths, the difference is not

much. In summary, the tendency of safety factor depending on water depths that satisfies the criteria for performance-based design method shows close similarity between the solid-wall caisson breakwater and the perforated-wall caisson breakwater.

Fig 4. 19~Fig 4. 21 show a comparison of caisson width between the performance-based design method and the deterministic design method depending on water depths. Here H_{0D} is the design wave height, B_p is the width of perforated-wall caisson breakwater in the performance-based design method, B_d is the width of perforated-wall caisson breakwater that satisfies the safety factor 1.2 in the deterministic design method. If the relative caisson width$\left(B_p / B_d\right)$ is less than 1, it means that the performance-based design method requires a smaller caisson width than the deterministic design method. For cases that the allowable expected sliding distance satisfies 0.3 m, the performance-based design method requires a bigger width than the deterministic design method and is non-economical in throughout the water depths, except inside the surf zone. If the exceedance rate of $S < 0.3$ m satisfies 10 % which is under the ultimate limit state, for both bottom slopes, in all water depths, except the location where the wave breaking occurs, the performance-based design method requires a bigger width and non-economical than the deterministic design method. In the repairable limit state, for both bottom slopes in all water depths, the performance-based method requires a smaller width and is economical than the deterministic design method. The tendency of the result is very similar each other for the allowable

expected sliding distance (Fig 4. 19) and the ultimate limit state (Fig 4. 20). In the repairable limit state (Fig 4. 21), there is no noticeable difference between different bottom slopes, and it shows the relative width of close to 1 when the water depth is the greatest and smallest, and it shows the value of less than 1 when it falls somewhere between. As it is shown in the researches by Kim et al. (2009), it is believed to be more reasonable to evaluate with the results of exceedance rate rather than with the allowable expected sliding distance.

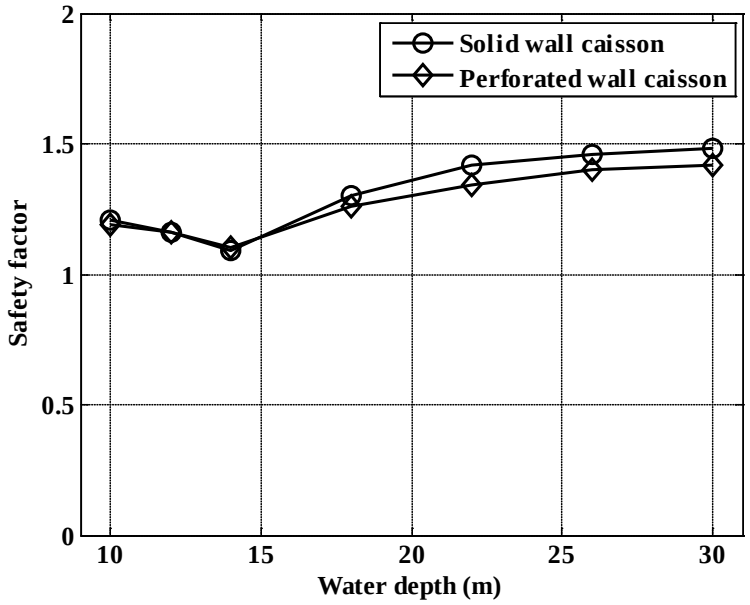

(a)

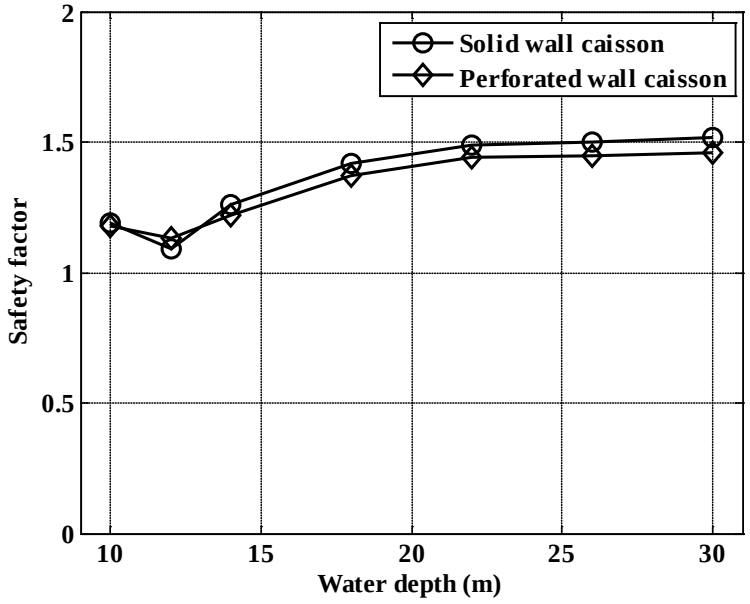

(b)

Fig 4. 16 Comparison of safety factors corresponding to allowable expected sliding distance of 0.3 m in different water depth of (a) bottom slope=1/50 (b) bottom slope=1/20

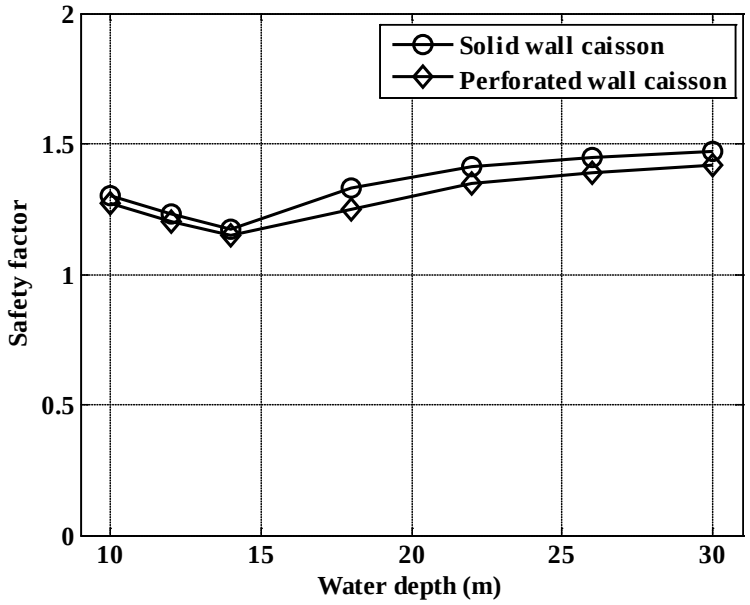

(a)

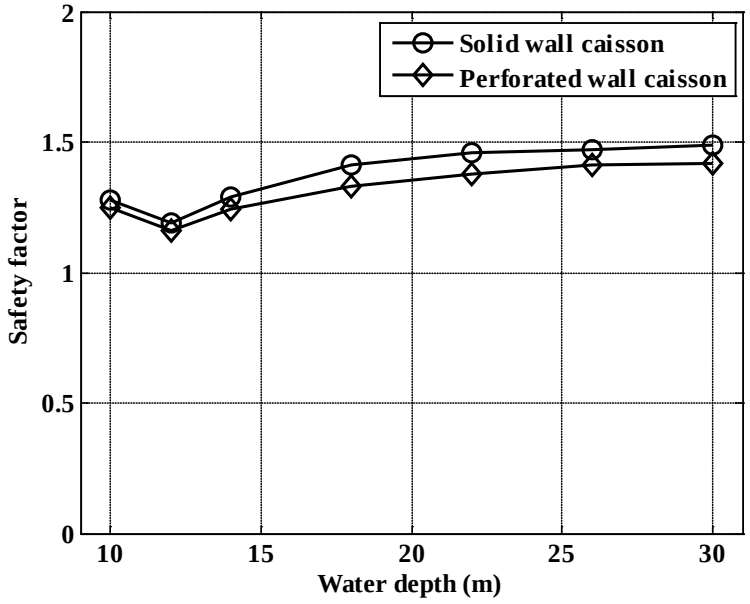

(b)

Fig 4. 17 Comparison of safety factors corresponding to exceedance rate for ultimate limit state in different water depths of (a) bottom slope=1/50 (b) bottom slope=1/20

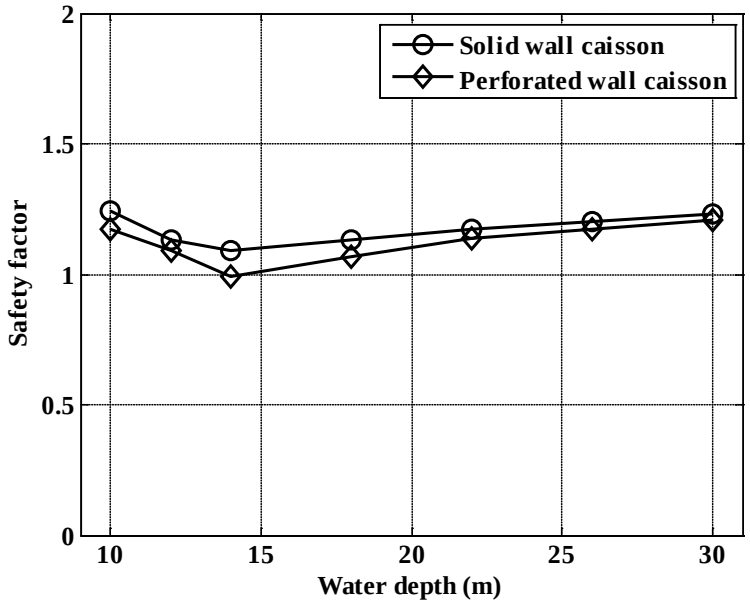

(a)

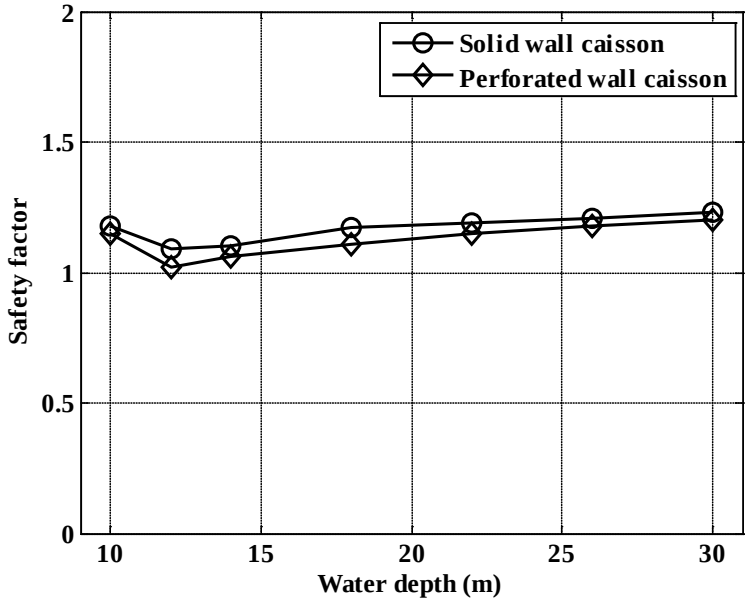

(b)

Fig 4. 18 Comparison of safety factors corresponding to exceedance rate for repairable limit state in different water depths of (a) bottom slope=1/50 (b) bottom slope=1/20

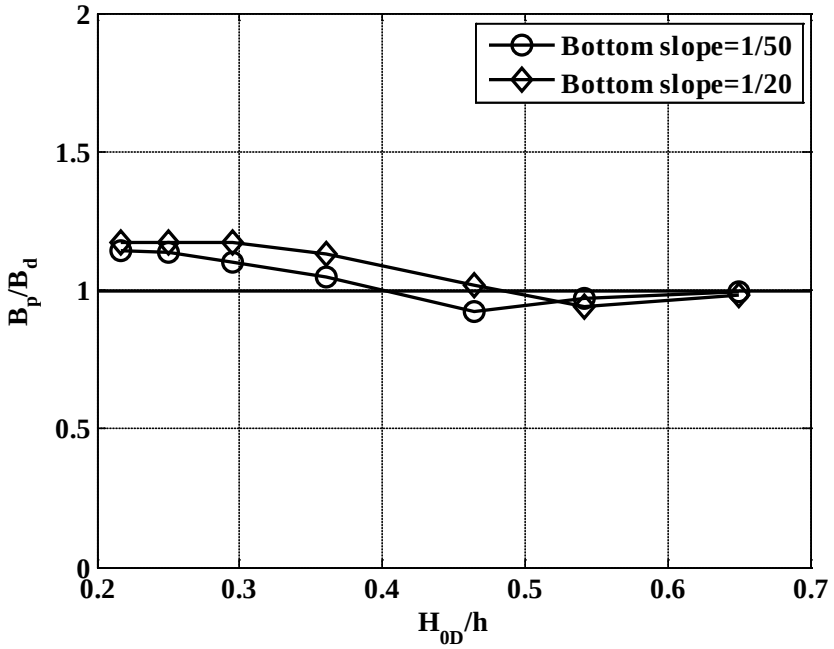

Fig 4. 19 Relative caisson width based on expected sliding distance of 0.3 m

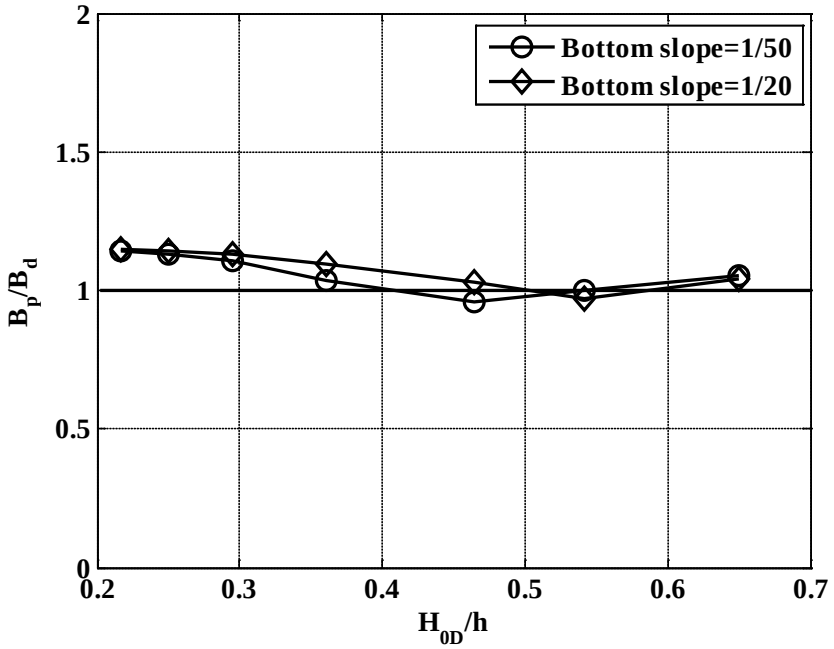

Fig 4. 20 Relative caisson width based on ultimate limit state (Exceedance rate of 10 % for total sliding distance of 0.3 m)

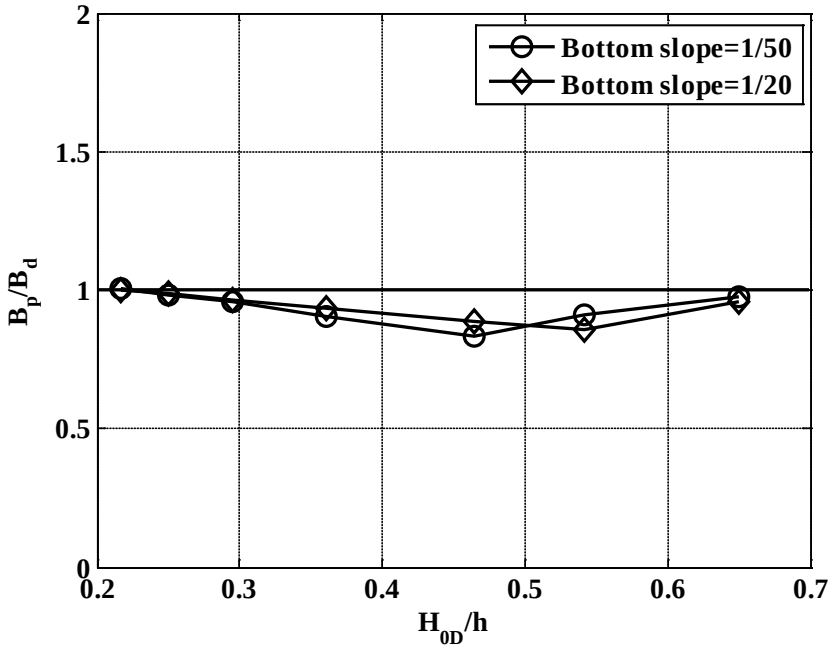

Fig 4. 21 Relative caisson width based on repairable limit state (Exceedance rate of 30 % for total sliding distance of 0.1 m)

CHAPTER 5 CONCLUSIONS AND FUTURE STUDY

5.1 Conclusions

This research was conducted by expanding and applying the performance-based design method that has been applied to the solid-wall caisson breakwater to the perforated-wall caisson breakwater. Also, after determining the cross-section by varying the safety factor, which is used in the deterministic design method, the analysis was mad by applying the cross-section to the performance-based design method. The analysis method employed the allowable expected sliding distance proposed by Takahashi et al. (2001), and the exceedance rate for an allowable sliding distance used by Kim et al. (2009) for the analysis.

The first purpose of this research is to examine the applicability of the model by comparing and analyzing the results from the performance-based design method used for the solid-wall caisson breakwater and the perforated-wall caisson breakwater. The solid-wall caisson breakwater's front wall consists of solid walls and there exists a high impulsive wave component since it absorbs the wave directly in the front. On the other hand, the perforated-wall caisson breakwater has the dissipating effect of wave force brought on by frontal perforated walls and wave chambers, there is a relatively low impulsive wave element compared to the solid-wall caisson breakwater. Therefore, the results of perforated-wall caisson breakwater (expected sliding distance, exceedance rate) show a safe result in overall compared to the solid-wall caisson breakwater, and their tendencies are

identical. Accordingly, there is little problem in applying the performance-based design method for the conventional solid-wall caisson breakwater to the perforated-wall caisson breakwater. Questions about which breakwater is more economical should be considered as a separate issue. The perforated-wall caisson breakwater has a relatively superior performance in wave reflection than the solid-wall caisson breakwater as shown in previous studies. The perforated-wall caisson requires a smaller weight since its safety factor is smaller than that for the solid-wall caisson breakwater. However, it is difficult to judge which is more economical since the reduction of weight of a perforated-wall caisson may cause an increase of caisson width compared with the solid-wall caisson. And since the perforated-wall caisson breakwater has a relatively more complexity in its configuration than the solid-wall caisson breakwater, the costs incurred in production and construction cannot be ignored. It is not possible to judge that the perforated-wall caisson breakwater is more economical than the solid-wall caisson breakwater just because the former is superior in caisson sliding.

The second purpose is to compare and analyze the results of the perforated-wall caisson breakwater between the performance-based design method and the conventional deterministic design method. Analysis of the allowable expected sliding distance and the exceedance rate under the ultimate limit state requires a bigger value than the estimated width in the deterministic design method, and therefore indicates that the performance-based design method is non-economical one. However, if it is a condition where requires a high safety factor by the judgment of an engineer, since a

bigger width can be determined even in the deterministic design method, it is not possible to simply determine that the performance-based design method to be non-economical for the allowable expected sliding distance and the ultimate limit state. Analysis of the exceedance rate under the repairable limit state requires a smaller value than the estimated width calculated by the deterministic design method, and therefore shows the performance-based design method an economical one.

Therefore, the design for sliding of the perforated-wall caisson breakwater by the performance-based design method in the repairable limit state (less than 30% of exceedance rate) is expected to be more efficient than the deterministic design method which uses the safety factor of 1.2 since it can reduce the width by 16%.

5.2 Future study

In the performance-based design for sliding of a caisson breakwater, the estimation of wave force and the distribution of time series have a strong influence on determining the sliding distance. For the solid-wall caisson breakwater, the estimation method of wave force and the time series have been proposed based on hydraulic model tests by numerous researchers. For the perforated-wall caisson breakwater, the estimation method of wave force was proposed based on hydraulic model tests under various conditions by Takahashi et al. (1991). Kim (2005) applied the wave pressure formula of Takahashi et al. (1991) to propose the times series of wave force acting on the perforated-wall caisson breakwater. This is an equation derived from the aspect of theoretical approach and is not derived from experiments. Although the calculated wave force is similar to the time series of wave force measured by the research of Takahashi et al. (1991), the wave force acting at the bottom of the wave chamber does not exists in the solid-wall caisson breakwater, so it may be unreasonable to assume the time series as a triangular distribution. Therefore, if the time series of the wave force on a perforated-wall caisson breakwater is proposed based on the experiments, more reasonable design results can be estimated in the future.

Secondly, since the reliability design method uses the probability distribution of design variables, the distribution estimation has a large influence on the design. The research on the distribution estimation of the solid-wall caisson breakwater has been actively conducted. However, the studies on the perforated-wall caisson breakwater are relatively scarce. This

study used the results of Takayama and Ikeda (1992) for the distribution of horizontal wave force acting on the perforated-wall caisson breakwater. However, since the formulae for wave force acting on the bottom of the wave chamber and uplift force have not been proposed, the formulae used for the solid-wall caisson breakwater were used. Therefore, the research on the probability distribution of the design variables applying to the perforated-wall caisson breakwater must be more actively conducted so that a more reasonable result of design can be predicted.

Third, the research for the allowable failure criteria for the sliding of a perforated-wall caisson breakwater is necessary. The allowable expected sliding distance and exceedance rate used in this research is the criteria that have been in use for the solid-wall caisson breakwater. For the perforated-wall caisson breakwater, it is believed that the allowable failure criteria for sliding is different from that of the solid-wall caisson breakwater and thereby needs a new allowable criteria.

References

Goda, Y. (1974). A new wave pressure formulae for composite breakwater, *Proc. 14th Int. Conf. Coast. Eng.*, ASCE, Copenhagen, 1702-1720.

Goda, Y. (1975). Deformation of irregular waves due to depth-controlled wave breaking. *Rep. of Port and Harbour Engineering,* 14(3), 5012-5018.

Goda, Y., and Suzuki, Y. (1975). Computation of refraction and diffraction of sea waves with Mitsuyasu's directional spectrum, *Tech. Note of Port and Harbour Res. Inst.* 230, 45.

Goda, Y., Takagi, H. (2000). A reliability design method of caisson breakwaters with optimal wave height. *Coast. Eng. J*. 42. 357-387.

Goda, Y. (2003). Revisiting Wilson's formulas for simplified wind wave prediction. *J. Waterw., Port, Coast. Ocean Eng.,* 129(2), 93-95.

Goda, Y. (2010). *Random seas and design of maritime structures, 3rd ed., World Scientific, 3rd ed,* World Scientific, Singapore.

Hong, S. Y., Suh, K.D., and Kweon, H.M. (2004). Calculation of expected sliding distance of breakwater caisson considering variability in wave direction. *Coastal Eng. J.*, 46(1), 119-140.

Huang, Z., Li, Y., Liu, Y. (2011). Hydraulic performance and wave loadings of perforated/slotted coastal structures: A review. *Ocean Eng*. 38, 1031-1053.

Iwagaki Y., and Sakai, T. (1968). On the shoaling of finite amplitude waves (2), *Proc. 15th Japanese Conf. Coastal Eng*, 59-106.

JPHA (2007). Japan Port and Habor Association, *Technical Standards and Commentaries of Port and Harbor Facilities in Japan* (in Japanese)

Kim, D.-H. (2005). Calculation of expected sliding distance of wave dissipating caisson breakwater, *J. Korea Society of Coast. Ocean Eng.*, 17(4), 213-220. (in Korean)

Kim, S.-W., Suh, K.-D., (2006). Application of reliability design methods to Donghae harbor breakwater, *Coast. Eng. J.* 48(1), 31-57.

Kim, S.-W., Suh, K.-D., Oh, Y. M., (2006). Comparative study of reliability design methods by application to Donghae harbor breakwaters: 2. Sliding of caissons, *J. Korea Society of Coast. Ocean Eng.*, 18(2), 137-146. (in Korean)

Kim, S.-W., Suh, K.-D. (2009). Exceedance probability of allowable sliding distance of caisson breakwaters in Korea, *J. Korea Society of Coast. Ocean Eng.*, 21(6), 495-507. (in Korean)

Kim, T. M., and Takayama, T. (2003). Computational improvement for expected sliding distance of a caisson-type breakwater by introduction of a doubly-truncated normal distribution. *Coast. Eng. J,* 45(3), 387-419

Korea Ocean Research and Development Institute. (1992). *Basic design study of offshore breakwater(Hydraulic model test-II).* (in Korean)

Ministry of Land, Transport and Maritime Affairs. (2011). *Standards for the breakwater reliability design.* (in Korean)

Mitsuyasu, H., Tasai, F., Suhara, T., Mizuno, S., Ohkuso, M., Honda T., and Rikiishi, K. (1977). Observations of the directional spectrum of ocean waves using a cloverleaf buoy, *J. Phys. Oceanogr.*, Vol. 5, 750-760.

Oumeraci, H., Kortenhaus, A., Allsop, W., de Groot, M., Grouch, R., Vrijling, H., Voortman, H. (2001). *Probabilistic design tools for vertical breakwater,* Sweta & Zeitlinger B.V., Lisse.

Overseas Coastal Area Development Institute of Japan (OCDI) (2009). Technical standards and commentaries for port and harbor facilities in Japan.

Shimosako, K., and Takahashi, S. (1998). Reliability design method of composite breakwater using expected sliding distance. *Rep. of Port and Harbor Res. Inst,* 47(3), 3-30. (in Japanese)

Shimosako, K., and Takahashi, S. (1999). Application of deformation-based reliability design for coastal structures, *Proc. Int. Conf. Coastal Struct., 1999,* A. A. Balkema, Spain, 363-371.

Shimosako, K., and Tada, T. (2004). Verification procedures of performance-based design on the sliding stability of composite breakwaters, *Proc. Tech-Ocean 2004.*, 53-58.

Suh, K.-D., Kweon, H.-D., Lee, D.-Y. (2008). Statistical characteristics of deepwater waves along the Korean coast, *J. Korea Society of Coast. Ocean Eng.*, 20(4), 342-354. (in Korean)

Suh, K-D., Kwon, H-D., Lee, D-Y. (2010). Some characteristics of large deepwater waves around the Korean Peninsula, *Coast. Eng.*, 57, 375-384.

Suh, K-D., Kim, S-W., Mori, N., Mase, H. (2012). Effect of climate change on performance-based design of caisson breakwaters. *J. Waterway, Port, Coast., Ocean Eng.*, 138, 215-225.

Suh, K-D., Kim, S.-W., Kim, S., Cheon, S. (2013). Effects of climate change on stability of caisson breakwaters in different water depths. *Ocean Eng.*, 71, 103-112.

Takahashi, S., Shimosako, K. and Sasaki, H. (1991). Experimental study on wave forces acting an perforated wall caisson breakwaters. *Rep. of port and harbor Res. Inst.* 30(4). 3-34 (in Japanese).

Takahashi, S., Tanimoto, K., and Shimosako, K. (1994). A proposal of impulsive pressure coefficient for the design of composite breakwaters. *Proc. Int. Conf. Hydro-Tech. Eng. Port and Harbour Const.*, Yokohama, Japan, 489-504.

Takahashi, S., Tanimoto, K., and Shimosako, K. (1994). Wave pressure on a perforated wall caisson. *Proc. Int. Conf. Hydro-Tech. Eng. Port and Harbour Const.*, Yokosuka, Japan, 747-764.

Takahashi, S., Shimosako, K., Kimura, K., Suzuki, K. (2000). Typical failure of composite breakwaters in Japan. *Proc. 27th Int. Conf. Coast. Eng.*, 1899-1910.

Takayama, T., Ikeda, N. (1992). Estimation of sliding failure probability of present breakwaters for probabilistic design. *Rep. of the Port and Hab. Res. Inst.*, 31(5), 3-32.

Tanimoto, K., and Takahashi, S. (1994). Design and construction of caisson breakwater – the Japanese experience. *Coast. Eng.*, 22, 57-77.

U.S. Army Coastal Eng. Res. Center. (1977). *Shore Protection Manual 3rd edn.*, U.S. Government Publishing Office, Washington, D.C., USA.

초 록

유공케이슨 방파제의 활동에 대한 설계법 비교 연구

서울대학교 대학원

건설환경공학부

김 남 훈

케이슨 방파제를 설계함에 있어서 방파제의 주요 파괴 모드인 활동에 대하여 안전율을 이용하는 결정론적 설계법이 사용되어 왔다. 하지만 구조물에 작용하는 하중과 구조물의 저항력 등에 대한 불확실성을 안전율이라는 간단하지만 경험적인 상수를 대신하기 때문에 활동량에 대한 정량적, 상대적인 평가가 어려워 구조물을 과대 혹은 과소 설계할 가능성을 내포하고 있다. 이러한 설계변수의 불확실성을 확률적 개념으로 고려하여 케이슨의 활동량을 계산하는 성능 설계법이 제안되고 있다. 무공케이슨 방파제의 성능 설계법은 과거 여러 연구자들에 의해 연구가 진행되어 왔으며, 현재 그 틀이 거의 잡혀져 있다 해도 과언이 아니다. 반면, 유공케이슨 방파제의 경우 전면의 유공벽 구조에 의한 파력 감쇄에 따라 구조물의 안정성이 증대되는 효과가 있음에도 불구하고 이와 관련된 연구는 국내·외적으

로 아직 많이 이루어지지 않았다.

본 연구에서는 기존의 무공케이슨 방파제의 성능 설계법 이론을 유공케이슨 방파제에 확장, 적용하여 이론의 적용 가능성 여부를 판단한다. 또한 결정론적 설계법의 결과와 비교 분석하여 합리적인 설계법을 결정 한다. 이는 유공케이슨 방파제의 성능 설계법에 대한 기준을 제시하기 위해 수행되는 기초 연구이다. 따라서 향후 유공케이슨 방파제의 성능 설계에 매우 중요한 지표가 될 것으로 예상된다.

주요어: 유공케이슨 방파제, 신뢰성 설계법, 성능 설계법, 기대활동량, 초과확률

학번: 2012-20892